RELEASED
2008/04/23

911118
Revision 0

Engineering Services for the Next Generation Nuclear Plant (NGNP) with Hydrogen Production

RPV and IHX Pressure Vessel Alternatives Study Report

Prepared by General Atomics
for the Battelle Energy Alliance, LLC

Subcontract No. 00060845
Uniform Filing Code UFC:820-3.1.2

GA Project 30283

GENERAL ATOMICS

Rolls-Royce

URS
Washington Division

TOSHIBA
Leading Innovation

OKBM

Korea Atomic Energy Research Institute

GENERAL ATOMICS

GA 1485 (REV. 08/06E)

ISSUE/RELEASE SUMMARY

☐ R & D ☐ DV&S ☒ DESIGN ☐ T&E ☐ NA	APPVL LEVEL	DISC	QA LEVEL	SYS	DOC. TYPE	PROJECT	DOCUMENT NO.	REV
	5	N	I	N/A	RGE	30283	911118	0

TITLE:

RPV and IHX Pressure Vessel Alternatives Study Report

CM APPROVAL/ DATE	REV	PREPARED BY	APPROVAL(S) ENGINEERING	APPROVAL(S) QA	APPROVAL(S) PROJECT	REVISION DESCRIPTION/ W.O. NO.
7 ISSUED APR 2 3 2008	0	M. Richards R. Meyer	A. Shenoy	K. Partain	J. Saurwein	Initial Issue A30283-0320

CONTINUE ON GA FORM 1485-1

* See list of effective pages

NEXT INDENTURED DOCUMENT(S)

N/A

COMPUTER PROGRAM PIN(S)

N/A

LIST OF CONTRIBUTORS

Name	Organization
Matt Richards	General Atomics
Richard Meyer	General Atomics
Brian Thurgood	BVPA Engineering
Yuko Kitajima	Toshiba Corporation
Ryoma Kato	Toshiba Corporation
Takanari Inatomi	Toshiba Corporation
Shigeki Maruyama	Toshiba Corporation
Dong-Ok Kim	KAERI
Min-Hwan Kim	KAERI
Won-Jae Lee	KAERI
John Garibaldi	URS Washington Division
Bill McTigue	URS Washington Division
Masaaki Nakano	Fuji Electric Systems
Nobumasa Tsuji	Fuji Electric Systems

LIST OF EFFECTIVE PAGES

Page Number	Page Count	Revision
Cover page	1	0
ii through xi	10	0
1 through 43	43	0
Appendix A	32	0
Appendix B	3	0
Appendix C	18	0
Appendix D	23	0
Back page	1	0
Total Pages	131	

EXECUTIVE SUMMARY

For the Next Generation Nuclear Plant (NGNP), two of the key long-lead items are the Reactor Pressure Vessel (RPV) and the vessel(s) for the Intermediate Heat Exchanger (IHX). This conceptual design study focuses on evaluating design options for these two vessels, taking into account the anticipated operating conditions for NGNP, the available materials and their associated metallurgical and physical properties, and acquisition, fabricability, and reliability factors that could impact NGNP startup by 2018.

For the RPV, both SA-508/533 steel [used for current generation Light Water Reactor (LWR) RPVs] and higher alloy steels with higher temperature capability [e.g., 9Cr-1Mo-V (Grade 91) steel] are being considered. Because of the relatively tight NGNP schedule (2018 – 2021 startup) and very limited experience base with the higher alloy steels for nuclear applications, SA-508/533 steel is emerging as a desirable material for the RPV in order to minimize schedule risks. Potential RPV and RPV component manufacturers have expressed concerns about manufacturing thick sections using higher alloy steels, and have indicated that supplying an RPV made from a higher alloy steel to support a 2018 – 2021 NGNP startup is highly unlikely.

In the absence of active vessel cooling, the RPV temperature during normal operation is determined by the design point selected for the primary coolant inlet temperature and the design of the reactor internal components, including the physical location of riser channels that route the coolant flow to the plenum above the reactor core. Assuming SA-508/533 steel is used as the Material of Construction (MOC) for the RPV, operation with a coolant inlet temperature above about 490°C will require use of an active Vessel Cooling System (VCS) to ensure compliance with ASME code limits. Thermal analyses performed by the Korea Atomic Energy Research Institute (KAERI) and Fuji Electric Systems (FES) indicate a VCS should not be required if it is possible to operate the NGNP with a coolant inlet temperature of 490°C and with inlet flow routed through risers in the Permanent Side Reflector (PSR) (which provides additional thermal resistance between the inlet flow and RPV). Design measures to optimize power and coolant flow distributions should result in acceptable fuel temperatures during normal operation with coolant inlet/outlet temperatures of 490°C/950°C. Some of these design measures (e.g., restraint mechanisms and sealing keys to reduce bypass flow) will require additional design work and technology development to demonstrate their feasibility and effectiveness. This design strategy would also require the reactor internal design to essentially preclude leakage flow from the PSR risers to the annular space between the core barrel and RPV.

For NGNP startup in the 2018 to 2021 time frame, SA-508/533 steel should be selected as the MOC for the RPV. With this choice, the NGNP design must ensure the RPV temperatures remain within ASME code limits, and should proceed along two parallel paths: (1) Operation

with a coolant inlet temperature of up to 490°C and design optimization to ensure acceptable fuel temperatures and prevention of leakage flow to the RPV; and (2) Operation with a more flexible inlet temperature in the range 490°C to 590°C with an active VCS. For a 2018 – 2021 startup, probably the only feasible backup material for SA-508/533 is 2.25Cr-1Mo (Grade 22) steel, especially if the configuration/application selected for NGNP is amenable for operation with a lower primary system pressure (e.g., 5 MPa instead of 7 MPa) that would permit somewhat thinner wall sections. This material has been manufactured in relatively thick sections, but for mostly non-nuclear applications. Although Grade 91 steel has been used for a variety of high-temperature applications, the manufacturing experience with this material has been fairly negative, especially for manufacturing the thick sections required for an RPV. Potential issues with this material include the following:

- All completed welds have to be normalized and tempered to obtain the tempered martensitic structure.
- Local normalizing and tempering of welds will likely result in microstructural problems at the temperature transition areas and could lead to Type IV cracking.
- The cooling rates from the normalizing temperature required to produce a martensitic structure will be difficult to achieve throughout the thickness.
- Heat treatment tempering ranges are extremely critical in order to obtain the correct tempered martensitic condition, requiring the furnace temperature to be controlled to within ±5°C.

The first design path described above entails the risks associated with successful demonstration of the technology required to optimize the reactor internals design. The second design path may raise issues about demonstration of a fully passively-safe design. In principle, an active VCS should not impact the case for passive safety, since a SA-508 RPV could operate for extended periods with the VCS offline without exceeding damage limits. However, the VCS should be considered an investment protection system and should be designed with a high degree of reliability. For NGNP, the reactor internals should be designed for not requiring a VCS, but a VCS should be incorporated into the design to mitigate the relatively high design and licensing risks associated with a prototype reactor operating at temperatures well in excess of those for current generation LWRs. During NGNP operation, RPV temperatures can be measured with the VCS online and offline to confirm whether or not a VCS is actually required.

In addition to the parallel design paths described above, a parallel technology-development effort should also be performed to develop an RPV material with higher temperature capability, which could be beneficial for future Very High Temperature Reactor (VHTR) commercial plants. Candidate materials include Grades 91, 92, 22V, and 23 steels.

Toshiba Corporation has recommended SA-508/533 steel as the material of construction for IHX vessels and has included Kaowool insulation as part of the design to protect the vessels from creep damage. Use of SA-508/533 steel for the RPV, cross vessel(s), and IHX vessel(s) would eliminate any potential concerns associated with bimetallic welds in the primary coolant pressure boundary.

TABLE OF CONTENTS

LIST OF FIGURES

LIST OF TABLES

ACRONYMS AND ABBREVIATIONS

ANL	Argonne National Laboratory
ASME	American Society of Mechanical Engineers
ASTM	American Society of Testing and Materials
B&PV	Boiler and Pressure Vessel
BEA	Battelle Energy Alliance
CMTR	Certified Material Test Reports
CSEF	Creep Strength Enhanced Ferritic
DOE	U.S. Department of Energy
EPRI	Electric Power Research Institute
FBR	Fast Breeder Reactor
FES	Fuji Electric Systems
GA	General Atomics
GT-MHR	Gas Turbine Modular Helium Reactor
HAZ	Heat Affected Zones
HPCC	High Pressure Conduction Cooldown
HTGR	High-Temperature, Gas-Cooled Reactor
IHX	Intermediate Heat Exchanger
INL	Idaho National Laboratory
JSW	Japan Steel Works
KAERI	Korea Atomic Energy Research Institute
LMTD	Log Mean Temperature Difference
LOCA	Loss of Coolant Accident
LOFA	Loss of Flow Accident
LPCC	Low Pressure Conduction Cooldown
LWR	Light Water Reactor
MHR	Modular Helium Reactor
MOC	Material(s) of Construction
MWt	Megawatt thermal
NGNP	Next Generation Nuclear Plant
NDE	Nondestructive Examination
NRC	Nuclear Regulator Commission
PFHT	Post-Forming Heat Treatment
PSR	Permanent Side Reflector
PWHT	Post-Weld Heat Treatment
QC	Quality Control
R&D	Research and Development
RCCS	Reactor Cavity Cooling System

RPV	Reactor Pressure Vessel
SSCs	Structures, Systems, and Components
URS-WD	URS – Washington Division
VCS	Vessel Cooling System
VHTR	Very High Temperature Reactor

1. INTRODUCTION AND BACKGROUND

For NGNP, two of the key long-lead items are the Reactor Pressure Vessel (RPV) and the vessel(s) for the Intermediate Heat Exchanger (IHX). This study focuses on evaluating design options for these two vessels, taking into account the anticipated operating conditions for NGNP, the available materials and their associated metallurgical and physical properties, and acquisition, fabricability, and reliability factors that could impact NGNP startup by 2018.

This report includes the following:

- A review of previous material evaluations performed by Argonne National Laboratory (ANL) [Natesan 2006a, 2006b], INL [INL 2007], and others.
- Detailed thermal and structural analyses performed by KAERI of prismatic-block Modular Helium Reactor with RPVs manufactured from both industry-proven SA-508/533 steel and more developmental 9Cr-1Mo-V steel, in order to assess requirements for an active VCS and to estimate structural design margins.
- Parametric, accident-condition analyses performed by FES to estimate the sensitivity of peak fuel and RPV temperatures to key design parameters, in order to better establish priorities for technology development.
- An assessment performed by URS-WD and GA of 9Cr-1Mo-V and other high-alloy steels for potential use as the RPV MOC, and recommendations provided by Toshiba Corporation for the IHX MOC based on their IHX designs for various NGNP configurations that are currently under consideration.
- Information provided by JSW on their current and future capabilities for manufacturing large forgings from SA-508/533 steel and high-alloy steels.
- Information provided by a Korean supplier on their RPV fabrication capabilities and issues associated with transportation and on-site assembly of an RPV.

The current workscope for this phase of Conceptual Design Studies also includes preparation of a white paper [Richards 2008] on characterizing the effect of NGNP operating conditions on the uncertainty of meeting project cost and schedule objectives. This white paper is a separate deliverable and includes discussions on how NGNP operating conditions and schedule could impact the RPV and IHX designs.

2. RPV AND IHX PRESSURE VESSEL MATERIAL EVALUATIONS

GA staff and consultant Brian Thurgood reviewed the candidate materials for the RPV and IHX Pressure Vessel.[1] URS-WD staff independently evaluated candidate materials for the RPV. GA also reviewed the published data from ANL [Natesan 2006a, 2006b], INL [INL 2007] and others. As a current member of various ASME B&PV Code Committees, Mr. Thurgood has access to all ASME Code data and was a part of the original subgroup that prepared the NH Subsection for ASME Section III Class 1 Components in Elevated Temperature Service. The following sections comprise material evaluations performed by Mr. Thurgood, GA staff, and the staff of URS-WD.

2.1. RPV Materials

This section addresses the acceptability of MOC for the NGNP RPV under current ASME Code definitions, allowable properties, and design stresses. Applicable, relevant regulatory and industry guidelines concerning potentially suitable candidate MOC were reviewed to meet the RPV operating conditions of this VHTR for the NGNP.

The various candidate MOC for evaluation included the LWR steels (ASME SA-508/SA-533), 2.25Cr-1Mo, 2.25Cr-1Mo-V, 9Cr-1Mo-V, and other potential MOC candidates as identified by GA and URS-WD. An assessment was made of the time and effort required to extend or develop new ASME Code cases as necessary for candidate MOC not qualified for use under the current ASME Code Section III, Division 1, Subsection NH for Class 1 Components in Elevated Temperature Service [649°C (1200°F)] for the NGNP.

2.1.1. Alternative RPV MOC Candidates

RPV Design Conditions and Requirements for MOC

The VHTR, with helium as the coolant and graphite as the moderator, has been selected by the U.S. Dept. of Energy (DOE) for the NGNP to demonstrate emissions-free, nuclear powered electricity and hydrogen production. The NGNP reference concepts are helium-cooled, graphite-moderated, thermal neutron spectrum reactors with a design goal reactor outlet temperature of 850°C - 950°C. The GA design for the NGNP [GA 2007] is based upon the gas turbine-modular helium reactor (GT-MHR) employing a prismatic graphite block core. This GA NGNP preconceptual design for electrical power production includes the following design parameters:

Core Thermal Power	600 MWt

[1] This report only covers materials for the RPV and IHX pressure vessel. High temperature materials for the IHX itself are covered in the IHX and Secondary Heat Transport Loop Alternatives Study Report [GA 2008].

Core Inlet Temperature	590°C
Core Outlet Temperature	950°C
System Pressure	7 MPa
He Coolant Flow Rate	321 kg/s
NGNP Design Life	60 years

The candidate MOC being considered for the primary coolant pressure boundary system must meet the required design criteria for this NGNP RPV based upon current ASME Code and Nuclear Regulatory Commission (NRC) regulations for LWR licensing per 10CFR50.55a. ASME B&PV Code Section III, Division 1, Subsection NB covers Class 1 Components up to 371°C (700°F). If the NGNP design requires the RPV to operate at temperatures above this limit, the candidate MOC should meet the rules and requirements of the ASME B&PV Code Section III, Division 1, Subsection NH, Class 1 Components in Elevated Temperature Service [up to 649°C (1200°F)].

The main baseline properties of MOC candidates include tensile strength, yield strength, elongation, reduction in area, creep-rupture strength, low-cycle fatigue, creep-fatigue, and fracture toughness (impact strength). Other key MOC characteristics include availability, fabricability, weldability, and good high temperature corrosion resistance within a helium environment containing low levels of chemical impurities. The RPV MOC must also possess high strength and stress intensities (allowable stresses) at elevated temperatures for extended operation under neutron irradiation

From a corrosion/erosion standpoint, the following factors and effects on the MOC must be addressed:

1. Effect of He coolant chemistry on MOC degradation (i.e., contaminants/impurities in He gas).
2. Corrosion effects on mechanical properties of candidate MOC.
3. Corrosion/erosion due to particulate-laden He gas flow velocities.

From a welding and heat treatment standpoint, the following factors should be adequately addressed:

1. Effect of welding processes and heat input on mechanical properties and microstructures.
2. Effect of post welding heat treatment (PWHT) on high temperature creep strength. PWHT needs to be optimized to maintain high temperature creep properties.
3. More data are needed on the mechanical properties of thick sections (> 6 inches).

4. Post-forming heat treatment (PFHT). The higher the amount of cold work performed, the lower the high temperature creep strength without a PFHT.

The LWR low-alloy steels Fe-0.75Ni-0.5Mo-Cr-V (UNS K12042), in accordance with ASME material specifications SA-508 and SA-533, are approved in the ASME B&PV Code Sect. III, Subsection NB, for Class 1 components only up to 371°C (700°F) for normal operation, well below the expected NGNP inlet core coolant temperatures in the range 490°C to 590°C. For accident conditions Code case N 499-2 allows limited excursions in the temperature range of 371°C -427°C for a cumulative time of 3000 hours and in the range of 427°C-583°C for 1000 hours. SA-508/SA-533 steels can be viable candidate materials for the RPV if routing the inlet coolant through the PSR or use of a VCS (if needed) result in limiting the normal vessel temperature to less than 371°C. [Natesan 2006a] notes that there is adequate data for the mechanical properties of SA-508 steel but not in a helium environment. More data is needed on thermal aging and the corrosion effects of impure helium. This low-alloy steel has only a small amount of chromium, and therefore will not form a protective surface oxide film to protect against carburization or decarburization. Since vessels of low-alloy steel have been used for light-water reactors, there is adequate experience in fabricating welded pressure vessels from ring forgings and thick plate. Although the NGNP RPV will be larger in diameter than most LWR vessels, the wall thicknesses required are comparable.

MOC Candidates for RPV Temperatures Above 371°C

[Natesan 2006a] presents some data for low alloy steels above 371°C, but there is a low probability that these materials would be approved by the ASME for normal temperatures above this level because of creep damage concerns. For normal vessel temperatures above 371°C, there are ferritic-alloy steels that appear to be potentially suitable as RPV forging and plate candidates for further consideration and investigation. Figure 2-1 presents allowable stresses vs. temperature for the four key ferritic steel grades: 22, 23, 91, and 92.

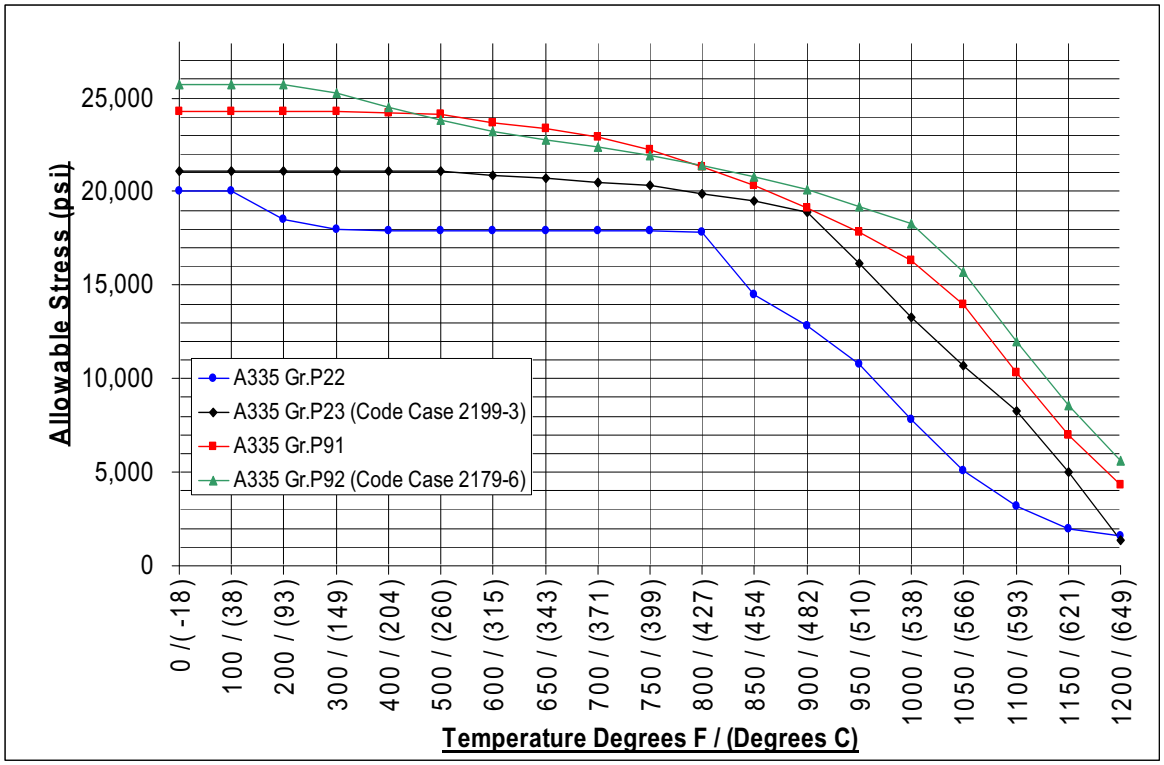

Figure 2-1. Allowable Stresses vs. Temperature of Various RPV MOC Candidates

Grade 22(Fe-2.25Cr-1Mo), UNS K21590, ASME SA-182 and SA-336, F22. The well-established Grade 22, used in both fossil and nuclear power plants, is approved in the ASME B&PV Code, Section III for use up to 593°C (1100°F). However, its lower, allowable stress values at NGNP RPV temperatures (490°C) would require greater RPV wall thicknesses to meet the above design conditions. This material may be suitable if RPV normal temperatures can be reduced to the range of 371°C - 427°C (700°F - 800°F). In this range the RPV wall thickness would probably be less than 10 inches at a system pressure of about 7 MPa. If the NGNP system pressure could be reduced to about 5 MPa, the RPV wall thickness would probably be in the range 7 to 10 inches. Thus, while applicable, this proven low-alloy steel is not considered to be an optimum RPV candidate due to excessive wall thickness and attendant loads. However, as described below, a vanadium (V) modified version of this steel has significantly higher stress intensities at elevated temperatures than Grade F22.

Grade 22V (Fe-2.25Cr-1Mo-0.25V), UNS K31835, ASME SA-182, SA-336, SA-541, F22V. Grade 22V is approved for use under the ASME B&PV Code, Section VIII but not under Section III. While there are adequate tensile strength data at 500°C, it is only approved up to 482°C (900°F). Limited high temperature creep and thermal aging data are available. There is thick section fabrication and welding experience derived from the oil and gas industry. As with other

MOC, more data are needed on compatibility with impure He gas. This steel has good hot-strength properties but requires an ASME code case for Sect. III, Div. 1, Class 1 applications up to at least 490°C (914°F), preferably per Subsection NH, which entails additional property testing and a series of quarterly ASME Code committee meetings to prepare and approve a code case.

Grade 91[2] *(Fe-9Cr-1Mo-V), UNS K90901, ASME SA-182, Grade F91 (forgings); ASME SA-387, Grade 91(plates)*. Grade 91 (modified 9Cr-1Mo) ferritic alloy (ferritic/martensitic) steel has the best mechanical properties and is the most industrially-mature of the high strength steels. Its superior hot-strength properties result from the addition of alloying elements such as V, Cb and N and optimum heat treatment. Grade 91 is designated as a creep strength enhanced ferritic (CSEF) steel. It is widely used in cogeneration power plants and supercritical fossil fuel power units up to the maximum temperatures and pressures. Grade 91 is approved for up to 649°C (1200°F) in ASME Section III, Division 1, Subsection NH, Class 1 component applications. This alloy is much more resistant to thermal fatigue than austenitic stainless steels because of its lower thermal expansion coefficient and higher thermal conductivity. Grade F91 provides excellent mechanical properties at elevated temperatures when produced and heat-treated to form the optimum tempered martensitic microstructure.

Proper PWHT and welding practices are essential for the successful use of Grade 91 steel as a durable RPV MOC. There are adequate data on long-term thermal aging with conservative creep-fatigue limits. As with all other potential MOC, additional data on hot He compatibility must be obtained. Also, more data are needed on the Grade 91 properties in the thick sections required for the RPV. Grade 91 is thus considered the best available high-strength ferritic-alloy steel regarding high temperature properties provided it is heat-treated and welded properly. Sound welding and PWHT are crucial to the successful use of P91 steel. Hardness testing is one QC/NDE method of measuring and monitoring the proper hardness of the base metal, weld metal and weld heat-affected zones (HAZ) of F91 forgings and plate to assure proper PWHT of this alloy. The Electric Power Research Institute (EPRI) has established hardness testing and other inspection programs to assess and confirm the P91 properties. Certified Material Test Reports (CMTR) of Grade 91 and all RPV grades are essential to confirm the chemical and mechanical properties including hardness at both the mill and in the field.

Although Grade 91 steel has been used for a variety of high-temperature applications, the manufacturing experience with this material has been fairly negative, especially for manufacturing the thick sections required for an RPV. Potential issues with this material include the following:

[2] Grade 91 is referred to as P91 in rolled-plate form and F91 for ringed forgings.

- All completed welds have to be normalized and tempered to obtain the tempered martensitic structure.
- Local normalizing and tempering of welds will likely result in microstructural problems at the temperature transition areas and could lead to Type IV cracking.
- The cooling rates from the normalizing temperature required to produce a martensitic structure will be difficult to achieve throughout the thickness.
- Heat treatment tempering ranges are extremely critical in order to obtain the correct tempered martensitic condition, requiring the furnace temperature to be controlled to within ±5°C.

Table 2-1 provides the comparison of allowable stresses for 2.25Cr-1Mo and 9Cr-1Mo-V steels taken from the ASME B&PV Code Section III Division 1—Subsection NH Class 1 Components in Elevated Temperature Service and, in certain cases where directed by the NH subsection, they were taken from ASME Section II Part D. These cases are noted. Also included are the proposed weld reduction factors which are applicable to pipe fusion welded long seams only, but which probably will eventually be applied to all long seams, including those in vessels. Table 2-2 shows a comparison of allowable stresses for three materials (2¼Cr/1Mo, 2¼Cr/1Mo/V and 9Cr/1Mo/V) at the maximum allowable temperatures in Section VIII Div 1 for 2¼Cr/1Mo/V at 482°C (900°F).

As discussed below, some other candidate MOC for the RPV also offer superior high temperature properties.

Grade 23 (2.25Cr-1.6W-V-Cb), UNS K41650, ASME SA-182 (Forgings) and SA-387 (Plate). Grade 23 ferritic-alloy steel is another modification of Grade 22 in which W, V, and Cb are used as alloying elements to obtain superior elevated temperature properties. Its high-temperature tensile strength and allowable stresses are significantly better than Grade 22 up to 649°C (1200°F). In fact, the stress intensities of Grade 23 are only slightly less than Grade 91 up to 649°C and are essentially equal to Grade 91 in the 482°C - 510°C (900°F – 950°F) temperature range, covering the 490°C (914°F) inlet He gas coolant temperature. An ASME Code Case 2199-3 on Grade 23 was approved on 04/18/06 allowing the use of Grade 23 for Section I construction, which lists its allowable stresses up to 649°C (1200°F) as forgings (SA-182), plate (SA-387), pipe (SA-335), and tube (SA-213). The next step would be a Code case for use in Section III, Class 1 components, Subsection NH. Grade 23 has the necessary hot strength if heat-treated properly as specified by this code case. It appears to be the economically best option in the 490°C - 580°C (914°F - 1076°F) core inlet temperature range. Grade 23 would permit thinner wall components than Grade 22 and is more fabrication-friendly than Grade 91. However, tight controls of fabrication are required to prevent possible reheat cracking

Table 2-1. Allowable Stress Intensities and Strength Reduction Factors (Section III Materials)

Stresses	2 ¼ Cr/1Mo		9Cr/1Mo/V	
	405°C (923°F)	565°C (1049°F)	405°C (923°F)	565°C (1049°F)
Tensile Stress Reduction Factor (Section III)[1]	0.84	0.71	0.98	0.89
Yield Stress Reduction Factor (Section III)[1]	0.89	0.72	1.0	1.0
Tensile Strength Values S_u	57.8 ksi[2]	49.2 ksi	64.5 ksi[2]	51.4 ksi
Allowable Stress Intensity S_m	10.1 ksi	4.7 ksi	20.5 ksi	11.5 ksi
Allowable Stress Intensity S_t	10.1 ksi	4.7 ksi	21.1 ksi	11.5 ksi
Yield Strength Values S_{y1}	31.8 ksi[3]	22.4 ksi	44.7 ksi[3]	36.6 ksi
Maximum Allowable Stress Intensity S_o	12.2 ksi	5.7 ksi	17.0 ksi	12.9 ksi
Proposed Weld Strength Reduction Factors[4]	0.88	0.77	1.0	0.91

1. Specified by the ASME in Section III Div.1, Subsection NH, Tables 3225-1 through 3225-4. The factors apply when the materials are to be used for extended periods at elevated temperatures.
2. ASME Section II Part D Table U
3. ASME Section II Part D Table Y-1
4. Currently proposed for long seam fusion welds in pipe

Grade 24 (2.25Cr-1Mo-0.25V-Ti-B), ASME SA-182 (Forgings). Grade 24 ferritic-alloy steel is economically comparable to Grade 23 and, unlike Grade 23, is not susceptible to reheat cracking. It is also expected to be more fabrication-friendly than Grade 23. However, Grade 24 is not yet approved for use by ASME Code Section I, much less Section III. It has very good high temperature properties but lacks the necessary ASME Code approvals.

Table 2-2. Allowable Stress Intensities (Section VIII Criteria)

Product Specification	482°C (900°F)		
	2 ¼ Cr/1Mo	2 ¼ Cr/1Mo/V	9 Cr/1Mo/V
SA 182 Forgings	15.8 ksi	20.3 ksi	19.1 ksi
SA 336 Forgings	15.8 ksi	20.3 ksi	19.1 ksi
SA 387 Plate Class 1	13.6 ksi	----	----
SA 387 Plate Class 2	15.8 ksi	----	----
SA 542 Plate Grade B Class 4	20.4 ksi*	----	----
SA 542 Plate Grade D Class4	----	20.3 ksi	----
SA 832 Plate Grade 22V	----	20.3 ksi	----
SA 387 Plate Grade 91	----	----	19.1 ksi

*454°C (850°F) maximum

Grade 92 (9Cr-2W), ASME SA-182 (Forgings, seamless). Grade 92 has among the best elevated temperature tensile properties of any of the above ferritic-alloy steels at both 490°C (914°F) core inlet temperature and at 649°C (1200°F). For example, its approximate stress intensities are: 482°C (900°F): 20 ksi; 510°C (950°F): 19 ksi; 593°C (1100°F): 12 ksi; and 649°C (1200°F): 5.6 ksi. These are outstanding allowable design stresses over the entire temperature range from ambient (almost 26 ksi) to 649°C (1200°F). It would enable the RPV designer to use lighter wall forgings and components than with most of the other ferritic steel grades. ASME Code Case 2179-6 was approved on 08/04/06 for the use of seamless Grade 92 tubes, pipes, and forgings in both Sections I and VIII, Division 1 construction. As with all of the other ferritic-alloy steels, proper heat treatment and welding are critical for its successful applications. Again, Grade 92 needs ASME Section III, Division 1, Subsection NH approval, but it has some of the best high-temperature properties available as an RPV MOC for the NGNP. The potential issues discussed above for Grade 91 steel would also likely be applicable to Grade 92 steel.

Other Ferritic Alloy Steels. Other potential ferritic alloy steels that are being researched and tested for elevated temperature power plant service conditions include Grade E911 (9Cr-1Mo-0.2V-Cb-N). Grades such as E911 have shown significantly improved high temperature strength versus Grade 91, but need ASME code cases for Section III, Class 1, Subsection NH

to justify serious consideration as a viable RPV pressure boundary MOC. Grade E911 is covered in ASME SA-182 specification for forged alloy (and SS) piping components for use in pressurized systems.

2.1.2. ASME Code Case Considerations for RPV MOC Candidates

Grade 91 steel is currently the leading candidate for RPV MOC for use above 371°C because it is approved for ASME Code Section III, Division 1, Subsection NH for Class 1 Components in Elevated Temperature Service (to 649°C) and has excellent high-temperature properties and extensive power plant service duty. Grade 91 was approved for Subsection NH in both the 2004 and 2007 ASME Codes. The other alloys with superior elevated temperature properties are Grades 22V, 23 and 92, both comparable in hot strength to Grade 91. Their ASME Code status is as follows: (1) Grade 23 was approved for Code Section I construction by Code Case 2199-3 with allowable stresses up to 649°C and offers good MOC economics with its lower-alloy content; and (2) Grade 92 was approved for both Code Section I and VIII Div. 1 construction by Code Case 2179-6 with superior high temperature strength properties. Grades 23 and 92 appear to warrant the development of code cases for Sect. III, Div. 1, Subsection NH use to provide alternate RPV MOC to Grade 91. If code cases for Grades 22V, 23 and 92 in forgings and plate for Subsection NH use were actively pursued, it should be possible to prepare and issue such code cases within about one year, which includes four Code committee meetings. Without an active sponsor to champion these code cases, the approval process would probably take approximately two years. Additional high-temperature property testing must also be conducted on these two grades to qualify them for Sect. III, Subsection NH use. Thus, Grade 91 needs the least additional testing and code work to certify its use as an RPV MOC. Grades 23 and 92 merit the necessary code case time and efforts for Sect. III, Div. 1, Sub. NH usage.

If a new alloy chemistry is proposed as a MOC that cannot be included into an existing ASME Section II approved grade or as a modification of an existing grade, then the time frame for approval would be at least another year beyond the time required for ASME Code approval (i.e., two+ years). ASME requires the proposed MOC already be accepted by a major materials society such as ASTM before being considered for inclusion as an approved ASME material. Table 2-3 below summarizes the comparison of major RPV MOC Candidates.

The data that is currently available on the alloys listed below are contained in the following code cases:

Grade 92 – Code Case 2179-6
Grade 91 – Code Case 2192-5
Grade 23 – Code Case 2199-3

All of the above code cases, however, do not include a request for inclusion in the ASME B&PV Code, Section III, Division 1, Subsection NH. Grade 91 has been approved for plate, piping, and tubing in Section III, Subsection NH since the 2004 edition of the ASME Code. The above

Table 2-3. Comparison of Major RPV MOC Candidates (Ferritic Steels)

RPV MOC UNS No.	ASME CODE STATUS	RPV MOC RECOMMENDATION
ASME SA-508/533 UNS K12042 (Fe-0.75Ni-0.5Mo-Cr-V)	Sect. III, Div. 1, Sub. NB for use up to 371°C.	Preferred but applicable only if RPV temperatures do not exceed 371°C
Grade 22 UNS K21590 (2.25Cr-1Mo)	Sect. III, Div. 1, Sub. NH for use up to 593°C.	Applicable to inlet (490°C-590°C) temp (only limited by lower allowable stress)
Grade 22V UNS K31835 (2.25Cr-1Mo-0.25V)	Sect. VIII up to 482°C	Needs code case for Sect. III/1/NH.
Grade 23 UNS K41650 (2.25Cr-1.6W-Cb)	Code Case 2199-3 allows use in Sect I construction.	Has high allowable stresses to 649°C. Needs code case for Sect. III/1/NH.
Grade 91 UNS K90901 (9Cr-1Mo-V)	Sect. III, Div. 1, Sub. NH up to 649°C.	Most industry mature & widely used MOC. Best current RPV candidate.
Grade 92 UNS K92460 (9Cr-2W)	Code Case 2179-6, allows use in both Sect. I & VIII.	Highest allowable stresses to 649°C. Needs code case for Sect. III/1/NH.

Grade 91 Code Case deals with requesting permission to use a modified chemistry for use in castings. Table 2-4 presents a more detailed summary of the advantages and disadvantages of the RPV MOC candidates including an indication of the effort needed to gain acceptance by the ASME B&PV Code, Section III, Subsection NH.

Data for ASME Code Case Submission

It is the policy of the ASME Boiler and Pressure Vessel Committee to adopt for inclusion in Section II (Material Specifications) only base metal specifications that have been adopted by the American Society for Testing and Materials (ASTM) or other recognized national or international organization. All materials discussed in this report, and included in Table 2-4, except the new material, are already recognized by ASME and ASTM. Typically, the material data contained in code cases include chemistry ranges, mechanical properties, and maximum allowable stress values. This data is a prerequisite to any code case submission. More detailed information regarding the data that is needed to develop a code case for new material, or to expand the code coverage of an existing material, is contained below and will pertain to the materials discussed in this report. The information below is not intended to specify every detailed

requirement needed to be included in a code case. Different requirements are expected to be included in a code case submission depending on its intended application and purpose in service. The information below concentrates on the expected requirements for a high temperature creep strength material that will require welding as part of the fabrication process.

Table 2-4. NGNP RPV Materials of Construction Summary

Material	Chemistry	Current ASME Code Status	ASME Action Needed	Advantages	Disadvantages (Note 2)	Time for ASME NH Approval
SA-508/S533	Fe-0.75Ni-0.5Mo-Cr-V	Section III, NB approved to 371°C	None	o Widely Used for LWR Vessels o ASME Section III, NB approved	o Limited to use below 371°C	Already approved for NB
Grade 91	9 Cr 1 Mo V	Section III, NH approved to 649°C	Extend NH Rules to apply to thick sections	o Excellent High temperature properties o Widely Used o ASME Section III, NH approved	o Sensitive to weld and PWHT variations o Lack of suppliers for thick-section material	1 year
Grade 92	9 Cr 2 W	Section I & VIII approved	Section III, NH approval – Code Case	o Best elevated temperature properties o Allows use of the thinnest sections	o Sensitive to weld and PWHT variations o Not ASME, NH approved	1 year
Grade 23	2.25 Cr 1.6 W Cb	Section I approved	Section III, NH approval – Code Case	o Not as sensitive to welding and PWHT variations o More economical than Gr. 91	o Susceptible to reheat cracking o Less stress intensity factors than Grade 91 o Not ASME, NH approved	1 year
Grade 24	2.25 Cr 1 Mo 2.5 V Ti, B	No Approvals	Section III, NH approval – Code Case	o Good high temperature properties o Not as susceptible to reheat cracking o Not as sensitive to weld and PWHT variations	o No ASME approvals o Need greater thicknesses to meet design conditions	1 year
Grade 22V	2.25 Cr 1 Mo 0.25 V	Section VIII approved	Section III, NH approval – Code Case	o Good high temperature properties o Widely used	o Limited high temperature property data available o Only approved to 482°C	1 year
New	TBD	No approvals	Section III, NH approval – Code Case	o Have ability to choose alloy with potentially superior high temperature properties	o Significant time to produce o Significant costs to produce o No track record of performance	2-3 years

Notes:
1. Given the temperatures in the NGNP it is assumed that all material must be ASME Section III, Subsection NH approved in order to qualify for use.
2. All above grades need data on thick section performance and compatibility with impure hot He.
3. The time for ASME approval column includes approximate time frame for inclusion into ASME Section III, Subsection NH. There is no guarantee, however, that approval will be given for use in temperatures equal to Grade 91. The only exception to this is Grade 92. It is very likely that Grade 92 would be approved to the same temperatures of Grade 91 or beyond.

Application. For new materials to be incorporated, the code case submitter needs to identify to the Committee, Sections, and/or Subsections, the temperature range of application, and whether cyclic service or external pressure is to be considered. The submitter must identify all product forms, size ranges, and specifications for which incorporation is desired.

Mechanical Properties. The code case submitter must furnish the Committee with adequate data on which to base design values for inclusion in applicable allowable stress tables. Such data includes values of ultimate tensile strength, yield strength, reduction of area, and elongation, at 100°F intervals, from room temperature to 100°F above the maximum intended use temperature. Any heat treatment that is required to produce the mechanical properties also needs to be described.

If the new or existing subject material is planned to be in service at temperatures at which time-dependent behavior could control design values, stress-rupture and creep rate data for these properties must be provided, starting at temperatures of about 50°F below the temperature where the time-dependent properties start and extending to about 100°F above the maximum temperature that the material is expected to experience in service. The longest rupture time at each test temperature must be in excess of 6000 hours and shortest time about 100 hours with at least three additional tests at equally spaced stress values in between. All of the materials discussed in this document fall into this category of needing time-dependent property analysis.

Minimum creep rate data must also be supplied over the same temperature ranges, with the lowest stress at each temperature selected to achieve a minimum creep rate of a certain percentage per hour or less.

For materials intended to be used in welded applications, sufficient time-dependent data must also be provided for weldments and filler metals to allow the ASME to assess the properties relative to the base material.

Notch toughness (impact strength) data may also be required depending on the temperatures to which the material will be exposed in service. The lower the temperature the material will experience in service, the more likely notch toughness data will be required.

Other Properties. The code case submitter must furnish data necessary to establish values for coefficient of thermal expansion, thermal conductivity and diffusivity, elastic modulus, shear modulus, and Poisson's ratio. This data must be provided over the range of temperatures for which the material is expected to experience while in service.

Weldability. The code case submitter must supply complete data on the weldability of the subject material, including data on welding procedure qualification tests made in accordance with the requirements of ASME Section IX. The welding qualification tests should be made over the full range of intended material thickness. The data should include postweld heat treatment (PWHT) requirements (if any), susceptibility to air hardening, effect of welding processes and procedures on the heat-affected zone (HAZ), weld metal notch toughness, and other mechanical properties.

Physical Changes. For new materials or materials where little data and/or service experience exist, it is important to know the degree of retention of properties with exposure to temperature. The effect of fabrication practices, such as forming, welding, and thermal treatment, on the mechanical properties, ductility, and microstructure of the material are important, particularly where degradation in properties may occur.

Requests for Additional Data. Any ASME Committee, Subcommittee, or Subgroup that the code case affects may request additional data, including data on properties, material behavior, or any other related subject (such as possible corrosion effects in a hot impure helium environment) at any time during the review and approval process particularly when considering new materials or extending coverage of existing materials.

2.1.3. Estimates of RPV Wall Thickness

The ASME B & PV Code Section III, Div 1, Subsection NB (equation NB-3324.1) gives a formula for "Tentative Pressure Thickness" of a cylindrical pressure vessel such as the NGNP RPV:

$T = PR/(S_m - 0.5P)$,
where:
P = pressure (psi)
R = inside diameter (inches)
S_m = Stress Intensity (psi from subsection NB)
T = Wall thickness (inches)

For the RPV described in the preconceptual design studies report:
P = 1000 psi
R = 142.25 inches
S_m = 20,500 psi for 9Cr-1Mo-V (from Table 2-1 above)

Therefore T = 7.1 inches and the current RPV side wall thickness of 8.5 inches should be acceptable for 9Cr-1Mo-V.[3] The ASME code states that NB-3324-1 establishes a tentative wall thickness for the conditions. A detailed stress analysis for the entire vessel would be required to demonstrate that stress intensities allowed by the ASME Code are not exceeded anywhere on the pressure boundary.

For an SA-508/SA533 vessel below 371°C, the tentative thickness per equation NB-3324.1 of the ASME code gives the following: T=(1000 psi x 142.25 in.)/(26,700 psi – 500 psi) = 5.43 in., or approximately 6 in. (152 mm) thick. The wall thickness at the supports would be about 8 in. (203 mm). The top and bottom heads could be thinner than the side wall, perhaps 4 to 5 in. (102 to 127 mm) thick.

2.1.4. Conclusions for RPV Materials Evaluation

Further optimization of the core inlet coolant flow, and/or possible direct vessel cooling to reduce the vessel wall temperature to less than 371°C, may allow the use of low-alloy steels SA-508/SA-533 for the RPV. This would result in reduced project schedule risk, reduced NRC licensing risk, and would minimize the additional material data required. However, if RPV wall temperature predictions remain above 371°C, there are a number of candidate materials that have been identified and evaluated.

A review of the literature leads to the conclusion that Grade 91 (9Cr-1Mo-V) is the leading MOC candidate for the RPV since it is ASME Code-approved for Section III, Division 1, Subsection NH service (to 649°C), well above the 490°C(or 590°C) inlet design temperature.[4] This CSEF steel has the best mechanical properties with the widest power industry use of all the ASME Code high temperature, high strength steels. Grade 91 forgings (Grade F91) appear to be ideally suited for the RPV environment and core coolant inlet temperature of 490°C (914°F). Grade 91 CSEF steel must be properly welded with proper PWHT. URS/Washington Division has Welding Engineers active on ASME Code committees who understand the criticality of welding and PWHT of Grade 91. If these operations are performed effectively, the superior high temperature properties of Grade 91 will be realized for very long-term performance, essential for a NGNP design life of 60 years.

The benefits of 9Cr-1Mo-V (Grade 91) over the other ferritic-alloy grades include superior hot-strength and oxidation resistance relative to Grade 22 with higher thermal conductivity and lower thermal expansion than the austenitic (300 Series) stainless steels. The alloying

[3] As discussed previously, the estimated RPV thickness using 2.25Cr-1Mo steel would be about 10 inches under the same operating conditions.
[4] As discussed previously, there are some potential issues associated with this material that must be resolved before any final determination can be made regarding its suitability as a MOC for the RPV.

elements (V, Cb, Nb) substantially increase the creep-rupture strengths and stress intensities compared to lower Cr-Mo steels. These enhanced properties allow the fabrication of RPV components with thinner walls, thus reducing thermal stresses and minimizing long-term thermal fatigue damage. To reiterate, the superior properties of Grade P91 steel depends of the proper additions of V, Cb, and Nb; optimum heat treatment to produce the correct microstructure; and maintenance of this microstructure during the P91 service life. Welding and PWHT are two key factors in creating this optimum microstructure, which can be indirectly measured/monitored by hardness testing per EPRI procedures, since Grade 91 hardness correlates well with its ultimate tensile strength.

Two other ferritic-alloy grades being considered are Grade P23 and Grade P92, both of which have excellent hot-strength properties. Grade P23 high temperature strength is somewhat below that for Grade P91, while Grade P92 is slightly stronger than P91. All three grades have good Code-allowable stresses up to 649°C (1200F). These latter two grades are covered by two ASME code cases. Code Case 2199-3 approved the use of Grade P23 for ASME Section I applications. Code Case 2179-6 approved the use of Grade P92 for both ASME Section I and VIII, Division 1 applications. Hence, both Grades 23 and 92 require further ASME Code cases to qualify for Section III, Class 1, Subsection NH applications. GA and URS Washington Division believe their attractive hot strength properties warrant code cases to qualify the two grades for Sect. III, Div. 1, Subsection NH use as alternatives to Grade 91. With active ASME Code committee members attending quarterly code meetings, it should be possible to issue such code cases within approximately one year. Additional testing of all three materials in hot He gas under neutron irradiation and other high temperature tests will also be necessary for Code and NRC approval in accordance with 10CFR50.55a requirements.

2.2. IHX Pressure Vessel Materials

The candidate materials discussed above for the RPV can also be used for the IHX pressure vessel. However, the IHX vessel does not have the requirement to radiate heat to the ultimate heat sink [reactor cavity cooling system (RCCS)] during accident conditions, which allows the use of insulation on the inner vessel surface to maintain vessel temperatures within ASME code limits.

Toshiba Corporation has developed IHX designs for two different configurations of the NGNP heat transport system [GA 2008]. The IHX designs include both more conventional concepts with helical coil tube bundles and compact concepts using modules based on the diffusion-bonded, printed-circuit heat exchanger technology developed by Heatric Corporation.[5] For the Toshiba designs, the IHX vessel is a pressure boundary for the primary helium coolant and will

[5] Additional information on this concept can be obtained from http://www.heatric.com/compact_heat_exchangers.html.

be designed according to the ASME Code, Section III. The material selected for the IHX vessel is SA-533/SA-508 steel, and the vessel is insulated with Kaowool to maintain operating temperatures at about 250°C during normal operation to prevent creep damage. Details regarding the IHX designs are given in [GA 2008]

3. RPV DESIGN CRITERIA BASED ON NRC REGULATORY GUIDANCE

Each of the three NGNP design configurations currently under consideration [GA 2008] were evaluated by URS-WD in the context of applicable regulatory criteria. Because Title 10 of the Code of Federal Regulations (10CFR) is the governing set of regulations for licensing domestic nuclear reactors, including Class 103 licenses and certifications for commercial reactors, URS-WD based their evaluation on a systematic review of 10CFR, and identified the criteria of interest for the design alternatives under consideration. The evaluation performed by URS-WD was compiled into a single report that included the RPV, cross vessel, IHX, secondary Heat Transport System, and the associated functions performed by these Structures, Systems, and Components (SSCs). This URS-WD report is included as a section in the IHX and Secondary Heat Transport Loop Study Report [GA 2008].

4. THERMAL/STRUCTURAL ANALYSES OF SA-508/533 RPV

Because of its extensive experience base as an ASME code-approved material for LWR RPVs, SA-508/533 steel is also being evaluated as a material for the NGNP RPV. As discussed in Section 6, this material may be the only viable option for a 2018 – 2021 NGNP startup because of the long-lead time to procure an RPV and the relatively tight schedule. As shown in Table 4-1, SA-508/533 steel was selected for an earlier, 350 MWt MHR concept with a steam cycle for power conversion. However, for the 600 MWt GT-MHR concept [Shenoy 2006], 9Cr-1Mo-V steel was selected as the RPV material to accommodate the GT-MHR's higher temperature design points for primary coolant inlet and outlet temperatures. Because the NGNP concept is expected to operate at temperature design points that are similar or higher than those for the GT-MHR, modifications to the reactor internal design are required to ensure an RPV manufactured from SA-508/533 steel operates within the ASME Section III code temperature limits given below:

Normal Operation (Service Level A):	371°C
Accident Conditions (Service Levels C and D):	538°C for up to 1000 h

Accident conditions include both loss of flow accidents (LOFAs) and loss of coolant accidents (LOCAs).[6]

For the GT-MHR, the inlet coolant flow is routed through riser channels between the core barrel and RPV (see Fig. 4-1). With this configuration, the design of the reactor vessel (especially materials selection) is driven in large measure by the coolant inlet temperature (see Table 4-1). As shown in Fig. 4-2, the MHR reactor internals can be designed to route the inlet flow through the PSR to provide additional thermal resistance between the inlet flow and reactor vessel, which may allow use of SA-508/533 steel for the RPV if the inlet temperature is not greater than about 490°C.[7] A VCS can also be incorporated into the reactor internal design to ensure the RPV operates at temperatures below the ASME code limit of 371°C. Preliminary evaluations of these design modifications were performed as part of the Pre-Conceptual Design Studies [GA 2007]. For this special study, KAERI and FES have performed additional evaluations, which include more detailed modeling of the reactor internals modifications and RCCS. The work performed by KAERI and FES is described in the following sections.

[6] For gas-cooled reactors, a LOFA is also referred to as a High Pressure Conduction Cooldown (HPCC), and a LOCA is also referred to as a Low Pressure Conduction Cooldown (LPCC).
[7] For this configuration, a pressure gradient will exist between the PSR riser channels and the reactor core. Cross flow through horizontal gaps is mitigated by incorporating sleeves in the PSR riser channels.

Table 4-1. RPV Design Parameters for 350 MWt and 600 MWt MHR Concepts

Parameter	350 MWt RPV	600 MWt RPV
Application	Electricity production, steam cycle	Electricity production, direct Brayton cycle (GT-MHR)
RPV Material	SA-508/533	9Cr-1Mo-V
Design Temperature, °C	288	495
Max. Operating Temperature, °C	210	474
Primary Coolant Inlet/Outlet Temperatures, °C	258/687	490/850
Design Pressure, MPa	7.2	8.0
Operating Pressure, MPa	6.4	7.1
RPV Outside Diameter (Shell), m	6.8	7.5
RPV Outside Diameter (Flange), m	7.4	8.2
RPV Thickness (Shell), m	0.133	0.216
RPV Total Height, m	22.0	24.0
RPV Weight, t	728	1328

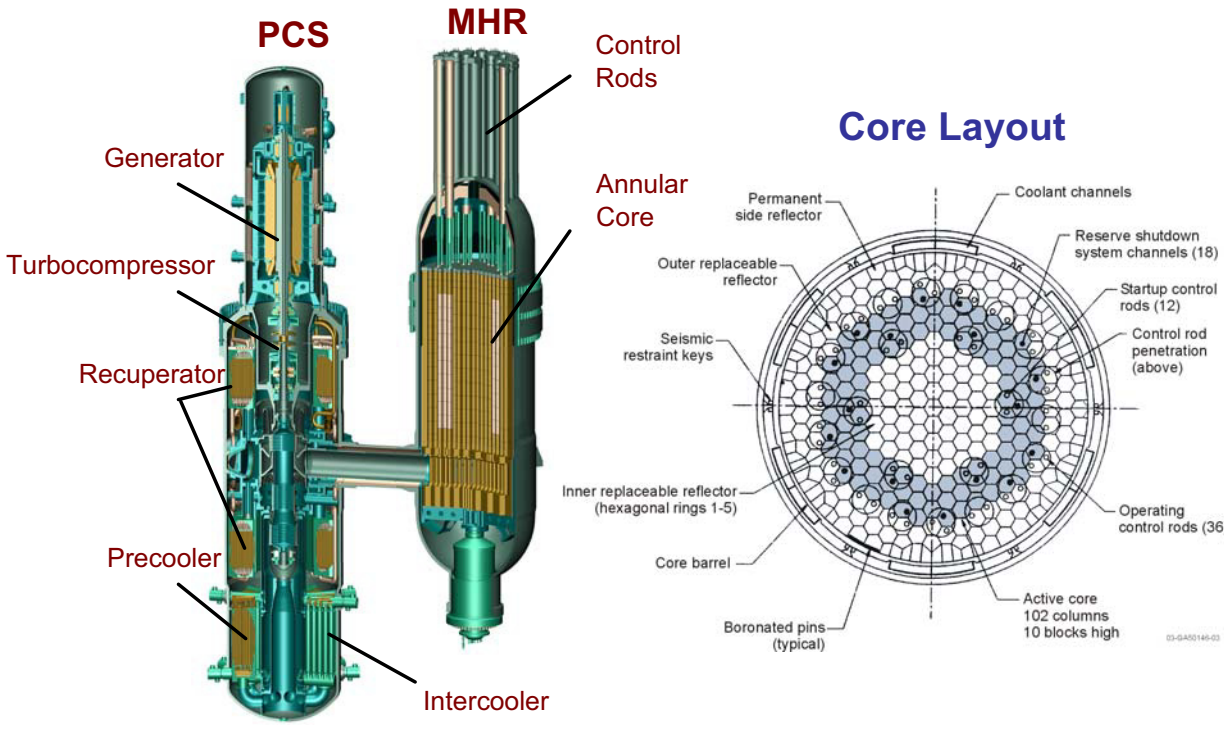

Figure 4-1. GT-MHR Concept and Core Layout

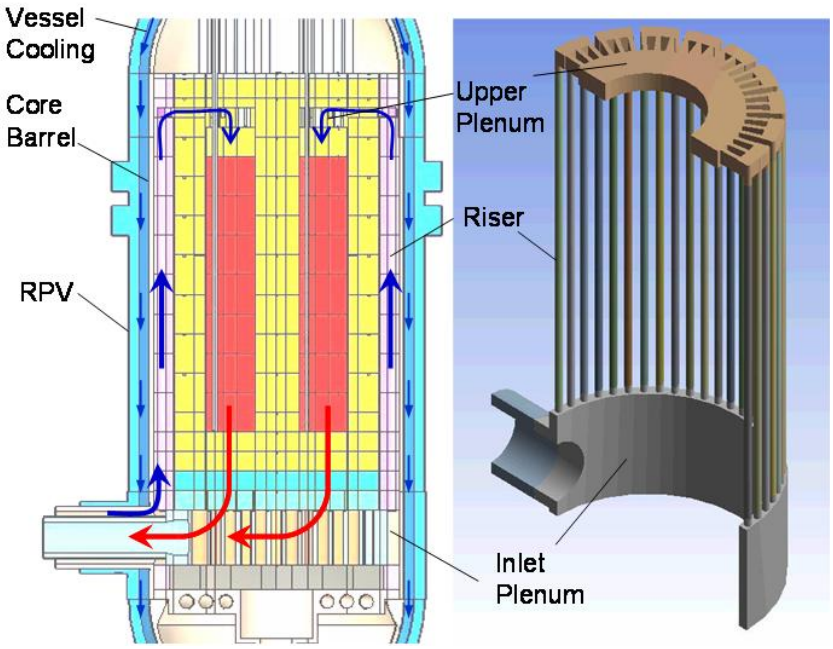

Figure 4-2. RPV and Reactor Internals Design with PSR Coolant Risers and Vessel Cooling

4.1. Evaluations Performed by the Korea Atomic Energy Research Institute

As part of this design study, KAERI prepared a report titled "A Preliminary Analysis for a Cooled SA-508/533 Reactor Pressure Vessel." This report is included as Appendix A. Key results from this report are summarized below.

Summary of Key Results

Both thermal and structural analyses were performed. Thermal analyses were performed using the GAMMA+ code (based on RELAP) and the commercial CFX code. CFX was used for detailed modeling of the region from the Permanent Side Reflector (PSR) to the RCCS.

Figure 4-3 shows the GAMMA+ model used to evaluate the cooled-vessel concept. This model includes the reactor coolant system, the reactor cavity, the RCCS, and the VCS. The solid regions include a total of 675 mesh points and are modeled in either two or three dimensions. The fluid regions include a total of 375 mesh points and are modeled using a combination of one- and two-dimensional flow networks. In particular, two-dimensional representations are used for the reactor cavity and annular space between the core barrel and RPV in order to model natural convection. Thermal radiation is modeled in the upper plenum, the annular space between the core barrel and RPV, the reactor cavity containing the RCCS panels, and the annular space between the RCCS downcomer wall and reactor cavity wall. As shown in Fig. 4-4, a detailed flow network model is used for the reactor core region, which accounts for bypass

flow through vertical gaps and cross flow through horizontal gaps. For this analysis, horizontal gaps were assumed to be 2 mm and vertical gaps were assumed to be 1.5 mm.

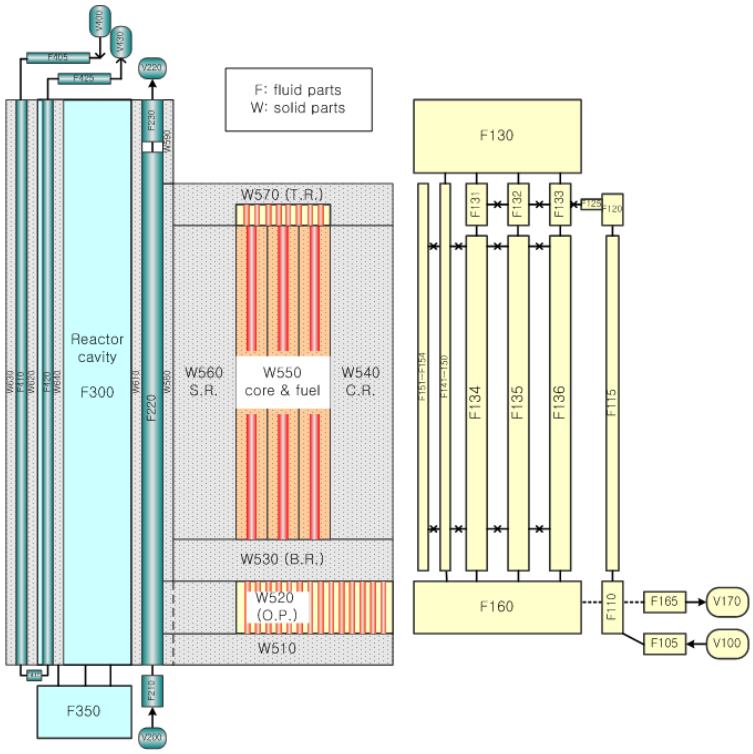

Component	Description	Meshes
F105,F165	Coaxial pipe	1,2
F110	Inlet bottom plenum	1
F115	Inlet riser holes	12
F120, F125	Inlet top plenum	1,2
F135	Top head	1
F131~3	Core top void	2
F134	Inner coolant channel	12
F135	Middle coolant channel	12
F136	Outer coolant channel	12
F141~150	FA bypass channel	14
F151,154	CR bypass channel	14
F152,153	RSC bypass channel	12
F160	Outlet plenum	4
F210,230	VCS inlet & outlet	1,1
F220	Vessel cooling channel	3x11
F300	Reactor cavity (RCCS)	3x20
F350	Reactor cavity (remain)	1
F405	RCCS inlet header	1
F410	RCCS downcomer	12
F415	RCCS lower plenum	1
F420	RCCS tube riser	12
F425	RCCS outlet header	1
W510	Bottom support	14x3
W520	Outlet plenum	14x2
W530	Bottom reflector	11x2
W540	Central reflector	5x10
W550	Fuel & core reflector	3x10
W560	Side reflector	3x10
W570	Top reflector	11x2
W580	Core barrel	3x14
W590	Upper shroud	3x3
W610	Reactor pressure vessel	5x20
W620	RCCS downcomer wall	3x20
W630	Reactor cavity wall	4x20
W640	RCCS panel	2x20x4

Figure 4-3. GAMMA+ Model for Evaluation of Cooled-Vessel Concept

As shown in Fig. 4-5, the CFX code was used to model a 1/54 sector corresponding to the region associated with a single PSR riser channel, extending in the radial direction from the PSR to the RCCS downcomer wall. The height of the computational domain is approximately 20 m.

As shown in Fig. 4-6, the KAERI configuration includes an upper plenum in the top reflector region.[8] More detailed design work needs to be performed for this configuration, including design of support posts and flow-distribution blocks in the upper plenum. Additional work also needs to be performed to assess potential bypass flow paths. As shown in Fig. 4-7, KAERI has developed two concepts for the flow distribution block. Both concepts provide a center well to

[8] The GT-MHR concept [Shenoy 1996] uses a metallic shroud and metallic upper core restraint (both made of Alloy 800H) to define the upper plenum. The flow passes through coolant holes in the upper core restraint and top reflector to the fuel blocks. A potential advantage of the KAERI concept is thermal protection of the upper plenum structure during core heatup accidents.

seat the support post and six large holes to collect the coolant flow. The first option uses small holes to distribute the flow to the fuel block, whereas the second option provides a cavity region at the inlet to the fuel block.

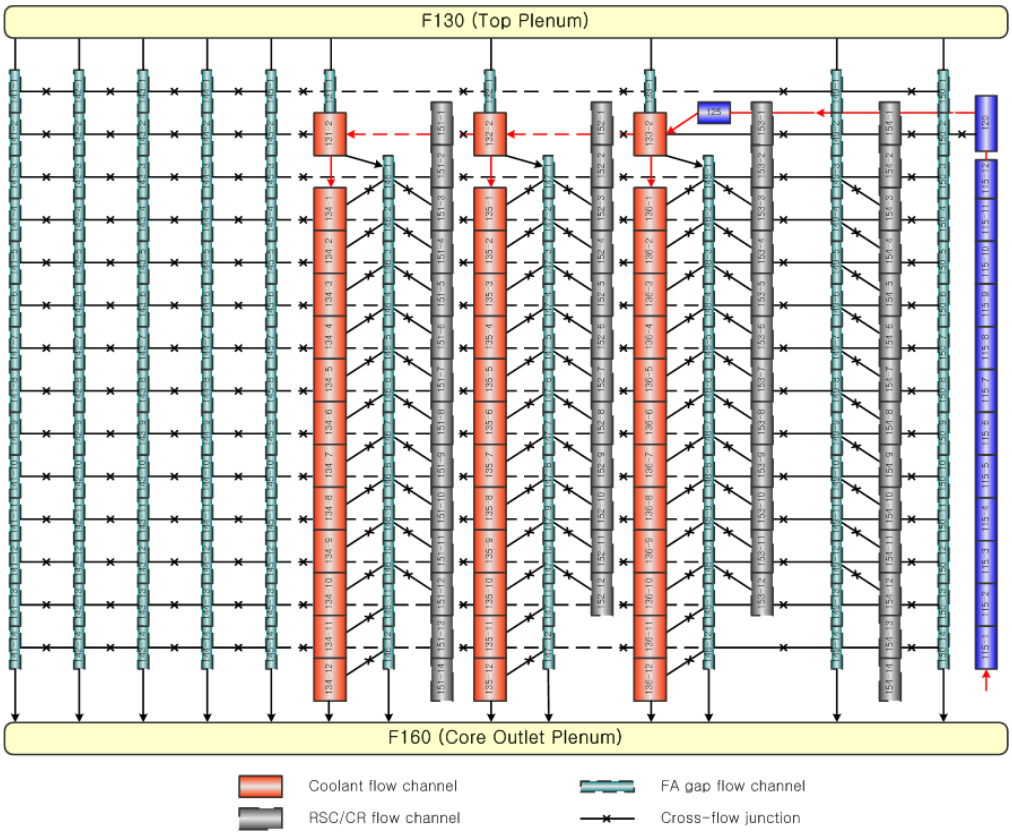

Figure 4-4. GAMMA+ Flow Network Model Used for Core Region

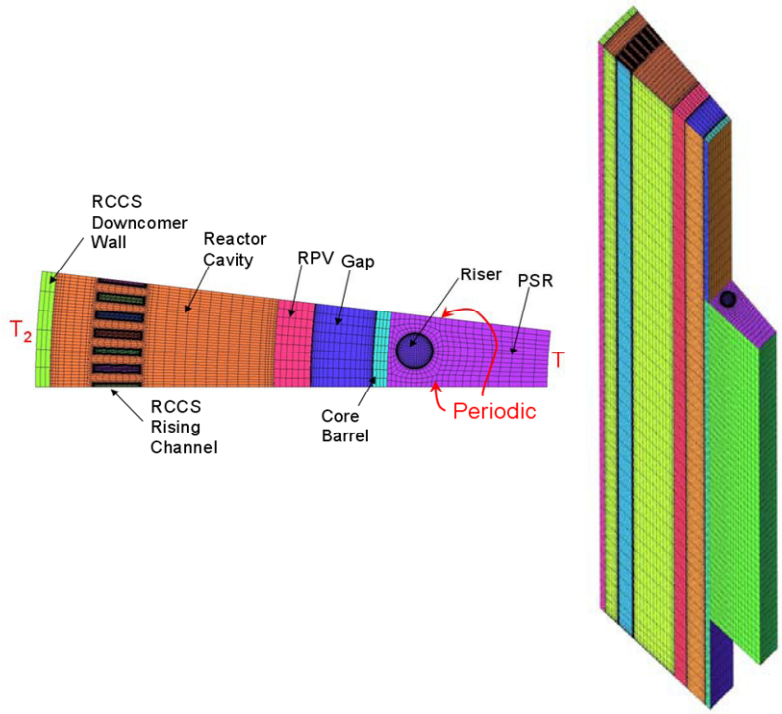

Figure 4-5. Computational Mesh Used for CFX Analyses

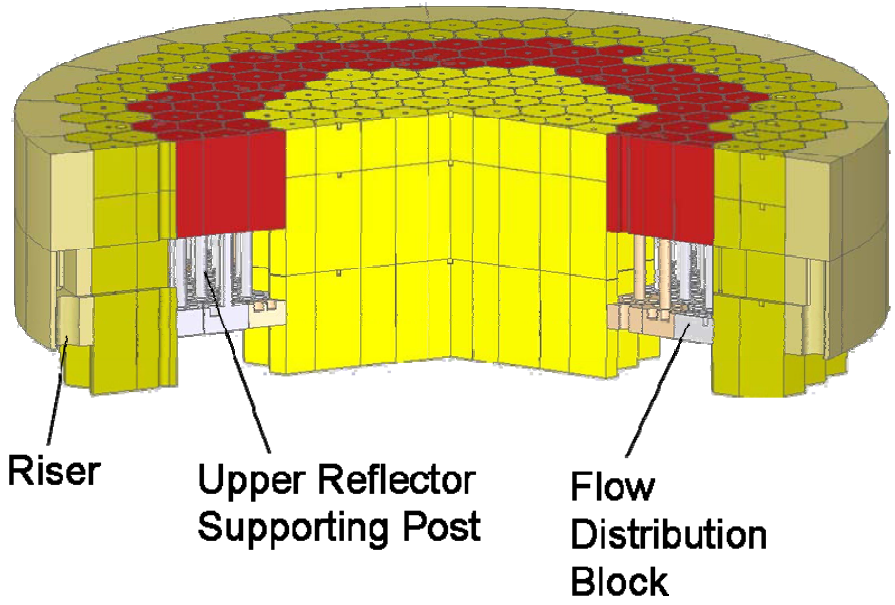

Figure 4-6. KAERI Concept for Upper Plenum in Top Reflector Region

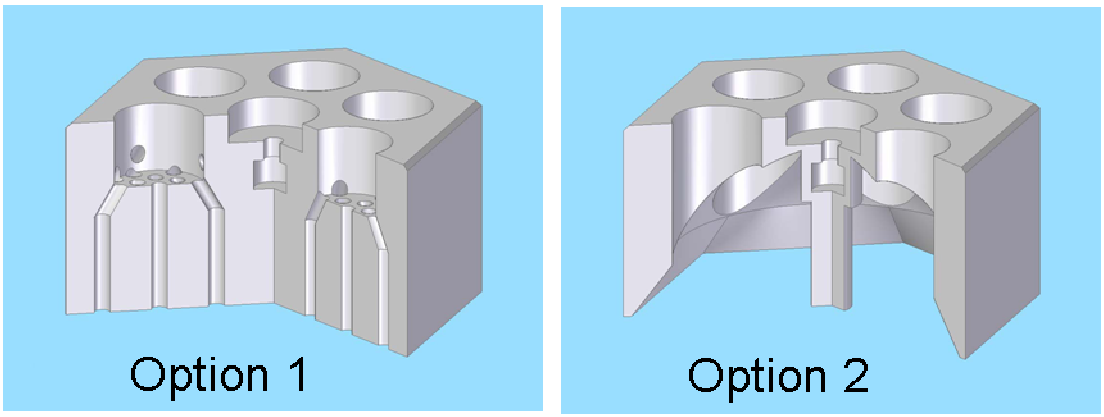

Figure 4-7. KAERI Concepts for Upper Plenum Flow Distribution Blocks

For an inlet temperature of 490°C, without vessel cooling, and an air-cooled RCCS, the peak RPV temperature is 348°C during normal operation and 519°C during a LPCC. Hence, for a 490°C inlet temperature, the ASME code limits can be satisfied for both normal operation and accident conditions without requiring an active VCS. For an inlet temperature of 590°C, an air-cooled RCCS, and a VCS with inlet temperature of 140°C and flow rate of 3.1 kg/s (less than 1% of primary coolant flow), the peak RPV temperature is 350°C during normal operation and 526°C during a LPCC. Hence, a VCS is required for inlet temperatures above approximately 490°C. Results for steady-state and transient analyses are summarized in Tables 4-2 and 4-3, respectively. RPV and peak fuel temperatures during HPCC and LPCC accidents are shown in Figs. 4-8 and 4-9, respectively. The RPV temperatures shown in Fig. 4-8 are for an air-cooled RCCS and coolant inlet/outlet temperatures of 490°C/950°C.

Table 4-2. Summary of Steady-State Results for Cooled Vessel Analyses

Cases	**Case 1**	**Case 2**	**Case 3**	**Case 4**	**Remarks**
Core thermal power, MW	600		600		
RCCS cooling type	Air-cooled RCCS		Water-cooled RCCS		
RCS inlet/outlet temperature, °C	490/950	590/950	490/950	590/950	
Heat removal, MW VCS RCCS VCS+RCCS	 N/A 1.76 1.76	 3.08 1.36 4.44	 N/A 2.08 2.08	 1.74 2.15 3.89	 VCS inlet temperature of 140 °C
VCS helium flow rate, kg/s	-	3.08	-	1.48	
Peak RPV temperature, °C	347.6	350.0*	313.7	350.0	

* Target RPV peak temperature limit during normal operation

Table 4-3. Summary of Transient Results for Cooled Vessel Analyses

Cases	**Case 1**		**Case 2**		**Case 3**		**Case 4**	
Inlet/Outlet, °C	490/950		590/950		490/950		590/950	
Accident	HPCC	LPCC	HPCC	LPCC	HPCC	LPCC	HPCC	LPCC
Peak fuel temp., °C	1358	1536	1375	1544	1344	1526	1365	1535
Peak RPV temp., °C	432	519	437	526	381	460	386	466
RCCS	Air-cooled				Water-cooled			
Event scenarios and assumptions	1. Core power switches to GA decay curve at time zero 2. RCS & VCS flows decrease to zero in 60 seconds (HPCC), and in 10 seconds (LPCC) 3. RCS & VCS pressures remain at 70 bar (HPCC), and decrease to 1 bar in 10 seconds (LPCC) 4. RCCS panel temperature increases from 65°C to 140°C in 5 hours for the water-cooled RCCS option							

Results using the GAMMA+ code show the heat removed during normal operation by a water-cooled RCCS is approximately 20% greater than that for an air-cooled RCCS, which lowers vessel temperatures by approximately 30°C. However, multidimensional analyses using the CFX code showed complex flow phenomena in the vessel cavity that essentially mitigated any benefit of the water-cooled RCCS (see Appendix A). These phenomena need to be evaluated in more detail.

A structural analysis of the RPV was performed using the ANSYS code. For temperatures less than 371°C (normal operation), design criteria from Section III, Subsection NB of the ASME code were used. At temperatures above 371°C (accident conditions), design criteria from Code Case N-499-2 and the Subsection NH assessment procedure was used. This analysis confirmed the structural integrity of the RPV. Internal pressure dominated the stress intensity and stresses from thermal loads during normal operation and accidents had a minor impact on structural integrity.

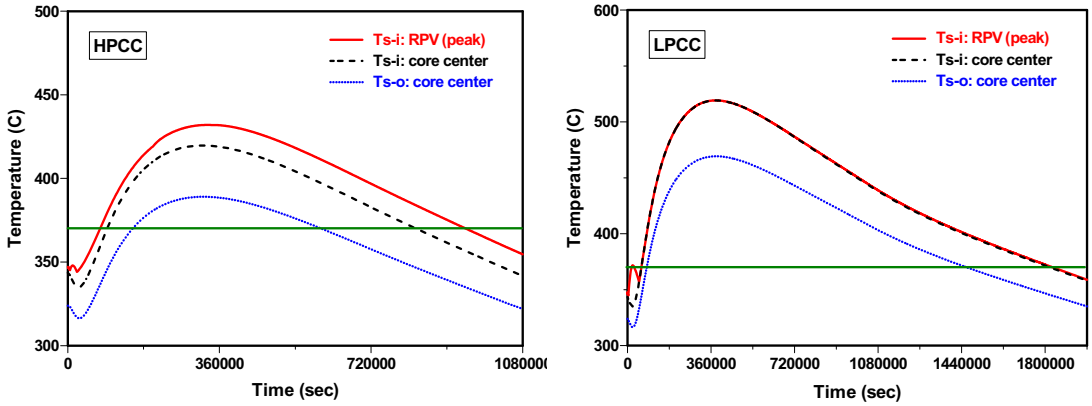

Figure 4-8. RPV Temperatures during HPCC and LPCC Events

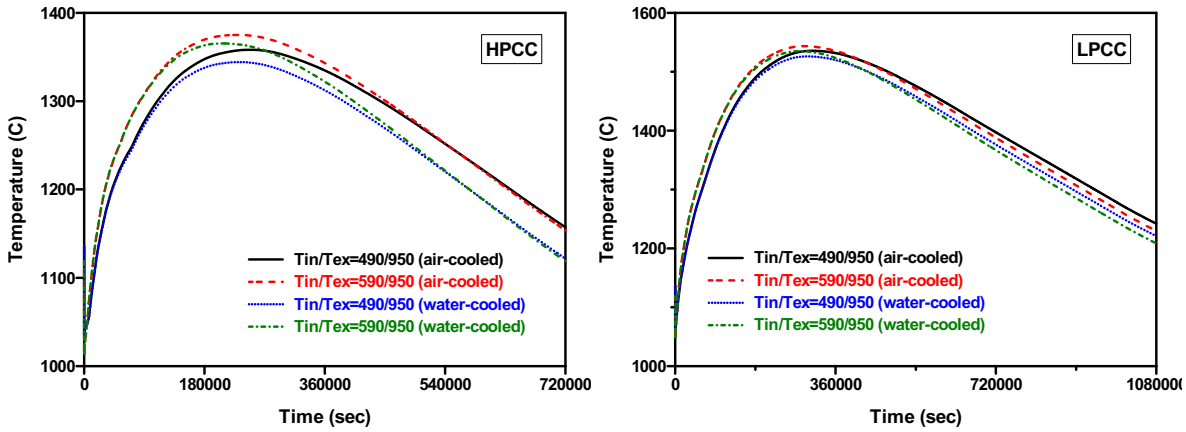

Figure 4-9. Peak Fuel Temperatures during HPCC and LPCC Events

4.2. Evaluations Performed by Fuji Electric Systems

As part of this design study, FES prepared a report titled “Analysis of follow-on to the accidental condition analyses using 3D ANSYS model” [FES 2008]. Because of Japanese nuclear export control restrictions, this reference will be provided to BEA as a separate document with appropriate restrictions for distribution. Key results from this report are summarized below.

Summary of Key Results

The calculations performed by FES consisted of a set of parametric studies of LPCC and HPCC accidents using the 30-degree sector ANSYS model shown in Fig. 4-10. The FES model does

not include a VCS and incorporates a 100-mm thick layer of carbon insulation on the PSR to reduce RPV temperatures during accident conditions. This insulation layer also includes B_4C to reduce fast neutron flux to the RPV. For normal operation, the FES results are consistent with the KAERI results described in Section 4.1 (i.e., a VCS is not needed to satisfy ASME code limits for an inlet temperature of 490°C, but a VCS would be required for an inlet temperature of 590°C). A total of 21 calculations were performed and the following parameters were varied:

Reactor Thermal Power:	500 MW, 550 MW, and 600 MW
Coolant Inlet Temperature:	490°C and 590°C
Coolant Outlet Temperature:	900°C and 950°C
Decay Heat:	nominal and 15% higher than nominal
RCCS:	air cooled and water cooled
Graphite Thermal Conductivity:	unirradiated, irradiated, and irradiated + annealed

The FES model is similar to the model used for the Preconceptual Design Studies [GA 2007], but with several improvements to improve the modeling and numerical accuracy. These improvements include a more detailed radiation exchange model between the RPV and RCCS, a more rigorous treatment of neutron-irradiation effects on graphite thermal conductivity, and more detailed treatment of temperature-dependent properties. As a result of these modeling improvements, peak RPV temperatures are approximately 40°C lower and peak fuel temperatures are approximately 10°C higher than results obtained using the previous model.

Most of the calculations were performed for a 108-column core, which reduces power density by about 5% but increases the heat-transfer path to the RCCS heat sink by about one-half the width of a graphite fuel element. For a LPCC event, the net effect is an increase in peak fuel temperature of about 30°C relative to a 102-column core and little or no impact on RPV temperatures.

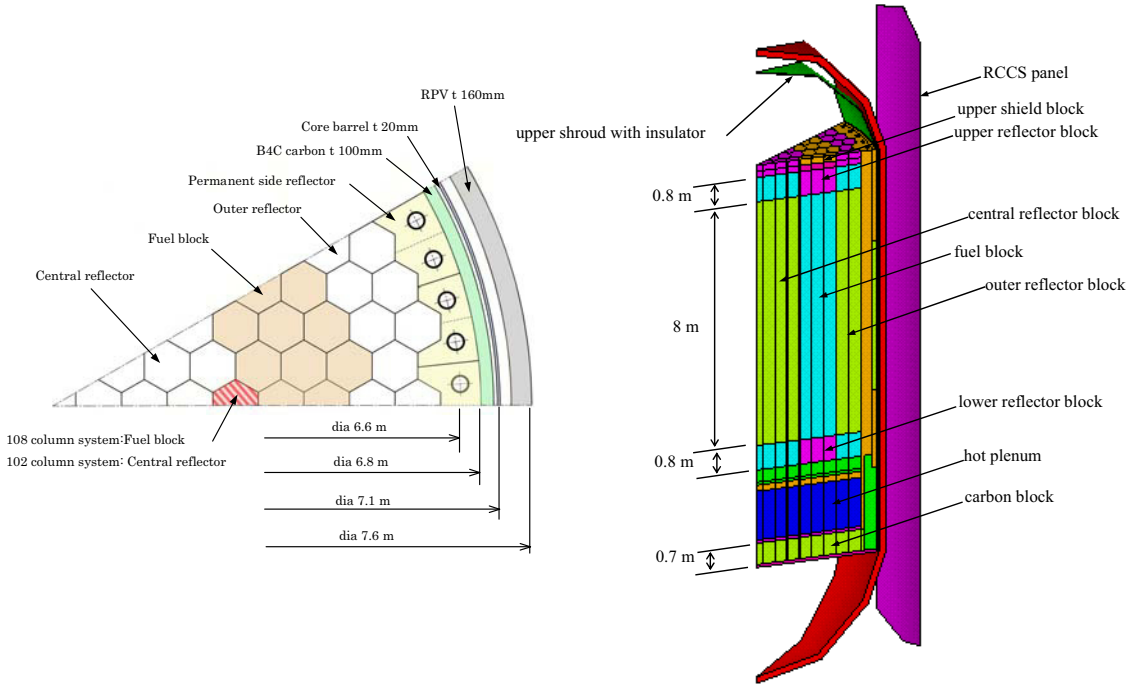

Figure 4-10. 30-Degree Sector ANSYS Model

Assuming decay heat is 15% higher than nominal to account for uncertainties results in an increase in peak fuel temperature of about 110°C and in an increase in peak RPV temperature of about 30°C. [9]

Graphite thermal conductivity has a significant impact on peak fuel temperatures but a negligible impact on RPV temperatures. For fully-irradiated graphite, peak fuel temperatures are approximately 165°C higher than those for unirradiated graphite. Accounting for thermal annealing of irradiated graphite reduces peak fuel temperatures by about 60°C.

Assuming decay heat is 15% higher than nominal, irradiated graphite with annealing, and an air-cooled RCCS, a thermal power level between 550 MW and 600 MW will result in peak fuel temperatures below 1600°C and peak RPV temperatures below the ASME accident-condition limit of 538°C during a LPCC event. For these assumptions, Figure 4-11 shows the peak fuel

[9] Based on previous uncertainty assessments performed by GA, increasing the decay heat by 15% approximately accounts for the effects of uncertainties in graphite thermal conductivity, RPV emissivity, and other parameters on peak fuel temperatures. For future studies, more rigorous sensitivity studies should be performed to better quantify uncertainties. In response to an action item from the 90% design review meeting for this phase of NGNP conceptual design studies, KAERI has prepared a preliminary list of parameters for performing sensitivity studies. This list is included as Appendix B of this document.

and RPV temperatures and Fig. 4-12 shows the corresponding temperature distribution at the time of peak fuel temperature.

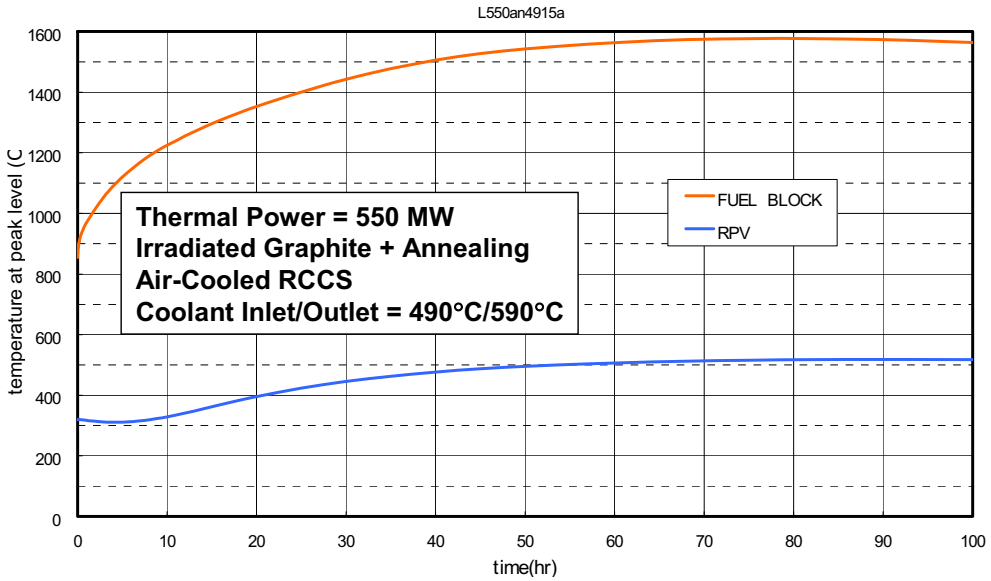

Figure 4-11. Peak RPV and Fuel Temperatures during LPCC with +15% Decay Heat

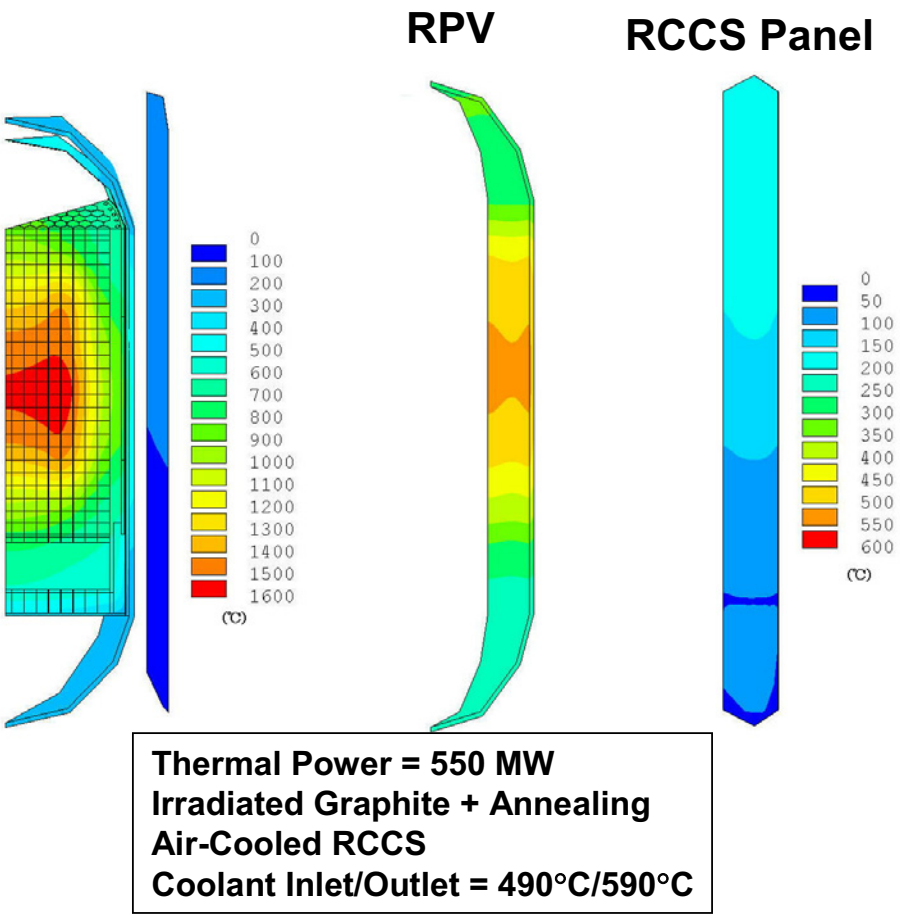

Figure 4-12. Temperature Distributions during LPCC with +15% Decay Heat

The FES results indicate a water-cooled RCCS at 65°C provides only a modest reduction (~9°C) in RPV temperatures relative to an air-cooled RCCS. If the RCCS is allowed to operate in boiling mode (140°C), there is no reduction in RPV temperatures relative to an air-cooled RCCS. For an air-cooled RCCS, increasing the panel flow area by 50% results in only a 3°C reduction in peak RPV temperature.

4.3. Control of Primary Coolant Leakage

As discussed in the previous sections, operation with a coolant inlet temperature of 490°C combined with routing the inlet flow through riser channels in the PSR should result in RPV temperatures during normal operation and accident conditions that would allow the use of SA-508/533 steel for the RPV without requiring active vessel cooling. However, if this design strategy is used, the reactor internals must be designed to essentially preclude any leakage of the inlet flow to the annular space between the core barrel and RPV. Figure 4-13 shows results from a previous parametric study [Richards 2007a] in which a fraction of the inlet flow was assumed to leak into the annular space between the core barrel and RPV. For this study, the

inlet temperature was assumed to be 510°C, which resulted in a peak RPV temperature of about 370°C with no leakage flow. As shown in Fig. 4-13, a leakage flow of 2% of the total flow will increase the vessel temperature by about 40°C.

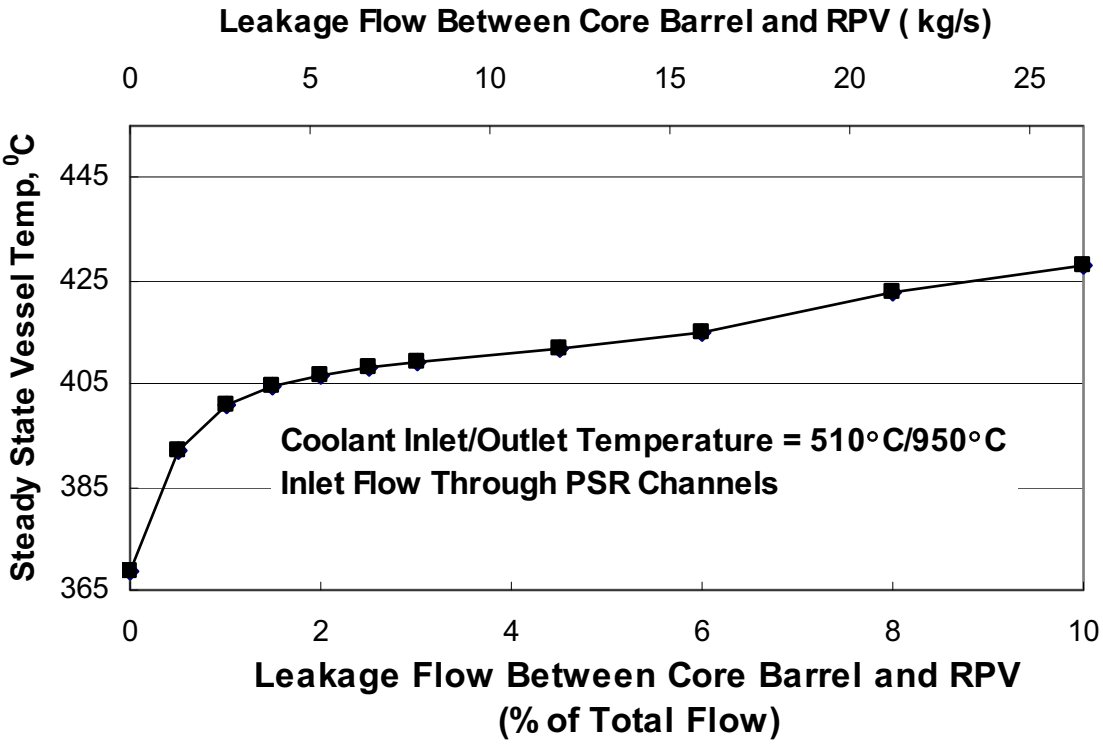

Figure 4-13. Effect of Leakage Flow on Normal Operation RPV Temperatures

5. THERMAL/STRUCTURAL ANALYSES OF 9Cr-1Mo-V RPV

As part of this design study, KAERI prepared a report titled “A Preliminary Analysis for a High-Cr NGNP Reactor Pressure Vessel.” This report is included as Appendix C.

The modeling approach is nearly identical to that described in Appendix A for the SA-508/533 vessel. The structural analyses confirmed that an RPV manufactured using 9Cr-1Mo-V steel would satisfy ASME code requirements. However, as discussed in Sections 2 and 6, the capability to manufacture and weld thick sections using 9Cr-1Mo-V steel needs to be proven before this material can be considered a viable candidate for the RPV.

6. VESSEL FABRICATION, TRANSPORTATION, AND ON-SITE ASSEMBLY ISSUES

6.1. Assessment of Japan Steel Works Forging Capability

Toshiba Corporation assessed the capabilities of Japan Steel Works (JSW) to fabricate forgings for the RPV for a 600-MWt prismatic block NGNP from the various candidate materials currently under consideration (SA-508, 2.25Cr-1Mo, and 9Cr-1Mo-V). Toshiba Corporation also assessed the current backlog for forging construction at JSW to determine the approximate date by which forgings for the RPV would have to be ordered to obtain delivery of the RPV in time for a 2018 NGNP startup.

Toshiba Corporation met with JSW to discuss the current capabilities of JSW. In addition, JSW provided answers to specific questions posed by GA (see Table 6-1). As indicated in Table 6-1, JSW is starting to develop capability to supply 9Cr-1Mo-V forgings to support the Fast Breeder Reactor (FBR) program in Japan,[10] but this program is still in the very early stages, and it is highly unlikely JSW would be able to supply forgings of this material in time to meet a 2018 NGNP startup. For this reason, JSW strongly recommends use of SA-508 steel for the NGNP RPV. Estimates for the RPV thickness using SA-508 steel are given below:

Cylindrical Shell:	152 mm (6 in.)
Hemispherical Domes:	102 mm – 127 mm (4 in. – 5 in.)
Vessel Support Interfaces:	203 mm (8 in.)

Figure 6-1 shows the dimensional capabilities of the JSW forging facilities. Ring forgings are limited to heights of 10 m and outside diameters of 10 m. Further limitations are imposed by the round furnace and quench tank, both of which are can accommodate ring forgings with diameters of 9 m and heights of 6 m. However, because the quench tank has water-circulation nozzles installed on the tank wall, ring forging diameters are further limited to 8.2 m, unless the height of the forging is below the height of the nozzles. JSW did previously manufacture a ring forging for the Monju FBR with dimensions 8.760 m OD × 7.780 m ID × 0.783 m H.

Manufacturing large-sized forged products requires large-sized ingots. JSW has used ingot sizes of 600 t for SA-508. For 2.25Cr-1Mo, the largest ingot size used by JSW is 250 t, but this size was determined by product requirements. It may be possible to use larger-sized ingots for 2.25Cr-1Mo, but quality requirements need to be confirmed. For 9Cr-1Mo-V, the ingot weight is currently limited to 120 t, because segregation causes difficulty with making homogeneous ingots. As discussed above, Research and Development (R&D) efforts have been initiated for the purpose of making large-sized ingots with 9Cr-1Mo-V, in order to manufacture large-size

[10] Japan intends to re-start the Monju prototype FBR in the near term and intends to start deployment of advanced FBRs around 2030 [Richards 2007b].

forgings for the Japan's advanced FBR concept. Regardless of the original ingot weight, product weights are typically 30% or less of the ingot weight, and as little as 10% of the ingot weight for complex shapes.

Table 6-1. JSW Answers to Questions from GA

Question from General Atomics	Answer from Japan Steel Works
For what materials does JSW have existing nuclear pressure vessel component forging manufacture capability (forging process equipment, process technology and ASME B&PV code qualification)?	The manufacturing facilities are not specific material and are used for LWR RPV material, turbine rotor material (high-Cr steel) and other materials.
What are the basic steps and process conditions used by JSW for manufacture of nuclear pressure vessel forgings?	The basic steps for manufacturing of the nuclear reactor pressure vessel can be obtained from the home page of JSW: http://www.jsw.co.jp/en/guide/facilities.html Basically, it involves, melting, refining, pouring, ingot-making, heat treatment, machining, and products.
What size limitations does the JSW nuclear vessel component forging manufacturing process have (finished weight, finished ring forging ID & OD, and finished ring forging length)?	The product size and weight are strongly affected by the maximum possible ingot weight. The maximum possible ingot weights are 600 t for SA-508, 250 t for 2.25Cr-1Mo, and 120 t for 9Cr-1Mo-V. The product weights are typically results less than about 30 % of the ingot weights (~10 % in case of complex shapes).
In previous discussions, the maximum JSW finished ring forging OD has been indicated to be about 8.2m and that the maximum OD was limited by the size of the existing quench tank. Could the quench tank size be increased, or could an alternative quench process be used (e.g., water spray)?	At present, there are no plans to increase the size of the quench tank, and current operations at JSW do not provide any schedule leeway to remodel any major facilities. The 8.2 m diameter limitation for RPVs results from water-circulation nozzles on the inside of the tank wall, which has an ID of 9 m. If the product height is sufficiently small (below the height of the tank nozzles), larger diameter forgings can be put into the quench tank. An example is a ring forging for the Monju FBR (8.760 m OD × 7.780 m ID × 0.783 m H).
JSW has also previously indicated to GA that they will only supply SA-508 nuclear vessel forgings based on their currently developed forging process. If this is still the case, could JSW develop the necessary forging process capability, including ASME code qualification, for the alternative NGNP nuclear vessel materials under consideration (2¼Cr-1Mo and 9Cr-1Mo)? If so, what would be the order of magnitude for both the cost and schedule of the process development work for each of these alternative NGNP vessel materials? If the development work is done, what would be JSW's projection of the finished forging size limitations for the alternative materials?	JSW still recommends using SA-508. Technically, 2¼Cr-1Mo is possible. But the product height is relatively small and the number of the welding lines increases because of the relatively small ingot weight of 250t. Also, further study is needed for the cross vessel joint region to maintain the required height. For 9Cr-1Mo-V the ingot size is limited because of segregation. Because of the current emphasis on FBR development in Japan, work has started on developing large-sized forged products of 9Cr-1Mo-V appeared for FBR in Japan, but this work is still in the design study phase. Because of the segregation problem, experimental work is also needed . Also, ingot manufacturing facilities require reservations of 5 to 6 years in advance. Hence, the cost, schedule, and forging size limitations cannot be determined at this time.
Does JSW have nuclear vessel welding process capability for joining forged components (process equipment, process technology and ASME B&PV code qualification)? If so, for what materials and what are the size limitations for finished welded assemblies?	JSW performs prefabrication of nuclear vessel components. However, welding and fabrication of these components into final products are conducted by other companies, typically heavy industries companies. JSW does not perform ASME certification of nuclear components. These certifications are performed on the final product by other companies.

According to JSW, ingot manufacturing facilities require reservations of 5 to 6 years in advance. An additional 3 to 4 years is required to produce the final RPV product. Hence, even if the recommendation by JSW to use SA-508 steel is adopted, the RPV could not be procured in time to support a 2018 NGNP startup, unless an effort is made to assign a high priority to production of the NGNP RPV. This would likely require some sort of government-to-government cooperation between the U.S. and Japan on NGNP. However, development of the FBR and deployment of additional LWRs currently have a much higher priorities in Japan relative to development of the Very High Temperature Reactor (VHTR) [Richards 2007b].

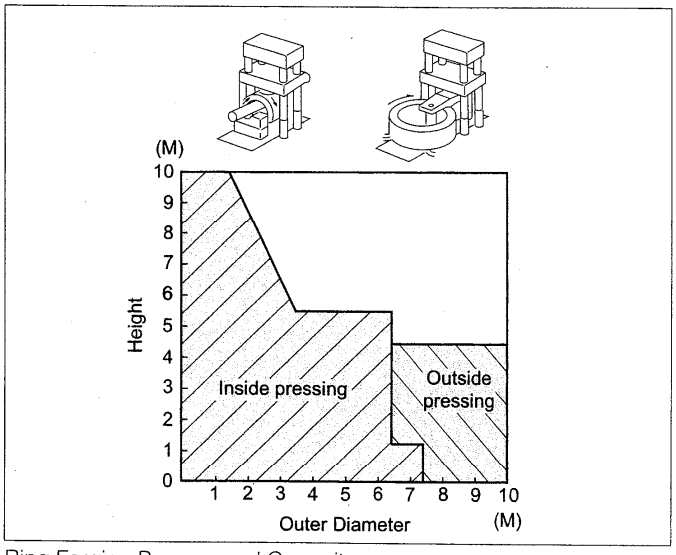

Ring Forging Process and Capacity

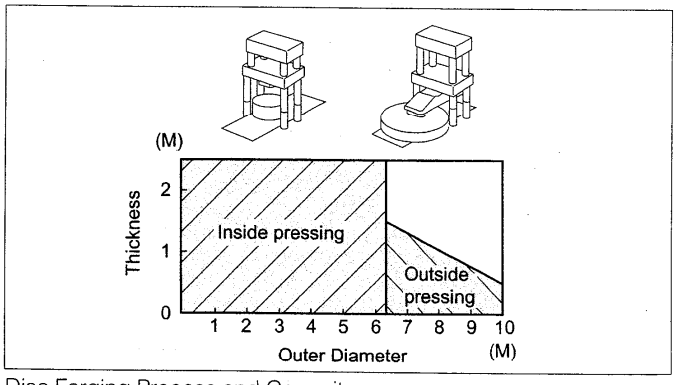

Disc Forging Process and Capacity

FACILITIES

14,000 Ton Hydraulic press with facility for outside pressing
8,000-Ton Hydraulic Press with facility for cross die forging
3,000-Ton Oil Hydraulic Press with numerical control

Figure 6-1. Dimensional Capabilities of JSW Forging Facilities

6.2. Assessment Performed by KAERI

As part of this design study, KAERI[11] prepared a report titled "Manufacturability Evaluation for NGNP Pressure Vessels." This report is included as Appendix D. Key results from this report are summarized below.

Summary of Key Results

As shown in Fig. 6-2, the Korean local supplier is considering two options for manufacture and transportation of the RPV. For both options, the upper head assembly (above the flange) is manufactured separately. For the first option, the RPV body is an integrated unit consisting of an upper body (mid section) and a lower body. For the second option, the RPV body is split into two components, with the lower body consisting of the cross-vessel region and below. Figure 6-3 shows the dimensions and weights for the two options.

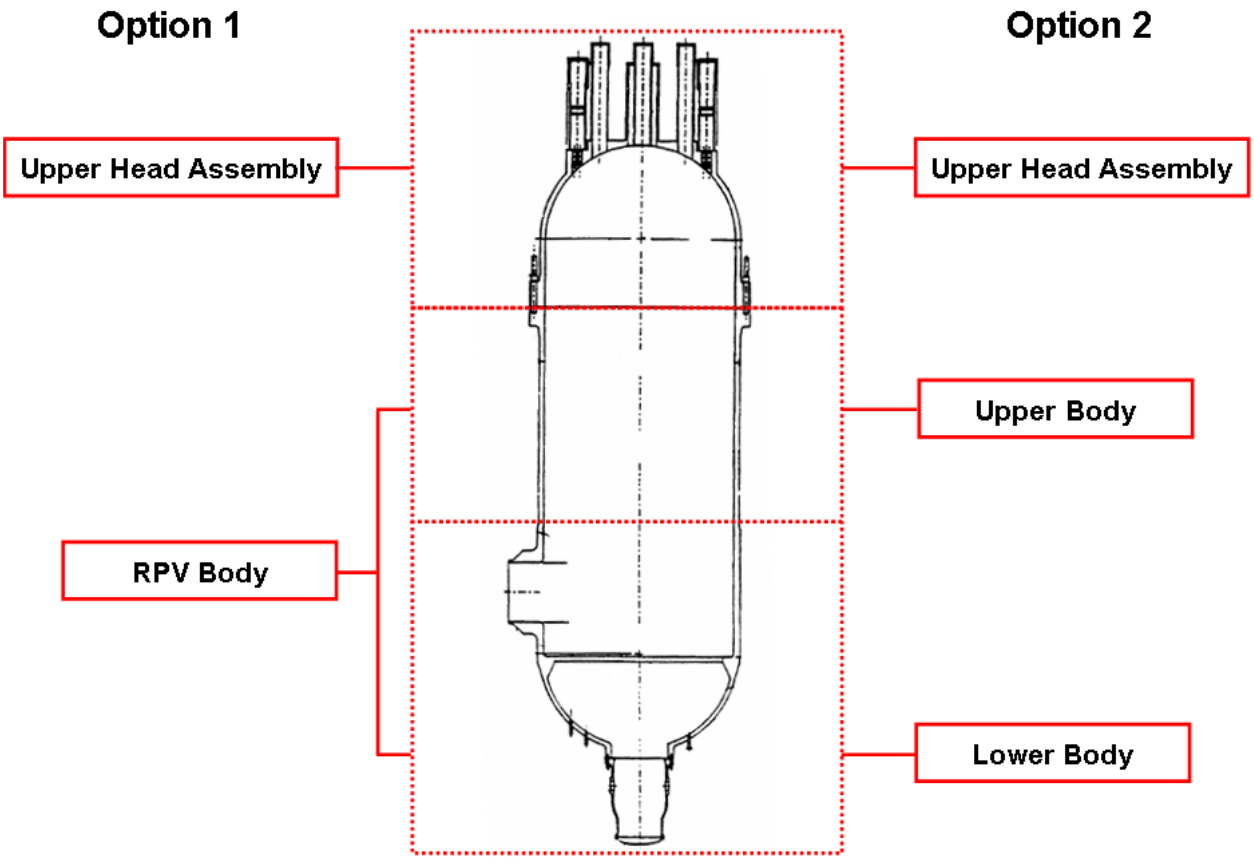

Figure 6-2. Options for Manufacture and Transportation of RPV

[11] In the areas related to RPV manufacture and transport, KAERI consults with the local Korean supplier, DOOSAN Heavy Industries and Construction.

Option 1 (1 piece RPV body)

Component		OD (mm)	ID (mm)	Height (mm)	Weight (ton)
RV	Head	8,420.1	7,226.3	10,207.5	435*
	RPV Body	8,420.1	7,226.3	21,008.3	924*
	Total	8,420.1	7,226.3	31,215.8	1,364

* The weight of stud and gasket is excluded. (But it is included in total weight)

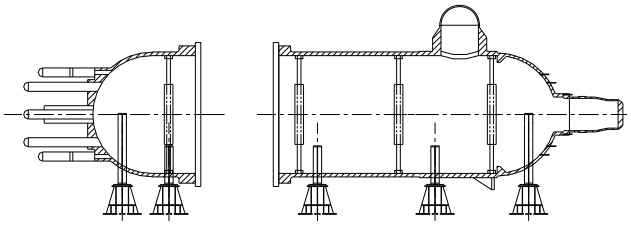

Option 2 (2 RPV piece body)

Component		OD (mm)	ID (mm)	Height (mm)	Weight (ton)
RV	Head	8,420.1	7,226.3	10,207.5	435*
	Upper Body	8,420.1	7,226.3	8588.5	325
	Lower Body	8,420.1	7,226.3	12419.8	599*
	Total	8,420.1	7,226.3	31,215.8	1,364

* The weight of stud and gasket is excluded. (But it is included in total weight)

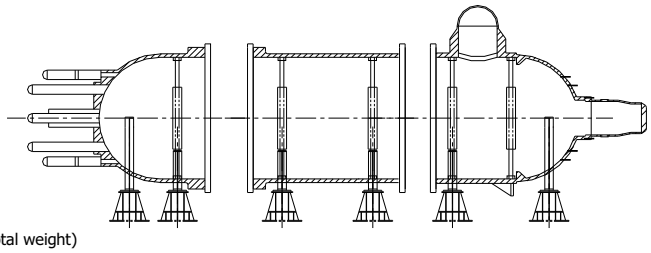

Figure 6-3. Dimensions and Weights for RPV Options

The Korean local supplier has extensive experience with manufacturing RPVs using SA-508/533 steel, and has also manufactured large vessels using 2.25Cr-1Mo steel for the fossil-fuel industry. Figure 6-4 shows a vessel with diameter of about 10 m and height of about 44 m that was manufactured using rolled plates for the Jammnagar Refinery Project. The Korean local supplier prefers to use 2.25Cr-1Mo steel for higher-temperature applications but does not preclude the use of 9Cr-1Mo-V steel. For manufacturing components from either 2.25Cr-1Mo or 9Cr-1Mo-V steels, the Korean local supplier indicates that elaborate controls are required to prevent segregation and cracking in the forging process.

Plate Bending **Rolled Half Shell** **Completed Vessel**

Figure 6-4. 2.25Cr-1Mo Vessel for Jammnagar Refinery project

As is the case for JSW, the Korean local supplier has practical limitations on the sizes of forged shells because of restrictions imposed by the melting furnace and other equipment. For this

reason, the Korean local supplier recommends using rolled plates for vessels approaching the size of the NGNP vessel.

7. CONCLUSIONS AND RECOMMENDATIONS

Information provided by both JSW and the Korean local supplier confirm that use of SA-508/533 for the RPV material of construction is essentially required in order to support a 2018 – 2021 NGNP startup date. Use of Grade 91 steel (or other high-alloy steels) may be a better material in terms of design optimization, but it is highly unlikely an RPV manufactured from this material could be procured in time to support a 2018 startup date, even with a dedicated, international effort. A key issue associated with Grade 91 steel is uniformity of properties in the ingot sizes required to manufacture the large forgings needed for an RPV. Developmental work should continue on Grade 91 steel (and other high-alloy steels, including Grades 22, 22V, and 23), since higher temperature capability could be a significant advantage for follow-on commercial plants. Opportunities for collaboration with Japan on development of Grade 91 steel (and other high-alloy steels) should be investigated, since Japan has started developmental work on this material to support deployment of advanced FBRs in the 2030 time frame.

Assuming SA-508/533 steel is used as the material of construction for the RPV, operation with a coolant inlet temperature of 590°C will require use of an active VCS to ensure compliance with ASME code limits. Thermal analyses performed by KAERI and FES indicate a VCS should not be required if it is possible to operate the NGNP with a higher core ΔT (and lower coolant mass flow) by lowering the inlet temperature to 490°C, with inlet flow routed through risers in the PSR. Design measures to optimize power and coolant flow distributions should result in acceptable fuel temperatures during normal operation with coolant inlet/outlet temperatures of 490°C/950°C. Some of these design measures (e.g., restraint mechanisms and sealing keys to reduce bypass flow) will require additional design work and technology development to demonstrate their feasibility and effectiveness. This design strategy would also require the reactor internal design to essentially preclude leakage flow from the PSR risers to the annular space between the core barrel and RPV.

For NGNP startup in the 2018 to 2021 time frame, SA-508/533 steel should be selected as the MOC for the RPV. With this choice, the NGNP design must ensure the RPV temperatures remain within ASME code limits, and should proceed along two parallel paths: (1) Operation with an inlet temperature of 490°C and design optimization to ensure acceptable fuel temperatures and to prevent leakage flow to the RPV; and (2) Operation with a more flexible inlet temperature in the range 490°C to 590°C with an active VCS. For a 2018 – 2021 startup, probably the only feasible backup material for SA-508/533 is Grade 22 steel, especially if the configuration/application selected for NGNP is amenable for operation with a lower primary system pressure (e.g., 5 MPa instead of 7 MPa) that would permit thinner wall sections. The first design path entails the risks associated with successful demonstration of the technology required to optimize the reactor internals design. The second design path may raise issues

about demonstration of a design with complete passive safety. In principle, an active VCS should not impact the case for passive safety, since a SA-508 vessel could operate for extended periods with the VCS offline without exceeding damage limits. However, the VCS should be considered an investment protection system and should be designed with a high degree of reliability. For NGNP, the reactor internals should be designed for not requiring a VCS, but a VCS should be incorporated into the design to mitigate the relatively high design and licensing risks associated with prototype reactor operating at temperatures well in excess of those for current generation LWRs. During NGNP operation, RPV temperatures can be measured with the VCS online and offline to confirm whether or not a VCS is actually required.

Stress analyses using the ANSYS code have confirmed the structural integrity with respect to ASME code guidelines of RPVs manufactured from either SA-508/533 or 9Cr-1Mo-V (Grade 91) steel.

Toshiba Corporation has recommended SA-508/533 steel as the material of construction for IHX vessels and has included Kaowool insulation as part of the design to protect the vessels from creep damage. Use of SA-508/533 steel for the RPV, cross vessel(s), and IHX vessel(s) would eliminate any potential concerns associated with bimetallic welds in the primary coolant pressure boundary.

8. REFERENCES

[FES 2008] "RPV and IHX Vessel Alternatives, Analysis of follow-on to the accidental condition analyses using 3D ANSYS model," FGN-F009-R0, Fuji Electric Systems, Kawasaki, Japan, March 2008.

[GA 2007] "Preconceptual Engineering Services for the Next Generation Nuclear Plant (NGNP) with Hydrogen Production," RGE 911107, Rev. 0, General Atomics, San Diego, CA, July 2007.

[GA 2008] "IHX and Secondary Heat Transport Loop Alternatives Study," RGE 911119, Rev. 0, General Atomics, San Diego, CA, April 2008.

[INL 2007] "Next Generation Nuclear Plant Pre-Conceptual Design Report," INL/EXT-07-12967, Rev. 1, Idaho National Laboratory, Idaho Falls, ID, November 2007.

[Natesan 2006a] K. Natesan, S. Majumdar, P. Shankar, and V. Shah, "Preliminary Materials Selection Issues for the Next Generation Nuclear Plant Reactor Pressure Vessel," ANL/EXT-06-45, Argonne National Laboratory, Argonne, IL, September 2006.

[Natesan 2006b] K. Natesan, A. Moisseytsev, S. Majumdar, and P. Shankar, "Preliminary Issues Associated with the Next Generation Nuclear Plant Intermediate Heat Exchanger Design," ANL/EXT-06-46, Argonne National Laboratory, Argonne, IL, September 2006.

[Richards 2007a] M. Richards, W.J. Lee, Y.H. Kim, N.I. Tak, and M. Reza, "Thermal Hydraulic Optimization of a VHTR Block-Type Core," 15th International Conference on Nuclear Engineering, Nagoya, Japan, April 22-26, 2007, Paper ICONE-10290.

[Richards 2007b] M. Richards, "Deployment of FBR/VHTR Systems for Japan's Future Energy Demands," GA-A25934, General Atomics, San Diego, CA, October 2007.

[Richards 2008] "Characterizing the Effect of NGNP Operating Conditions on the Uncertainty of Meeting Project Cost and Schedule Objectives," PC 000566, General Atomics, San Diego, CA, April 2008.

[Shenoy 2006] A. Shenoy, "GT-MHR Conceptual Design Description Report," RGE 910720, Rev. 1, General Atomics, San Diego, CA, July 1996.

APPENDIX A – KAERI Cooled Vessel Study

KAERI

Nuclear Hydrogen Project

Calculation Note

Document No: NHDD-KA-07-RD-CA-022, Rev.01

Title : A Preliminary Analysis for a Cooled SA-508/533 NGNP Reactor Pressure Vessel

Prepared by :	Min-Hwan Kim	Date : Mar. 17. 2008
Reviewed by :	Hong-Sik Lim	Date : Mar. 20. 2008
Reviewed by :	Dong-Ok Kim	Date : Mar. 24, 2008
Approved by :	Won Jae Lee	Date : Mar. 26, 2008

SUMMARY

This report is on a cooled-vessel study which is a part of NGNP CDS subtask, WBS NHS.000.S01-RPV and IHX Pressure Vessel Alternatives. The main purpose of the task is to perform a preliminary structural analysis for a cooled SA508/533 NGNP RPV under normal operating conditions and anticipated transients. It is assumed that the reactor outlet temperature is 950°C while the reactor inlet temperatures are 490 °C and 590 °C. A cooled-vessel concept was derived and its basic dimensions for the analysis were determined. Thermal boundary conditions for the structural analysis were obtained from the thermo-fluid analysis using GAMMA+ code, in which both an air-cooled RCCS and a water-cooled RCCS were considered. Along with the GAMMA+ analysis, a CFD analysis using CFX code were conducted for the detailed design study and its results are used not only to investigate detailed flow and heat transfer phenomena that occur in the cooled-vessel but also to verify the GAMMA+ results. The structural analysis was performed using ANSYS code and the integrity of RPV was examined in accordance with ASME B & PV Code.

Record of Revisions

No.	Date	Description	Prepared by
00	Feb. 22, 2008	Initial Issue	Min-Hwan Kim
01	Mar. 26, 2008	Tables 5.4, 5.5, 5.6, 5.7, 5.8, 5.9 – to update data All - To correct descriptions and sentences	Min-Hwan Kim

NHS.000.S01 #2130

A Preliminary Thermo-fluid and Structural Analysis for a Cooled SA-508/533 NGNP Reactor Pressure Vessel

March 27, 2008

Revision 01

RPV and IHX Pressure Vessel Alternatives

NGNP Project - Conceptual Design Studies

Korea Atomic Energy Research Institute

TABLE OF CONTENTS

LIST OF FIGURES

LIST OF TABLES

1. INTRODUCTION

Current GT-MHR design requires high-Cr materials, such as 9Cr-1Mo-V or 2¼Cr-1Mo, for the reactor pressure vessel in order to keep the vessel integrity at higher temperature. However, there are still open issues in manufacturing and procuring high-Cr vessels. As an alternative design, KAERI proposes a cooled-vessel design that enables the use of conventional SA508/SA533 vessel as used in the light water reactors (LWRs). The cooled-vessel design prevents a direct contact of coolant with the reactor vessel by routing the coolant flow paths inside the permanent side reflector and the core-top graphite structures. And, the vessel is cooled by slip-stream of helium flow from the helium purification system. Thus, the reactor vessel temperature can be maintained under the design limit during both normal and transient conditions.

During the NGNP preliminary conceptual design study, KAERI showed that the cooled-vessel design could be a feasible option for the NGNP. In this conceptual design studies, more detailed design study is carried out in order to demonstrate the applicability of the cooled-vessel design to the 600MWth NGNP.

The objective of this task is to perform a preliminary structural analysis of the cooled-vessel design under normal operating conditions and anticipated transients. To achieve this goal, a design concept of cooled-vessel is derived and the basic dimensions are determined. Using these data, the thermal-fluid analysis is carried out using GAMMA+ code to provide thermal boundary conditions for the structural analysis. It is assumed that the reactor outlet temperature is 950°C, while the reactor inlet temperatures are 490°C and 590°C respectively. And, both the air- and water-cooled RCCS designs are considered in the analysis. For detailed design study, the CFX analysis is carried out and its results are used not only to investigate detailed flow and heat transfer phenomena that occur in the cooled-vessel but also to verify the results of GAMMA+ analysis. Structural analysis is conducted by using ANSYS code and the integrity of reactor vessel is assessed based on the ASME B&PV code.

2. COOLED-VESSEL DESIGN

2.1 Description of cooled-vessel design

GA has proposed a prismatic core VHTR as a candidate of NGNP reactor, which is based on the GT-MHR and has the reactor outlet temperature of 950°C and the reactor inlet temperature of 590 °C. The material of RPV (reactor pressure vessel) considered is 2¼Cr-1Mo or 9Cr-1Mo-V steel. This material provides creep resistance property at higher temperatures, whereas there are still open issues in using these materials not only in the manufacturability such as welding procedure but also in the procurement of materials. So, as an alternative, we propose the cooled-vessel design that allows the use of SA-508/533 vessel as used in the commercial light-water reactors by maintaining the vessel temperature below its operating structural limit.

A cooled-vessel is shown in Figure 2.1. The design is such that a direct contact of inlet coolant with the vessel wall is precluded by routing the coolant flow paths inside the vessel internal graphite structures and an additional vessel cooling system is introduced if necessary.

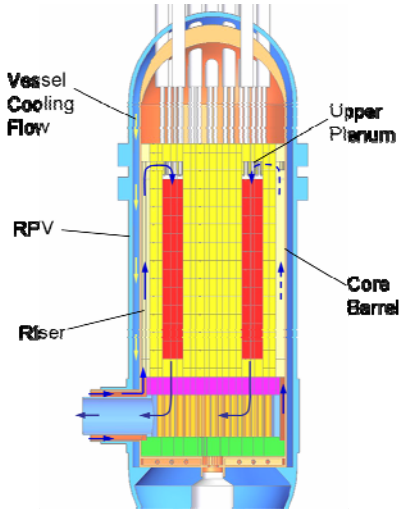

Figure 2.1. Configuration of the cooled-vessel design

The cooled-vessel design is characterized by the internal flow path through the permanent side reflector and a vessel cooling system dedicated to cooling the internal surface of the RPV. The flow path is divided into three parts consisting of the inlet plenum, the riser and the upper plenum. The incoming flow from the outside of coaxial duct is supplied to the inlet plenum, a large annular space below the permanent side reflector, in which the flow is distributed into the riser. The riser consisting of 54 cylindrical holes connects the inlet plenum and the upper plenum. After going through the riser holes, the flow gathers at the upper plenum and is supplied downward to the core. At the upper plenum, three riser holes are grouped to buffer the non-uniform flow from the riser then the flow is supplied to the upper part of the core through the slits in the graphite structure. Figure 2.2 shows the fluid regions of the flow path inside the graphite structure.

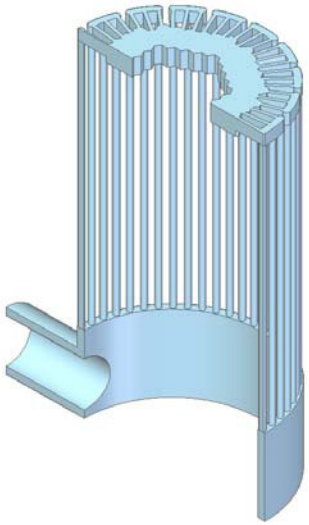

Figure 2.2 Fluid regions of the flow path inside the graphite structure

The vessel cooling system supplies cold helium flow to an annular gap between the RPV and the core barrel. The position of the cooling flow injection can be either the top or the bottom of the RPV, which will be determined after investigating the results of a thermo-fluid and structural analysis. The cold helium can be supplied by using a

slipstream flow from the helium purification system (HPS). If the required amount of cooling flow is too large to be supplied by the HPS, a dedicated vessel cooling system is to be installed.

There are two design issues arising from the internal flow path. One is a direct bypass flow from the riser to the core through the cross-flow gap between the reflectors. According to the NGNP PCD results of the FES (Fuji Electric Systems), the total amount of bypass flow due to the inlet flow path is as large as 17%, if without any measures to reduce the bypass flow. One of the countermeasures is to install inner tubes in the risers.

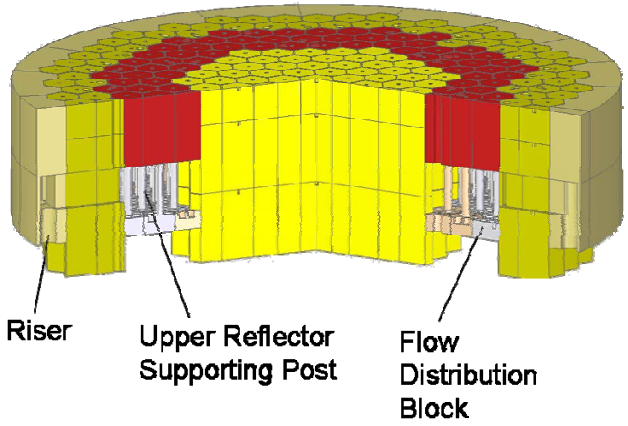

Figure 2.3 Upper plenum structure

The other issue is how to stack the graphite blocks to make the upper plenum structure. An upper plenum structure suggested in this study is shown in Figure 2.3. It introduces the supporting post and the flow distribution block. The cylindrical post is to support the upper reflectors. When the post is directly installed on the fuel block, part of flow channel is blocked because the cross-section of the post is larger than the distance between the coolant channels in the fuel block. Therefore, the flow distribution block is introduced not only to place the supporting posts but also to connect the flow paths between the upper plenum and the core flow channel. Two options for the flow distribution block are shown in Figure 2.4. The both options have a seating place for the post at the center of upper surface. Six holes around the seating place provide flow paths from the upper plenum to the inlet of the core. In the option 1, the connection to the fuel

channel is provided by small holes, while the option 2 has a cavity region at the inlet of the fuel block.

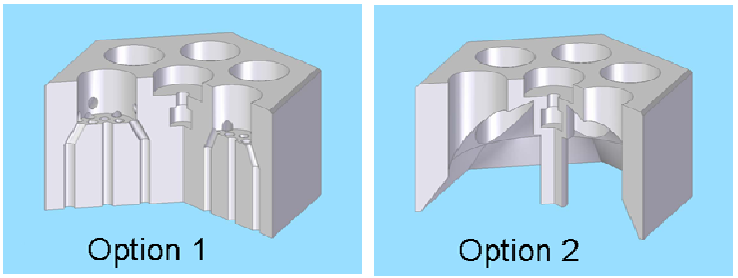

Figure 2.4 Options for a flow distribution block

2.2 Key dimensions

Basic dimensions for the cooled-vessel design should be determined before the thermo-fluid and structural analysis. Most dimensions are based on the GT-MHR except for those related to the cooled-vessel. Schematics and key dimensions in horizontal and vertical cross sections are shown in Figures 2.5 and 2.6.

The effect of the location of riser holes was already investigated in the previous work [Kim, 2007]. The results showed that moving the riser holes closer to the core side provided benefits in reducing the vessel temperature. However, a space for the inlet plenum below the permanent side reflector is to be secured for the connection to the riser holes. So, a compromised location of the riser is selected. The diameter of 54 riser holes is determined to maintain a total area comparable to that of the coolant channel of the GT-MHR, 1.64 m^2. The annular gap distance between the core barrel and the RPV is selected to secure a space for elements such as core lateral restraints.

The thickness of the RPV is determined as follows. According to the ASME Code [ASME, 2004], tentative pressure thickness can be determined by Eq. (1).

$$t = \frac{Pr}{S_m - 0.5P} \qquad (1)$$

Here, where P, r and t are pressure, inner radius and thickness of the vessel, respectively. The stress intensity S_m is determined from the subsection NB. Key dimensions for the thermo-fluid and structural analysis are listed in Table 2.1.

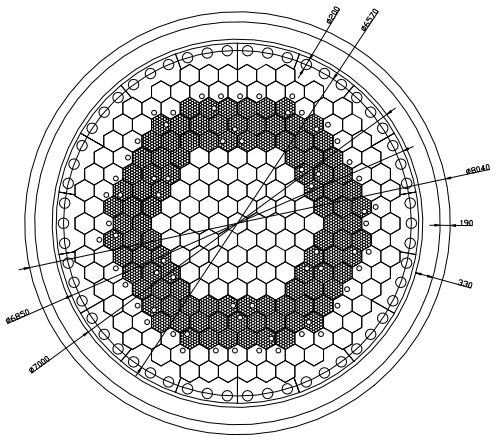

Figure 2.5 Schematic of the cooled-vessel on a horizontal plane.

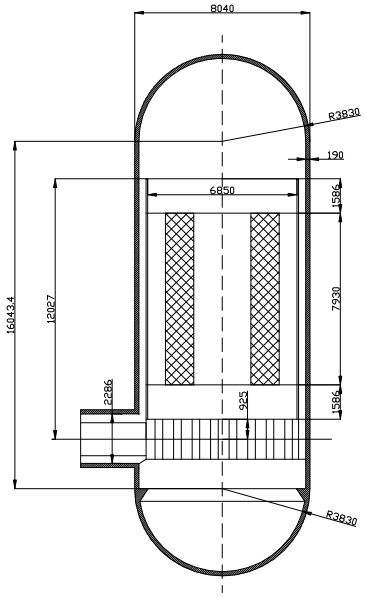

Figure 2.6 Schematic of the cooled-vessel on a vertical cross section

Table 2.1 Key dimensions for the thermo-fluid and structural analysis

RPV	Material	SA 508/533 steel
	Height	24.08m
	Inner Diameter	7.66m
	Outer Diameter	8.04m
	Thickness	0.19m
Distance between RPV and CB		0.33m
Core Barrel	Material	Alloy 800H
	Inner Diameter	6.85m
	Outer Diameter	7.00m
	Thickness	0.075m
Riser	Number of Holes	54
	Hole Diameter	0.2m
	Diameter of Hole Position	6.57m
Core	Height of Active Region	7.93m
	Height of Upper Reflector	1.586m
	Height of Lower Reflector	1.586m
Lower Plenum Height		1.85m

3. THERMO-FLUID ANALYSIS USING GAMMA+ CODE

The system thermo-fluid calculations are performed in order to obtain the temperature distributions of the reactor pressure vessel under the normal operating condition and the postulated accidents for the cooled-vessel design that uses the conventional carbon-steel material (SA508 or SA533). This section discusses the steady-state and transient analysis results performed by the GAMMA+ system analysis code. The results are supplied as boundary conditions for the RPV structural analysis as well as the CFD thermo-fluid analysis.

3.1 Description of system TF analysis model

The GAMMA code [Lim, 2006] was developed for the analysis of VHTR thermo-fluid transients including air ingress phenomena. The code capability was extended and the GAMMA+ code was developed to have enhanced capability for the following models; fluid transport and material properties, multi-dimensional heat conduction, multi-dimensional fluid flow, chemical reactions, multi-component molecular diffusion, fluid heat transfer and pressure drop, heat generation and dissipation, and radiation heat transfer.

The reference analysis inputs for the GT-MHR are taken from the GT-MHR conceptual design report [GA, 2002] and the INEEL ATHENA PMR input [INEEL, 2005]. Based on the reference inputs, the GAMMA+ code input was prepared for the NGNP preconceptual engineering services in 2007. In order to reflect the modified design of the cooled-vessel design, some modifications were made in the previous GAMMA code input.

Figure 3.1 shows the whole system modeling using the GAMMA+ code. It consists of the reactor coolant system, the reactor cavity and the reactor cavity cooling system (RCCS) and the vessel cooling system (VCS). All solid regions are two- or three-dimensionally modeled having total meshes of 675. The fluid regions are modeled by the combination of two- and one-dimensional flow networks with total meshes of 375. In particular the reactor cavity and the annulus between the core barrel and the RPV are modeled two-dimensionally in order to consider the natural circulation flow characteristics. The thermal radiation heat transfers are considered in the top plenum, the annulus between the core barrel and the RPV, the reactor cavity containing the RCCS panels, and the annulus between the downcomer wall and the reactor cavity wall.

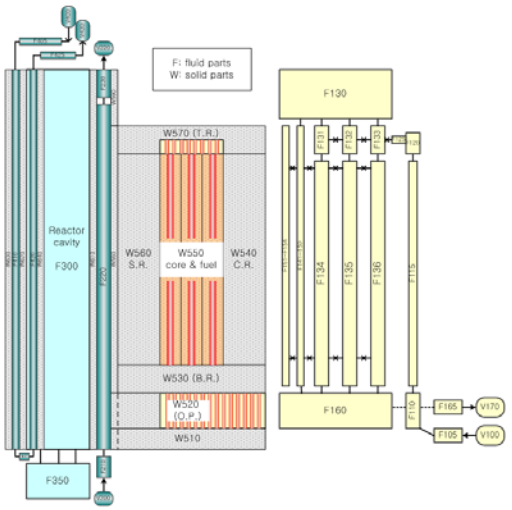

Component	Description	Meshes
F105,F165	Coaxial pipe	1,2
F110	Inlet bottom plenum	1
F115	Inlet riser holes	12
F120, F125	Inlet top plenum	1,2
F135	Top head	1
F131~3	Core top void	2
F134	Inner coolant channel	12
F135	Middle coolant channel	12
F136	Outer coolant channel	12
F141~150	FA bypass channel	14
F151,154	CR bypass channel	14
F152,153	RSC bypass channel	12
F160	Outlet plenum	4
F210,230	VCS inlet & outlet	1,1
F220	Vessel cooling channel	3x11
F300	Reactor cavity (RCCS)	3x20
F350	Reactor cavity (remain)	1
F405	RCCS inlet header	1
F410	RCCS downcomer	12
F415	RCCS lower plenum	1
F420	RCCS tube riser	12
F425	RCCS outlet header	1
W510	Bottom support	14x3
W520	Outlet plenum	14x2
W530	Bottom reflector	11x2
W540	Central reflector	5x10
W550	Fuel & core reflector	3x10
W560	Side reflector	3x10
W570	Top reflector	11x2
W580	Core barrel	3x14
W590	Upper shroud	3x3
W610	Reactor pressure vessel	5x20
W620	RCCS downcomer wall	3x20
W630	Reactor cavity wall	4x20
W640	RCCS panel	2x20x4

Figure 3.1 Analysis model of the GAMMA+ code for the cooled-vessel concept

The core fluid region is modeled in more detail to consider all the bypass flow paths as shown in Figure 3.2. The bypass flow paths modeled are those through the vertical and horizontal gaps between the fuel blocks, through the reserved shutdown and control rod holes. The cross-flow model is applied between the vertical bypass channels for lateral flow. The gap sizes used in the current analysis are 2 mm for the horizontal gaps and 1.5 mm for the vertical gaps between the fuel blocks, respectively.

The core power distribution is obtained from the GAMMA+/VSOP linkage calculation. Figure 3.3 shows the power distributions for the two different helium inlet temperatures of 490°C and 590°C, respectively. The beginning-of-cycle (BOC) core condition has higher peaking and, thus, conservatively selected for the analysis.

Free convection heat transfer occurs in the reactor cavity and the annulus between the core barrel and the RPV during the steady-state and the transients. In order to quantify the heat transfer from the core to the RCCS, the following heat transfer correlation for a vertical annulus [Keyhani, 1983] is used.

$$Nu = 1.406 Ra^{0.077}, \quad \text{for } Ra \le 6.6\times10^{3} \quad \text{(conduction regime)}$$
$$Nu = 0.163 Ra^{0.322}, \quad \text{for } Ra > 6.6\times10^{3} \quad \text{(boundary layer regime)}$$

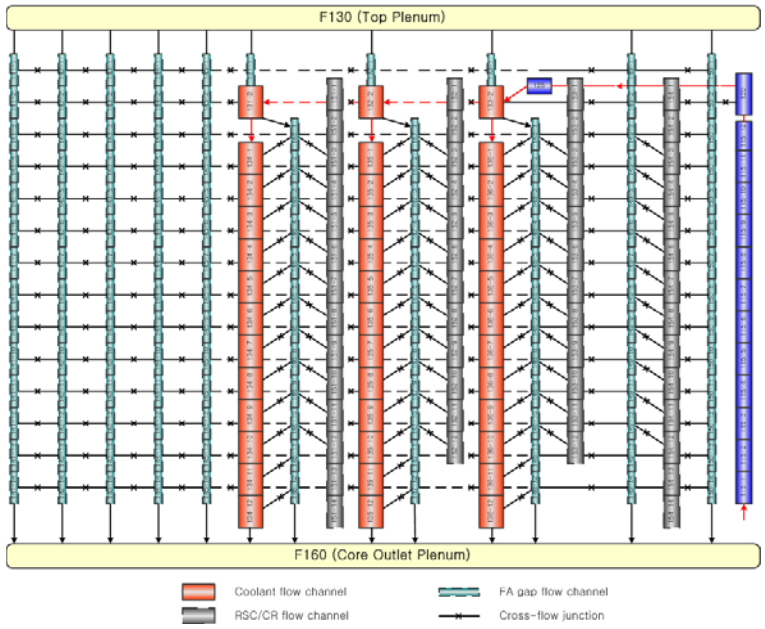

Figure 3.2 Flow network model of the GAMMA+ code for the inlet riser, core coolant, FA gap bypasses, and RSC/CR channels

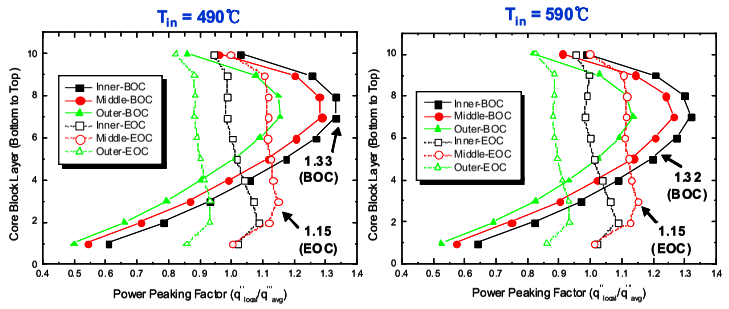

Figure 3.3 Core power distributions from the GAMMA+/VSOP linkage calculation

To consider the effect of the aspect ratios of height and radius, the correlation is re-formulated as follows:

$$Nu = 0.800 Ra^{0.077} H^{-0.052} K^{0.505}, \quad \text{for } Ra \le 6.6\times10^3$$
$$Nu = 0.187 Ra^{0.322} H^{-0.238} K^{0.442}, \quad \text{for } Ra > 6.6\times10^3$$

where H is the aspect ratio, height/width, and K is the radius ratio, R_o/R_i. The Rayleigh number is based on the width, $R_o - R_i$.

Both the air- and water-cooled RCCS are modeled in the analysis. The air-cooled RCCS is modeled one-dimensionally, referencing the GT-MHR design and assuming the inlet pressure and temperature of 1 bar and 43°C, respectively. For the water-cooled RCCS option, since the water-cooling loop design data is unavailable at present, we made simple assumptions based on the conditions of GT-MHR Burner [IAEA, 2000]. The RCCS panel average temperature is kept at 65°C without boiling during normal operation while it increases up to 140°C in 5 hours during the accident and the boiling is allowed inside the RCCS. The heat loss from the outside of the reactor concrete wall to an environment is modeled using a constant heat transfer coefficient of 5 W/m^2-K and an emissivity of 0.6 at an air temperature of 30°C.

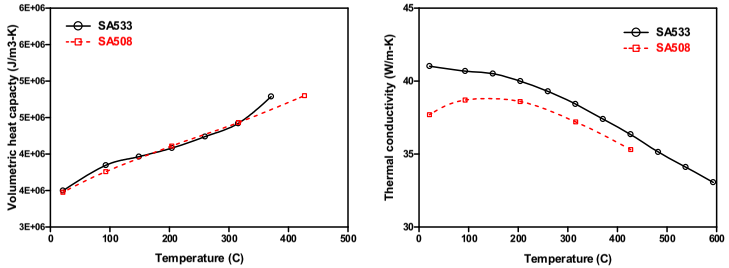

Figure 3.4 Material properties of the steel-alloy RPV for SA533 and SA508

The material properties of steel alloys considered in the cooled-vessel concept are shown in Figure 3.4. The heat capacities of SA533 and SA508 are similar each other, meanwhile the thermal conductivities are quite different. To be conservative, we selected the SA508 properties in the analysis.

3.2 Steady-state and transient analysis results

3.2.1 Analysis cases and major parameters from the analysis

Four analysis cases are defined in the cooled-vessel design studies; two helium inlet conditions of 490°C and 590°C and two RCCS cooling types, air-cooled and water-cooled. Table 3.1 shows the major parameters during the steady-state for four analysis cases. For the cases with the helium inlet temperature of 490°C, the peak RPV temperature is below the target temperature limit of 350°C even without the VCS flow. The heat loss to the RCCS is higher in the water-cooled RCCS option than in the air-cooled RCCS option. For the cases where the VCS is necessary (Tin=590 °C), however, the total heat loss to the VCS and the RCCS is higher in the air-cooled RCCS option than in the water-cooled RCCS option. It is because the required VCS flow to meet the target RPV temperature limit (350°C) is about twice larger in the air-cooled RCCS than in the water-cooled RCCS.

Table 3.1 Steady-state cases and major parameters from the analysis

Cases	Case 1	Case 2	Case 3	Case 4	Remarks
Core thermal power, MW	600		600		
RCCS cooling type	Air-cooled RCCS		Water-cooled RCCS		
RCS inlet/outlet temperature, °C	490/950	590/950	490/950	590/950	
Heat removal by, MW					
VCS	-	3.08	-	1.74	VCS inlet temperature of 140 °C
RCCS	1.76	1.36	2.08	2.15	
Sum=	1.76	4.44	2.08	3.89	
VCS helium flow, kg/s	-	3.08	-	1.48	
Peak RPV temperature, °C	347.6	350.0*	313.7	350.0	

Note *: target RPV peak temperature limit under normal operating condition

In the cases of Table 3, the VCS cold helium is injected at the bottom head of the RPV. In order to investigate the effect of VCS injection location, additional cases with VCS injection at the top of the RPV are analyzed and the steady-state results are shown in Table 3.2. The VCS flow required to keep the vessel temperature within the target limit is further reduced, and therefore the total heat loss becomes less. This is more prevailing

in the air-cooled RCCS option.

Table 3.2 Additional steady-state cases for VCS injection at RV top and major parameters from the analysis

Major parameters		Air-cooled RCCS	Water-cooled RCCS	Remarks
VCS injection nozzle location		RV upper head		
RCS inlet/outlet temperature, °C		590/950		
Heat removal by, MW	VCS	2.02	1.10	VCS inlet temperature of 140 °C
	RCCS	1.64	2.38	
	Sum=	3.66	3.48	
VCS helium flow, kg/s		2.14	1.06	

The transient analyses are performed for the High Pressure Conduction Cooldown (HPCC) accident that is the limiting case for vessel heatup at high pressure condition, and the Low Pressure Conduction Cooldown (LPCC) accident that is the limiting case for vessel heatup at low pressure. Transient flow and pressure boundary conditions for the transient calculation are described in Table 3.3. The predicted peak fuel and RPV temperatures show the consistent trend, that is, lower temperatures for lower inlet temperatures and for the water-cooled RCCS option that has larger heat removal capacity.

Table 3.3 Transient cases and major parameters from the analysis

Cases	Case 1		Case 2		Case 3		Case 4	
Initial condition	490/950		590/950		490/950		590/950	
Initiation event	HPCC	LPCC	HPCC	LPCC	HPCC	LPCC	HPCC	LPCC
Peak fuel temp., C	1358	1536	1375	1544	1344	1526	1365	1535
Peak RPV temp., C	432	519	437	526	381	460	386	466
RCCS	Air-cooled				Water-cooled			
Event scenarios and assumptions	1. Core power switches to GA decay curve at time zero 2. RCS & VCS flows decrease to zero in 60 seconds (HPCC), and in 10 seconds (LPCC) 3. RCS & VCS pressures remain at 70 bar (HPCC), and decrease to 1 bar in 10 seconds (LPCC) 4. RCCS panel temperature increases from 65 °C to 140 °C in 5 hours for the water-cooled RCCS option							

3.2.2 Case 1: Tin/Tout=490/950°C (Air-cooled RCCS)

Figure 3.5 shows the RPV temperature profile at full power normal operation. Even without the VCS flow, the peak RPV temperature remains below the target temperature limit of 350°C. The RPV temperature profile is almost flat and the hottest point locates beside the top reflector region, due to the natural circulation in the annulus between the core barrel (CB) and the RPV.

Figure 3.6 shows the RPV temperature transients during the HPCC/LPCC accidents. The peak RPV temperature locations are different in the HPCC and LPCC accidents. In the case of the HPCC accident where the RCS pressure remains at 70 bars, the peak RPV temperature occurs at the top reflector region like the steady-state case due to the natural circulation inside the CB/RPV annulus. In case of the LPCC accident where the RCS pressure is at 1 bar, the peak RPV temperature occurs at the center elevation of the active core because the radiation heat transfer dominates and the effect of free convection inside the CB/RPV annulus is negligible.

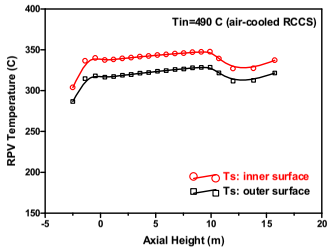

Figure 3.5 RPV temperature profiles at the inside and outside surfaces for Tin/Tout=490/950°C, air-cooled RCCS case

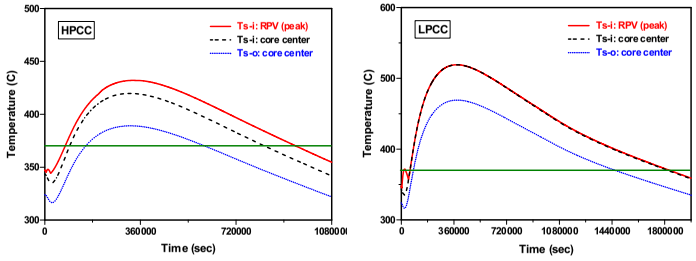

Figure 3.6 RPV temperature transient for Tin/Tout=490/950°C, air-cooled RCCS case (HPCC/LPCC)

3.2.3 Case 2: Tin/Tout=590/950°C (Air-cooled RCCS)

Figures 3.7 and 3.8 show the steady-state RPV temperature profile and the RPV temperature transients during the HPCC/LPCC accident for the Case 2. The VCS flow is required to meet the target RPV temperature limit. With the cold VCS flow from the RPV bottom, the RPV temperature profile becomes steep and the hottest point locates at the top reflector region, while the RPV temperature becomes flat and the hottest point occurs at the outlet plenum region with the cold VCS flow from the RPV top. The trend of the RPV temperature transients in Figure 3.8 are almost identical to those of Case 1, but the RPV peak temperature is slightly higher than that of Case 1 due to higher initial store energy with the helium inlet temperature of 590°C.

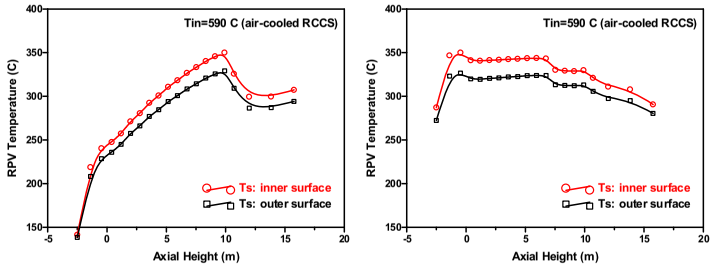

Figure 3.7 RPV surface temperature profiles for Tin/Tout=590/950°C, air-cooled RCCS case: VCS injection at bottom (left) and top (right)

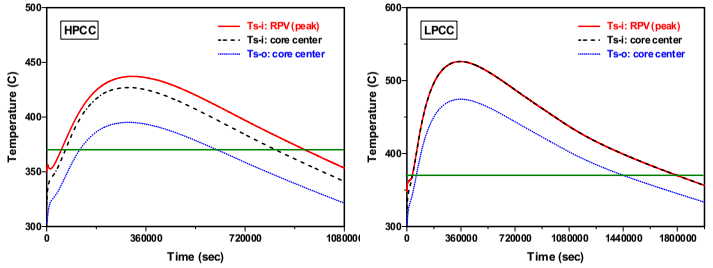

Figure 3.8 RPV temperature transient for Tin/Tout=590/950°C, air-cooled RCCS case (HPCC/LPCC)

3.2.4 Case 3: Tin/Tout=490/950°C (Water-cooled RCCS)

Figures 3.9 and 3.10 show the steady-state RPV temperature profile and the RPV temperature transients during the HPCC/LPCC accident for the Case 3. The RPV temperature profile and transients are similar to that of Case 1 (air-cooled RCCS). However, the peak RPV temperature is lower than that of Case 1 because the heat removal by the water-cooled RCCS is larger than that of the air-cooled case.

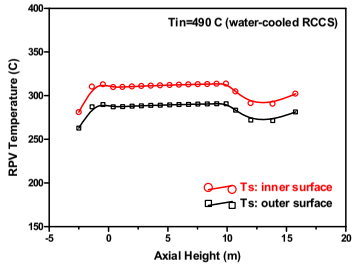

Figure 3.9 RPV temperature profiles at the inside and outside surfaces for Tin/Tout=490/950°C, water-cooled RCCS case

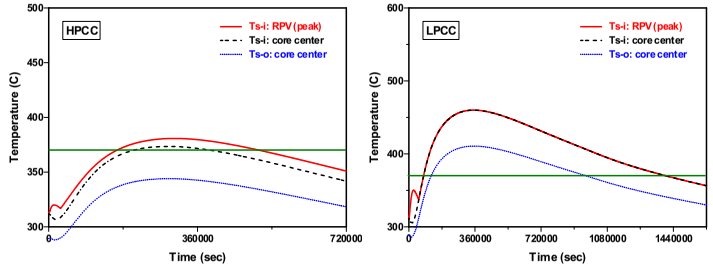

Figure 3.10 RPV temperature transients for Tin/Tout=490/950°C, water-cooled RCCS case (HPCC/LPCC)

3.2.5 Case 4: Tin/Tout=590/950°C (Water-cooled RCCS)

Figures 3.11 and 3.12 show the steady-state RPV temperature profile and the RPV temperature transients during the HPCC/LPCC accident for the Case 4. The RPV temperature profile and transients are similar to that of Case 2 (air-cooled RCCS), but the profile of RPV temperature is less steep than that of Case 2. It is because the required VCS flow is small due to the larger heat removal by the water-cooled RCCS. The RPV temperature transients in Figure 3.12 show similar trend with those of Case 2 (air-cooled RCCS). However, the peak RPV temperature is lower than that of Case 2 because of larger heat removal by the water-cooled RCCS.

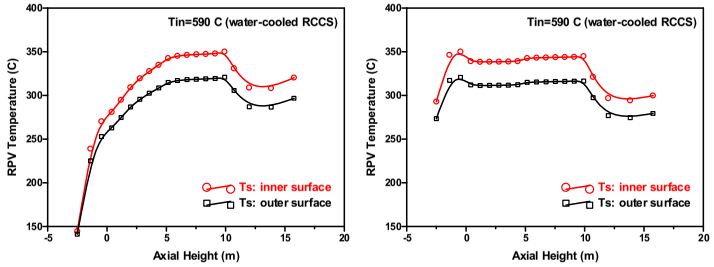

Figure 3.11 RPV surface temperature profiles for Tin/Tout=590/950°C, water-cooled RCCS case: VCS injection at bottom (left) and top (right)

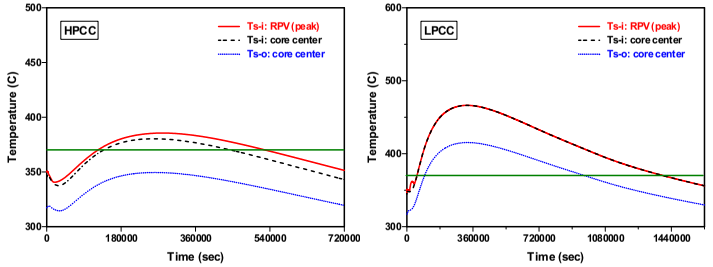

Figure 3.12 RPV temperature transients for Tin/Tout=590/950°C, water-cooled RCCS case (HPCC/LPCC)

3.2.6 Fuel temperature transients

The peak fuel temperatures transients during the HPCC and LPCC accidents are compared in Figure 3.13. Similar to the RPV temperature transients, the fuel temperature transient is less affected by the helium inlet temperatures. However, in contrast to the RPV temperature transients, the fuel temperature transients are not much affected by the RCCS cooling types, even though they are lower with the water-cooling RCCS.

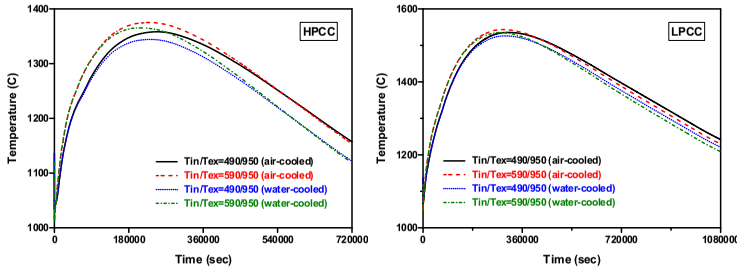

Figure 3.13 Peak fuel temperature and RCCS heat removal transients during the HPCC and LPCC accidents

4. THERMO-FLUID ANALYSIS USING CFX CODE

Detailed steady-state thermo-fluid analyses using a CFD model are conducted not only to investigate the detailed flow and heat transfer phenomena that occur in the cooled-vessel design but also to verify the results of the GAMMA+ analysis. A commercial CFD code, CFX [ANSYS, 2006], is used. This section describes a CFD model and its analysis results.

4.1 CFD analysis model

4.1.1 Computational domain

In order to get the core and RPV temperature distribution during steady-state, a heat transfer to the RCCS should be taken into account. Dimensions of the RPV internal structure are given in Section 3 and Figure 4.1 shows the layout of the RCCS adopted in this work.

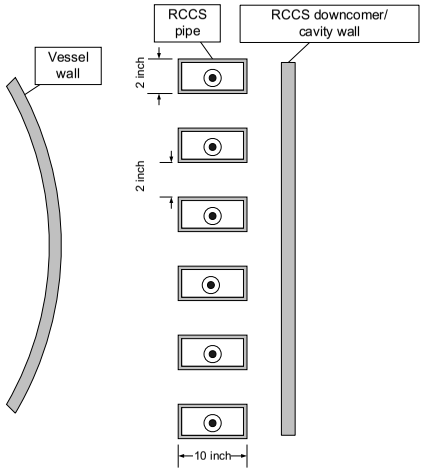

Figure 4.1 Layout of the considered RCCS system

In the case of the air-cooled RCCS, the design is assumed to be the same as that for the GT-MHR [General Atomics, 1996]. The width of the reactor cavity is 1.18 m. A total

of 292 tubes are vertically arranged in the reactor cavity. Each tube is a standard structural steel tube of rectangular cross section having external dimensions of 2 in. x 10 in. with 0.1875 in. wall thickness. The pitch between the tubes is 2 in. The same physical dimensions of the RCCS pipes are assumed for the water-cooled RCCS. A reflective surface/insulation (microtherm) is provided as a part of the downcomer wall in the air-cooled system. On the other hand, it is assumed that the concrete wall directly faces the RPV in the water-cooled system.

A CFD simulation of the entire vessel geometry including the reactor cavity and the RCCS requires tremendous computing resources. In this work, therefore, a 1/54 model is used for efficient calculations by using the symmetric assumptions. Complex geometries inside the RPV are also simplified. Such simplifications will not affect the thermal behavior of the RPV significantly.

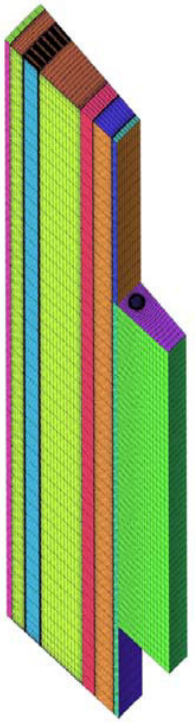

Figure 4.2 Isometric view of the computational meshes

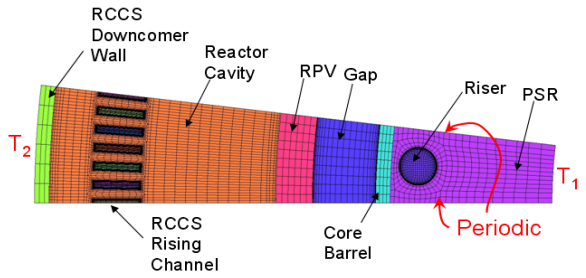

Figure 4.3 Top view of the computational meshes

Figure 4.2 shows the computational domain of the CFD analysis for the cooled-vessel design. Figure 4.3 shows top view of the computational meshes. The domain includes the 1/54 section of the graphite reflector, the riser hole, the gap for vessel cooling, the RPV, the reactor cavity, the RCCS tubes, and the downcomer wall (or cavity wall). The height of the domain is 19.873 m. Spherical shell geometry of the vessel head is simplified to be an annulus. Furthermore, it is assumed that six RCCS tubes are located in the 1/54 section, which results in a total of 324 tubes. The width of the RCCS tube is decreased by ~10% in order to conserve the radiation heat transfer area of the RCCS tubes of GT-MHR.

4.1.2 Numerical models

The CFD analysis of the cooled-vessel design needs to consider the thermo-fluid phenomena consisting of multi-dimensional heat conduction, conjugate heat transfer between solid and fluid, convective heat transfer, buoyancy, and radiation heat transfer. Buoyancy induced turbulent flows are expected in the reactor cavity and the gap between the RPV and the core barrel, where the Rayleigh numbers (based on the width) are estimated to be larger than 10^7 [Holman, 1986]. The Reynolds number of the flow at the inlet of the riser hole is ~765,000. Therefore, a highly turbulent flow is expected in the riser hole. The k-ε turbulence model with the scalable wall function is applied to the fluid flows in the reactor cavity, the gap between the RPV and the core barrel, and the riser hole. In order to consider the buoyancy, the full buoyancy model is used to the helium flow in the gap whereas the Boussinesq approximation model is used to the air flow in the reactor cavity. The estimated buoyancy reference temperature and buoyancy

reference density are used from the CFD solutions with initially guessed values. For the radiation heat transfer, the discrete transfer model (DTM) is applied with the option of "surface to surface transfer mode". High resolution scheme is selected for the advection scheme, in which the blending factors to blend between the first and the second order advection schemes vary throughout the computation domain based on the local solution filed [ANSYS, 2006]. The CFD database for the conductivities and emissivities of the solid materials is the same as those for the GAMMA+ analysis.

4.1.3 Boundary conditions

The boundary conditions for the CFD analysis are mainly based on the results of the GAMMA+ analysis. The boundary conditions imposed for the CFD analysis for the cooled-vessel design are summarized in Table 4.1.

Table 4.1 Summary of the boundary conditions imposed for the CFD analysis

Solid boundary	
- Graphite reflector surface	Temperature profile calculated by GAMMA+
- Inner surface of barrel	Temperature profile calculated by GAMMA+
- Inner side RCCS tube	Fixed temperature of 65 °C (water cooled RCCS only)
- Symmetric side surfaces	Rotational periodic boundary
- Outer surface of downcomer wall	Adiabatic
- Top and bottom walls	Adiabatic
Riser flow	
- Inlet	Mass flow calculated by GAMMA+ Inlet temperature of 490/590 °C
- Outlet	Pressure boundary
Vessel cooling flow (if exists)	
- Inlet	Mass flow calculated by GAMMA+ Inlet temperature of 140 °C
- Outlet	Pressure boundary/opening boundary
- Symmetric side surfaces	Rotational periodic boundary
RCCS flow (air cooled RCCS only)	
- Inlet	Mass flow calculated by GAMMA+ Inlet temperature calculated by GAMMA+
- Outlet	Pressure boundary
- Symmetric side surfaces	Rotational periodic boundary

Figure 4.4 shows the positions of the imposed boundary conditions. It should be noted that for the water-cooled RCCS, the fixed temperature of 65 °C is imposed on the inner side of the RCCS tube, which is the same boundary condition of the GAMMA+ analysis.

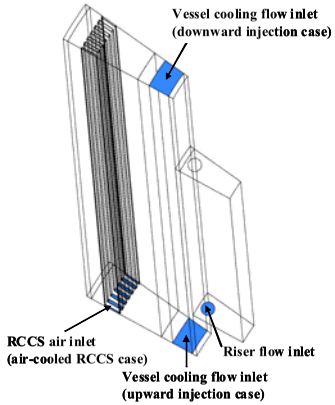

(a) Fluid inlet boundaries

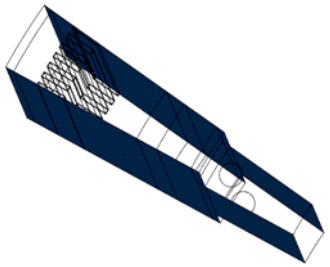

(b) Periodic boundary surfaces

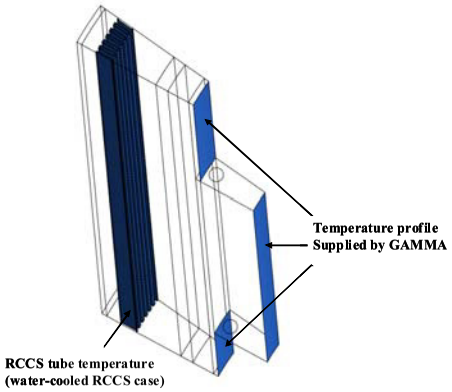

(c) Fixed temperature wall boundaries

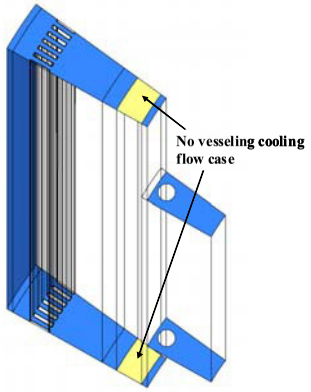

(d) Adiabatic wall boundaries

Figure 4.4. Positions of the imposed boundary conditions

4.2 Results of CFD analysis

Cases considered in the analysis are given in Table 4.2. Three cases are for the air-cooled RCCS and one case is for the water-cooled RCCS. For the air-cooled RCCS, one case is for the RPV inlet temperature of 490°C where the VCS is not required and two cases are defined for the RPV inlet temperature of 590°C where the VCS injection location is top and bottom. For the water-cooled RCCS, one case is selected for the RPV inlet temperature of 490°C without the VCS.

The other cases for the water-cooled RCCS at 590°C inlet temperature are not considered by two reasons; 1) the vessel cooling flow is adjusted to maintain the RPV temperature at the target temperature of 350°C and 2) the effect of the VCS injection location is expected similar to the cases for the air-cooled RCCS. The vessel cooling and RCCS flow for the air-cooled cases are given in Table 4.2 as obtained from the GAMMA+ results. For the water-cooled RCCS, the same configuration as the air-cooled RCCS is used, but the inner surface temperature of the RCCS rising channel is fixed at 65°C.

Table 4.2. Cases considered in the CFD analysis for steady state

Parameters	Case 1	Case 2a	Case 2b	Case 3
RCCS Type	Air-Cooled			Water-Cooled
T_{in}/T_{out} (°C)	490/950	590/950	590/950	490/950
Vessel Cooling System	No	Yes	Yes	No
VCS Helium Flow (kg/s)	N/A	2.33	2.20	N/A
VCS Flow Injection	N/A	Bottom	Top	N/A
RCCS Flow (kg/s)	12.58	11.84	12.44	Constant Wall T.
RCCS Inlet T (°C)	46	46	46	65

4.2.1 Air-cooled RCCS

Flow distribution inside the gap between the core barrel and the reactor vessel is investigated. Figure 4.5 shows the streamlines and velocity vectors in the gap. The case 1, 490°C of the inlet temperature and no vessel cooling flow, represents a typical pattern of natural circulation between two vertical plates. Counter-clockwise natural circulation

is formed, since the core barrel side is hotter than the RPV wall. However, the case 2a, 590°C of the inlet temperature and the vessel cooling flow from the bottom, shows a different flow pattern. Since the forced convection flow by the VCS is smaller than the buoyancy force that drives the natural convection, most of the flow injected for cooling moves upward along the core barrel. Thus, the cold helium flow at 140°C first cools down the bottom of the core barrel, which reduces the upward buoyancy force at that region. This results in the breach of the natural circulation flow. The result for the case 2b, 590°C of the inlet temperature and the vessel cooling flow from the top, shows a similar flow pattern to the case 1 but the amount of circulation flow is larger than that of the case 1, since the cold helium flow injected moves downward along the vessel surface and it makes a positive effect to the natural circulation.

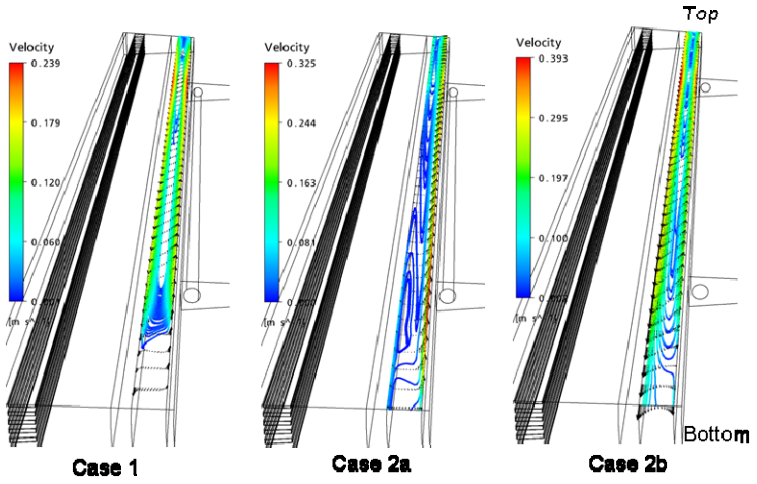

Figure 4.5 Flow distribution in the gap region

Figure 4.6 shows the flow distribution in the reactor cavity where different flow patterns are observed. The results from the case 1 show a fully-developed natural circulation flow across the whole height of the cavity. A wavy pattern of flow occurs between the rising channel and the downcomer wall of the RCCS due to temperature difference between them. The temperature of the downcomer wall side is higher than

that of RCCS channel surface due to the radiation reaching on the wall through the space between the channels. Therefore, the higher temperature at the downcomer wall heats the flow moving downward, which induces an adverse pressure gradient and results in the separation of the flow from the wall. As the flow downward along the downcomer wall meets the RCCS channel, the relatively low temperature of the channel surface cools the flow. Then, the flow moves back to face the downcomer wall and it is heated again, which results in a repeated wavy flow. The results from the case 2a show a similar pattern to the case 1. The vessel cooling flow makes the vessel temperature at the bottom region decrease, which results in a decrease of the buoyancy force along the vessel wall and reduction of the circulation size in the cavity. The flow pattern observed in the case 2b is different from the previous two cases. Vessel cooling flow from the top reduce the vessel temperature at the top region and makes buoyancy force small, which largely disturbs the natural circulation flow.

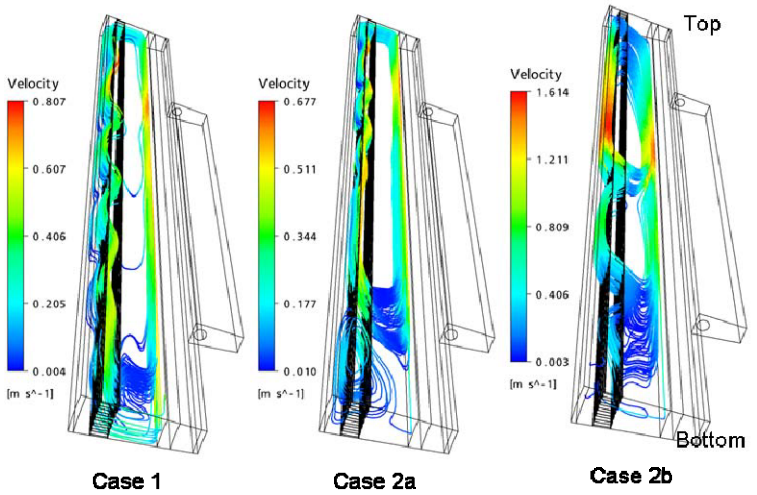

Figure 4.6. Flow distribution in the reactor cavity

Temperature distribution at the level of core center for the case 1 is presented in Figure 4.7. There is the highest temperature in the PSR and the lowest temperature at the inside of the RCCS channel. Except for the region around the riser in the PSR, almost same temperature distribution is observed along the line 1 and 2. At the region between the riser and the core barrel, the graphite temperature near the riser is relatively

high due to the helium coolant flowing through the riser at the temperature of 490°C while the graphite temperatures near the core barrel are the same by a lateral conduction from the lateral side. This results in a steep temperature gradient between the riser and the core barrel along the line 1. Other temperature drops at the surfaces of core barrel, RPV, RCCS channel and downcomer wall are mainly due to the reduced convection heat transfer.

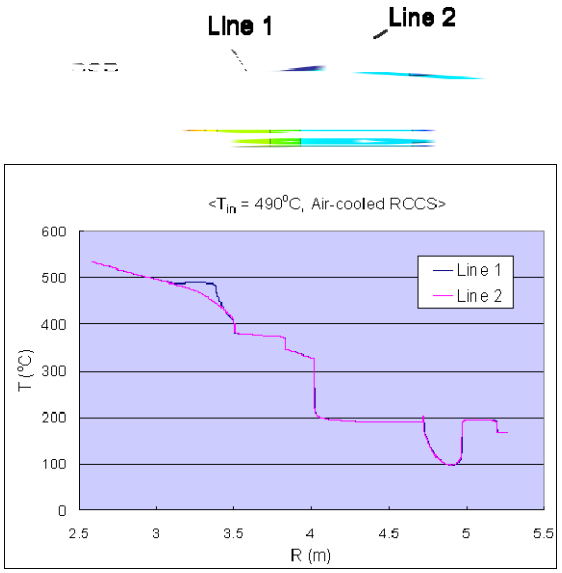

Figure 4.7. Temperature distribution at the level of core center (Case 1)

Comparison of RPV temperature between CFX and GAMMA+ results are shown in Figures 4.8, 4.9 and 4.10 for each case considered for the air-cooled RCCS. The case 1 shows that GAMMA+ results are well reproduced by the CFX, which means that the GAMMA+ model used in the present study is adequate for the prediction of cooled-vessel performance. The comparison for the case 2, shown in Figure 5, also shows good agreement. However, different distribution is observed for the case 2b. The CFX results show that the cold helium flow from the top makes the vessel temperature low at the upper region whereas the GAMMA+ analysis gives much higher temperature. The reason for the difference is that the gap region between the core barrel and the vessel is modeled as one-dimensional fluid cell in the GAMMA+ code in which the multi-

dimensional flow and heat transfer cannot be resolved.

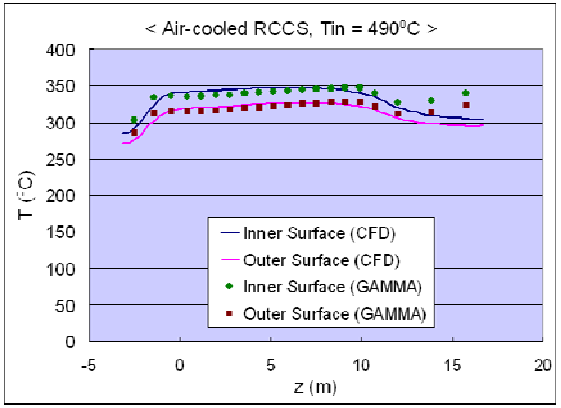

Figure 4.8. Comparison of RPV temperature between CFD and GAMMA+ results for the case 1

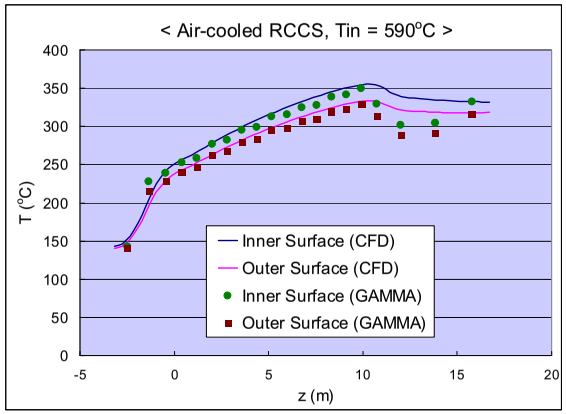

Figure 4.9. Comparison of RPV temperature between CFD and GAMMA+ results for the case 2a

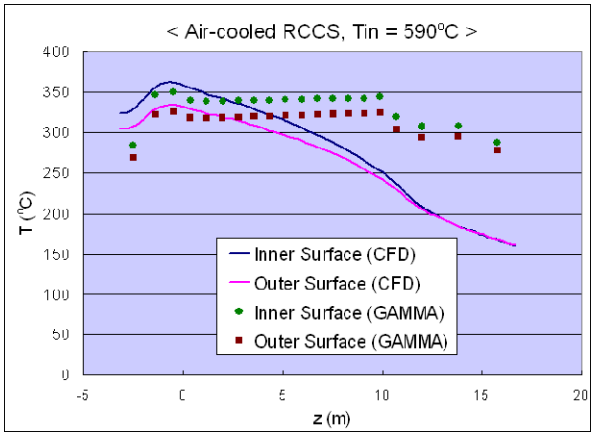

Figure 4.10. Comparison of RPV temperature between CFD and GAMMA+ results for the case 2b

Table 4.3. Comparison of maximum vessel temperature and het loss to RCCS

Parameter		Case 1	Case 2a	Case 2b
		Air-Cooled RCCS		
Tin/Tout (°C)		490/950	590/950	590/950
Vessel Cooling System		No	Yes	Yes
VCS Flow Injection		N/A	Bottom	Top
Max. Vessel T (°C)	CFX	347.2	355.4	363.0
	GAMMA+	347.7	350.0	350.0
RCCS Heat Loss (MWt)	Radiation	1.48 (84.3%)	1.30 (84.1%)	1.09 (82.3%)
	Convection	0.28 (15.7%)	0.25 (15.9%)	0.23 (17.7%)
	Total	1.76 (100%)	1.55 (100%)	1.32 (100%)
	GAMMA+	1.76	1.40	1.65
VCS Heat Loss (MWt)	CFX	N/A	2.68	2.62
	GAMMA+	N/A	2.73	2.04
Total Heat Loss (MWt)	CFX	1.76	4.23	3.94
	GAMMA+	1.76	4.13	3.69

Maximum vessel temperature and heat loss to the RCCS are given in Table 4.3 and compared with the GAMMA+ results. The result for the case 1 shows very good agreement with the GAMMA+ not only for the temperature but also for the heat loss to the RCCS. According to the results, radiation heat transfer accounts for about 84% of RCCS heat loss while that of convection is about 16% for the case 1, which emphasizes that emissivity of the RPV is a key parameter for heat transfer from the vessel to the RCCS. The results for the case 2a also show good agreement but a little difference is observed for the case 2b. As explained before, this is due to one-dimensional modeling of the gap in the GAMMA+ analysis, especially at the top region of the gap where the injected cold helium flows downward along the vessel wall.

4.2.2 Water-cooled RCCS

Although the GAMMA+ analysis result indicated that the air-cooled RCCS can provide a heat removal capacity for maintaining the vessel temperature below 350°C, it is needed to secure more safety margin for the cooled-vessel design. According to the GAMMA+ result, the water-cooled RCCS decreases the vessel temperature by about 30°C due to its higher heat removal capacity. Since the selection of RCCS option in the cooled-vessel design is so important, it is required to validate the GAMMA+ results using more detailed CFD results. As shown in Table 4.2, a case considered for the water-cooled RCCS is for the inlet temperature of 490°C without vessel cooling flow.

To examine the effects of the RCCS type on the flow and heat transfer, the results for the water-cooled RCCS (Case 3) are compared with those of the air-cooled RCCS (Case 1). Figure 4.11 shows flow distribution in the gap region. The flow pattern for the water-cooled RCCS is not different from the air-cooled RCCS, while the local flow velocity is increased by an enhanced heat removal to the water-cooled RCCS.

Flow distribution in the cavity region described in Figure 4.12 gives somewhat different flow pattern. The wavy pattern observed in the RCCS channel is much more severe than the air-cooled RCCS. Figure 4.13 shows temperature profiles for two RCCS types along the line at the height of core center. The larger heat removal capacity of the water-cooled RCCS results in a higher temperature gradient across the vessel than that of the air-cooled RCCS. Since the downcomer wall temperature is higher due to radiation than the RCCS channel surface, the local flow pattern near the downcomer wall is distorted and results in the three circulating cells. It affects the flow and heat transfer near the vessel wall.

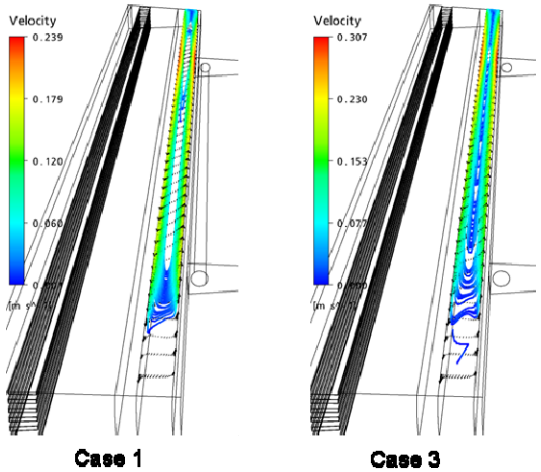

Figure 4.11 Comparison of flow distribution in the gap for two RCCS types

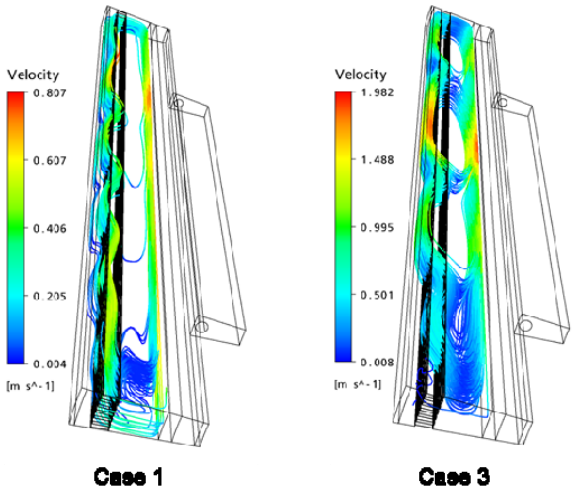

Figure 4.12 Comparison of flow distribution in the cavity for two RCCS types

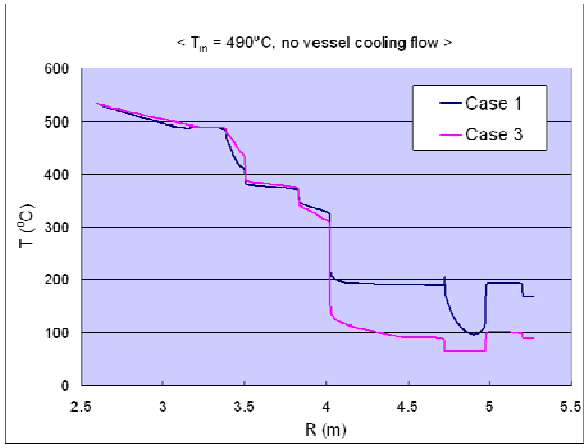

Figure 4.13 Comparison of temperature profiles for two RCCS types along the line at the height of core center

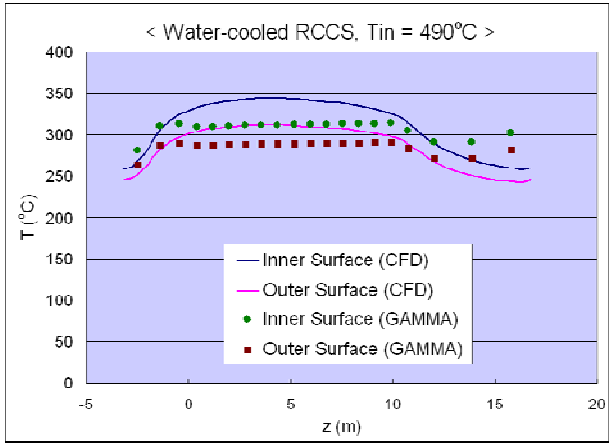

Figure 4.14 Comparison of RPV temperature between CFD and GAMMA+ results for the case 3

Figure 4.14 compares the RPV temperature distribution along the vessel between the CFX and GAMMA+ results. The CFX result gives higher temperature in the core region than that from the air-cooled RCCS. It is deemed that the wavy flow moving upward as shown in Figure 4.12 leads the difference between two results. Relatively coarse modeling of the reactor cavity of the GAMMA+ was not able to catch the flow distortion in the cavity that was observed in the CFX analysis.

To see how the flow for the water-cooled RCCS is deviated from the air-cooled RCCS, z-directional velocities along the line at the radial location of 38mm off the vessel surface are compared in Figure 4.15. The velocity variation for the water cooled RCCS is remarkably increased, while the variation for the air-cooled RCCS is relatively mild. Therefore, it is seen that the main reason for the difference of the vessel temperatures between two results comes from the local velocity and temperature distribution and consequent heat transfer.

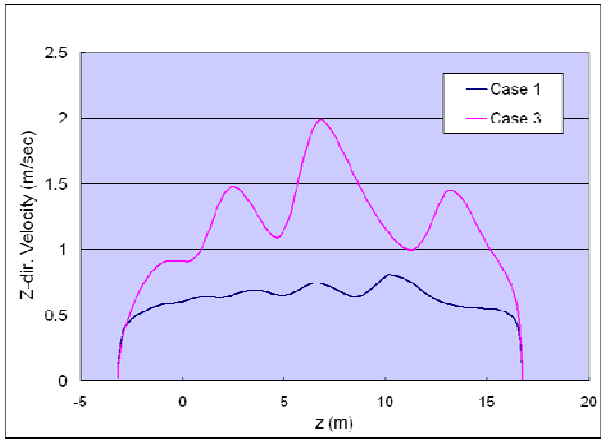

Figure 4.15 Comparison of z-directional velocity along a vertical line at r=4.4m

Table 4.4 summarizes of the maximum RPV temperature and the heat loss to the RCCS for results of two RCCS types. It is shown that the maximum vessel temperature does not decrease to the amount predicted by the GAMMA+ code for the case 3. In consequence, larger heat loss to the RCCS by the radiation is predicted by the CFD code. The convection heat transfer to the RCCS is also increased by local circulating flow in the cavity.

Table 4.4 Comparison of the maximum vessel temperature and heat loss to RCCS for two RCCS types

Parameter			Case 1	Case 3
RCCS Type			Air-cooled	Water-cooled
Tin/Tout (°C)			490/950	490/950
Vessel Cooling System			No	No
Max. Vessel T (°C)	CFX		347.2	343.8
	GAMMA+		347.7	313.7
RCCS Heat Loss (MWt)	CFX	Radiation	1.48 (84.3%)	1.77 (71.6%)
		Convection	0.28 (15.7%)	0.71 (28.4%)
		Total	1.76 (100%)	2.48 (100%)
	GAMMA+		1.76	2.08

5. STRUCTURAL ANALYSIS

The objective of this study is to evaluate the structural integrity of the RPV for a proposed cooled vessel design which adopts SA503/533 as RPV material under the selected normal operating conditions and accidents. The RPV integrity for four normal operating conditions that consist of the inlet temperature of 490°C and 590°C and of two different types of RCCS, that is, the air- and water-cooled RCCSs, has been selected for the steady state analysis.

As described in the sections 2 and 3, the RPV temperature during normal operation is maintained below 371℃ so that the conventional ASME Boiler and Pressure Vessel Code, Section III, Subsection NB is applicable for this evaluation. Two thermal transient conditions (HPCC and LPCC) initiated from the four normal operating conditions were considered in the evaluation of structural integrity as the accident conditions. When the RPV temperature exceeds 371℃ which is the limiting temperature for Subsection NB during thermal transients, the Code Case N-499-2 (CC N-499) shall be used to evaluate the structural integrity of SA533 Grade B, Class 1 material for the limited temperature service. The CC N-499 describes general guidelines and allows the ASME Boiler and Pressure Vessel Code, Section III, Subsection NH as an applicable design code for class 1 components using SA533 Grade B, Class 1 material in the elevated temperature service conditions.

The structural integrity of the cooled-vessel against the transient thermal loadings has been demonstrated per the ASME Code Subsection NB and the CC N-499. Total 8 different transient thermo-mechanical loadings were obtained from the transient analysis using the GAMMA+ system analysis code. The design by analysis procedures per ASME Code Subsection NH has been applied with the mechanical and physical property values at elevated temperatures in the CC N-499.

5.1 Preparatory works for structural analysis

In order to evaluate the structural integrity of the cooled vessel, the RPV is modeled and the thermo-mechanical analyses are conducted using the ANSYS finite element analysis code.. The schematic of the RPV is shown in Figure 5.1. The RPV is vertically divided into 21 elevations as the GAMMA+ model. The height, inner diameter, and thickness of the RPV are 24083mm, 7660mm, and 190mm, respectively.

5.1.1 Modeling of the RPV

Thermal analyses and corresponding structural analyses were performed using ANSYS finite element code. Total number of 4-node axisymmetric finite elements and nodes are 2964 and 3465, respectively as shown in Figure 5.2. In this conceptual design stage, a simple egg-shell shape RPV without geometric discontinuities such as nozzles or flanges was analyzed. Linear elastic analyses were performed and inelastic quantities such as accumulated inelastic strains at elevated temperature services are to be evaluated according to the contents of the CC N-499 and Subsection NH.

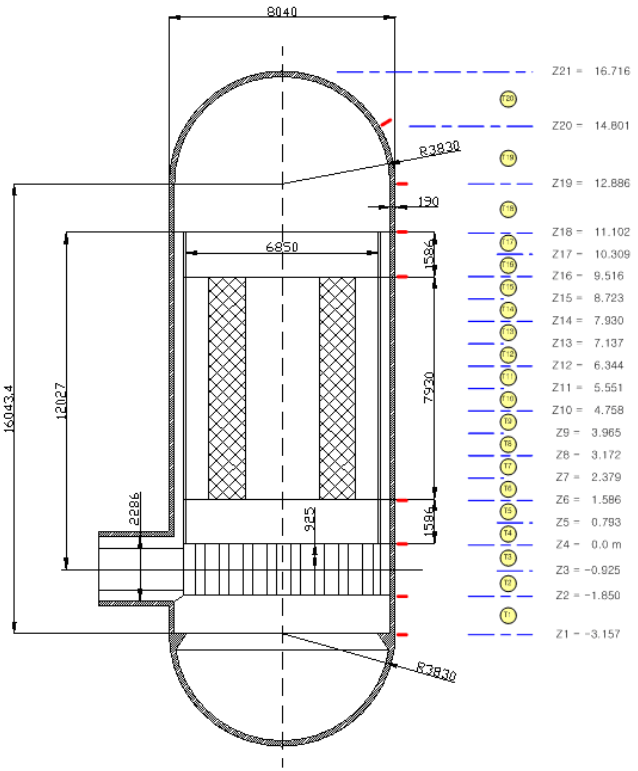

Figure 5.1 Schematic of the RPV adopting cooled-vessel concept

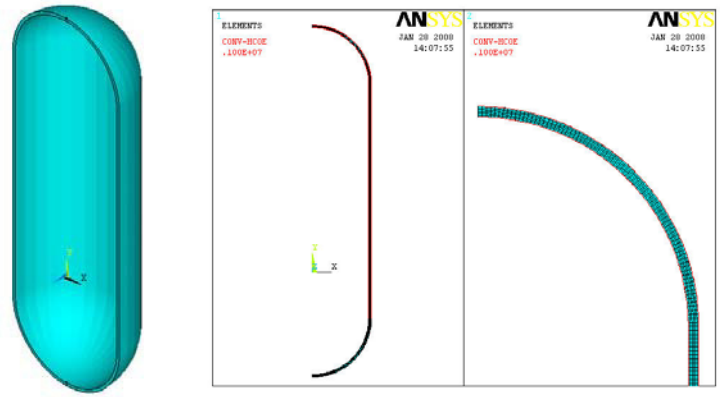

Figure 5.2 Finite element model of the RPV

5.1.2 Loading Conditions

During normal operation, the pressure inside the RPV is assumed 7MPa and the inlet/outlet gas temperatures are assumed either 490℃/950℃ or 590℃/950℃. By the combination of two gas temperature cases and two RCCS types, total four normal operation cases are considered. The two accidents considered in these analyses are the HPCC (High Pressure Conduction Cooldown) and the LPCC (Low Pressure Conduction Cooldown) initiated at the four normal operations. Total eight cases of transient conditions are considered as shown in Table 5.1, whose thermal transient loadings are provided by the GAMMA+ analyses and pressure loadings are assumed to be constant 7MPa for the conservatism of structural analysis even though they are assumed to decrease to 1 bar in 10 seconds in the GAMMA+ analyses. Support loads, nozzle loads, flange loads as well as seismic loads are not considered at this conceptual design stage.

Table 5.1 Transient cases and characteristics

Case number	Case 1	Case 2	Case 3	Case 4	Case 5	Case 6	Case 7	Case 8
Inlet/Outlet Gas Temperature	490℃/950℃				590℃/950℃			
RCCS type	Air cooled		Water cooled		Air cooled		Water cooled	
Transient type	HPCC	LPCC	HPCC	LPCC	HPCC	LPCC	HPCC	LPCC

5.1.3 Material properties

The RPV is made of the SA533, Grade B, Class 1 alloy steel which is a Manganese-Molybdenum-Nickel alloy (Mn-0.5Mo-0.5Ni) whose composition is shown in Table 5.2. Table 5.3 shows the mechanical and physical properties of the SA533, Grade B, Class 1 alloy steel at various temperatures in ASME Code, Section II, Part A, Part D and CC N-499.

Table 5.2 Chemical compositions of SA533, Grade B, Class 1 alloy steel

	Carbon, max	Manganese	Phosphorus, max	Sulfur, max	Silicon	Molybdenum	Nickel	Fe
Composition, %	0.25	1.07-1.62	0.035	0.035	0.13-0.45	0.41-0.64	0.37-0.73	Bal.

Table 5.3 Mechanical properties of SA533, Grade B, Class 1 alloy steel

Temp. (℃)	Thermal conductivity (J/s.m.℃)	Specific heat (J/Kg.℃)	Density (kg/m^3)	Thermal expansion coefficient (m/m/℃)	Young's modulus (GPa)	Poission ratio	Yield strength (MPa)
21.1	41.02	445.6	7850	1.260E-05	200	0.3	345
93.3	40.68	490	7850	1.314E-05	197	0.3	324
148.9	40.51	505	7850	1.332E-05	193	0.3	314
204.4	39.99	520	7850	1.368E-05	190	0.3	305
260	39.29	540	7850	1.386E-05	186	0.3	298
315.6	38.43	563.1	7850	1.404E-05	181	0.3	290
371.1	37.39	610	7850	1.422E-05	174	0.3	281
426.7	36.35	610*	7850*	1.440E-05	165	0.3	266
482.2	35.14	610*	7850*	1.458E-05	153	0.3	241
537.8	34.10	610*	7850*	1.476E-05	139	0.3	196

*: Values are not provided in the Code, and assumed constant above 371.1℃

5.1.4 Criteria of ASME Code, Section III, Subsection NB and CC N-499

Structural evaluation is performed in accordance with the ASME Code, Section III, Subsection NB and the CC N-499 for the NGNP RPV which adopts the cooled-vessel concept. The operating temperature of the RPV should be maintained below 371℃ for the SA533 Grade B Class 1 alloy steel to be within the jurisdiction of the Subsection NB. To use the SA533 Grade B Class 1 alloy as the vessel material at the service

temperature exceeding 371℃, the requirements of the CC N-499 should be satisfied. The allowable conditions for limited elevated temperature service of SA533 Grade B Class 1 alloy steel are as follows:

- Maximum allowable temperature limit for Level B Service Condition: 427℃
- Maximum allowable temperature limit for Level C & D Service Conditions: 538℃
- Maximum allowable cumulative time per temperature range
  * 371℃ ~427℃: 3000 hours (for Level B Service Condition)
  * 427℃ ~538℃: 1000 hours, number of events limit (3) (for Level C & D)

The design rules of the Subsection NB shall be satisfied for service conditions for which metal temperatures do not exceed 371℃, and the design rule of the Subsection NH shall be applied by the requirement of the CC N499 when metal temperature exceeds 371℃ for the Level B, C, and D Service Conditions. The CC N-491 only describes general guideline for the use of SA533 Grade B Class 1 material for limited elevated temperature services and provides the mechanical and physical properties at these elevated temperatures including isochronous stress-strain curves, stress-to-rupture values, elevated temperature fatigue strength, and the creep-fatigue damage envelop curve, which are the basic data for applying the Subsection NH. Design criteria of the Subsection NB and the Subsection NH are summarized in Table 5.4.

Table 5.4 Design criteria of Subsection NB and Subsection NH

		Design Condition	Level A and B Service Conditions	Level C Service Condition	Level D Service Condition
NB <371°C	Primary	$P_m < S_m$ $P_L+P_b < 1.5S_m$	P_m <110% S_m P_L+P_b<110% ($1.5S_m$) (for Level B)	$P_m < 1.2S_m$ $P_L+P_b < 1.8S_m$ (or $1.5S_y$)	$P_m < 2.4S_m$ $P_L+P_b < 3.6S_m$
	Secondary	-	P_L+Pb+Q < 3Sm $PL+P_b+Q+F<S_a$	-	-
N-499-2 >371°C (NH)	Load controlled stress limits	$P_m < S_o$ $P_L+P_b < 1.5S_o$	$P_m < S_{mt}$ $P_L+P_b < 1.5S_m$ $P_L+0.8P_b < S_t$	$P_m < 1.2Sm, S_t$ $P_L+P_b < 1.8S_m$ $P_L+0.8P_b < S_t$	$P_m < 2.4S_m, 0.7S_u$ $P_L+P_b < 3.6S_m$ $P_L+0.8P_b<0.67S_r$
	Strain and deformation limits	-	ε(membrane) <1% ε(membrane+bending)< 2% ε(peak) < 5% Creep fatigue damage : $D_c + D_f < D$		-

P_m : Primary membrane stress intensity
P_L : Primary local membrane stress intensity
P_b : Primary bending stress intensity
Q : Secondary stress intensity
S_m : Allowable stress intensity (time independent)
S_t : Allowable stress intensity (temperature and time dependent)
S_{mt} : Allowable stress intensity (lower value of S_m and S_t)
D_c : Creep damage value
S_r : Expected minimum stress-to-rupture strength
D_f : Fatigue damage value
S_o : Allowable stress intensity for design loadings
D : Total creep-fatigue damage

As seen in Table 5.4, it is enough to check the allowable stress criteria for low temperatures below 371℃. On the other hand, at elevated temperature above 371℃, it is necessary to check both the allowable stress criteria and the inelastic strain criteria as well as creep-fatigue damage. In these analyses, the criteria for the Level A&B Service Conditions are applied for structural integrity assessment instead of the criteria for the Level C&D Service Conditions for conservative evaluation even though the considered accidents of HPCC and LPCC are expected to be in the Level C&D Service Conditions. Also, the criteria of $P_m < S_m$ and $P_L+P_b < 1.5S_m$ which are the criteria for the Design Conditions are applied for the Level A&B Service Conditions to obtain conservative results.

5.2 Structural analysis and design adequacy

5.2.1 Normal operating conditions evaluation

The structural analyses with thermo-mechanical loadings have been performed for the four normal operating conditions corresponding to the cases given in Table 5.1. The temperatures of the RPV remain below 371℃ at all locations as expected. Membrane stresses intensities, P_m, induced by the design pressure of 7MPa are dominating and they satisfy the allowable stress limit S_m with design margin of 0.3. This margin can be increased by increasing the thickness of the vessel from 190mm to a bigger value if necessary. The combined primary and secondary stress intensities (P_L+P_b+Q) satisfy the allowable stress limit $3S_m$ with design margins between 1.9 and 2.2 as shown in Table 5.5.

Table 5.5 Design margins – steady state condition (for Sm and 3Sm)

Case	Loc.	T_{mean} (℃)	P_m (MPa)	P_L+P_b (MPa)	P_L+P_b+Q (MPa)	S_m (MPa)	$3S_m$ (MPa)	Margin	
1 & 2	Z4	327.9	145	151	180	184	552	0.3*	2.1**
3 & 4	Z16	301.8	145	151	181	184	552	0.3*	2.0**
5 & 6	Z16	338.2	145	151	178	184	552	0.3*	2.1**
7 & 8	Z16	334.4	145	151	192	184	552	0.3*	1.9**

*: $(S_m/P_m)-1$ **: $3S_m/(P_L+P_b+Q)-1$

Temperature profile along the RPV at the normal operation of Case 1 & 2 is shown in Figure 5.3 and the corresponding stress intensity distribution is shown in Figure 5.4. Figure 5.5 indicates the stress intensity profile along the inner and outer surfaces of the

RPV and it can be noticed that the stress intensities along the outer surface are larger than those of inner surface. This is typical throughout all the transient cases considered. Maximum stress intensity occurs near Z4 elevation indicated in Figure 5.1. All the other results of the normal operations of Cases 3&4, 5&6, and 7&8 show similar results, and the maximum location for stress intensities and their results are summarized in Table 5.5.

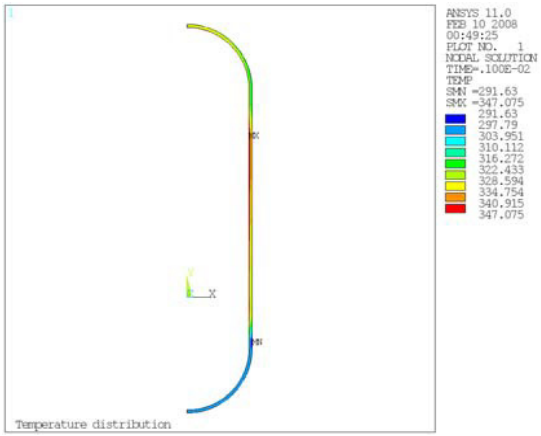

Figure 5.3 Temperature distribution for the normal operation of Case 1&2

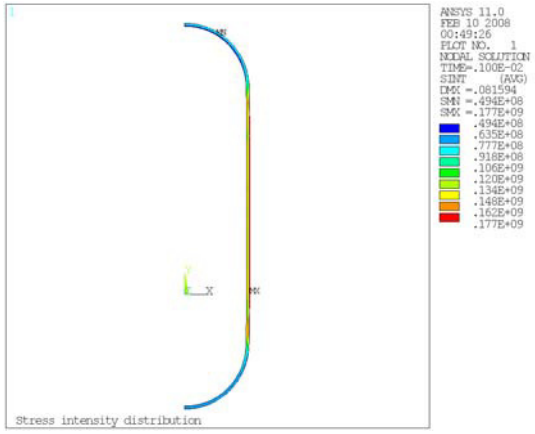

Figure 5.4 Stress intensity distribution for the normal operation of Case 1&2

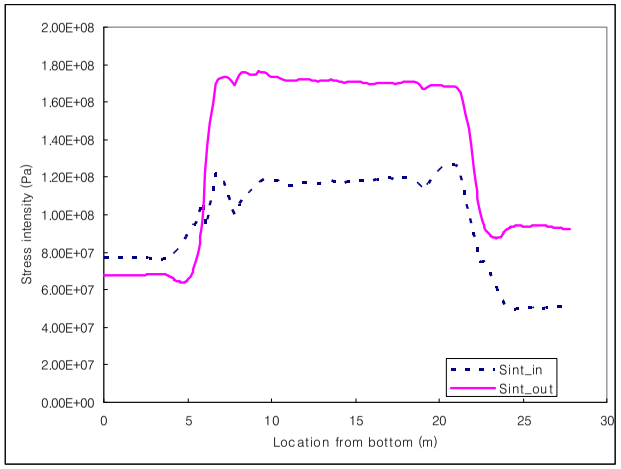

Figure 5.5 Stress intensity profile along inner/outer surfaces for the normal operation of Case 1&2

5.2.2 Accident conditions evaluation

The structural transient analyses have been performed for the transient pressure and thermal loadings corresponding to each case in Table 5.1. At elevated temperatures above 371℃, it is necessary to check both the load controlled stress limits and the strain and deformation limits as in Table 5.4. It is noted that the design criteria for the Levels A&B Service Conditions are applied for structural integrity assessment instead of using the design criteria for the Levels C&D Service Conditions conservatively.

For transient Case 1, temperature histories along the inner and outer surfaces at the selected elevations, Z4, Z6, Z12, Z16 and Z18 are shown in Figure 5.6. The temperature history pattern is varying with the elevation. The temperature at Z4 and Z6 regions remains below 371℃ throughout the transient while at the other regions the temperature exceed 371℃ and at Z16 it reaches up to 423℃. The maximum stress intensity reaches about 190MPa at Z12 and Z16 regions after 87 hours from the initiation of the transient and this is the typical characteristics of the HPCC transient cases. Figure 5.7 shows the stress intensity histories on the RPV inner and outer walls at the selected elevations.

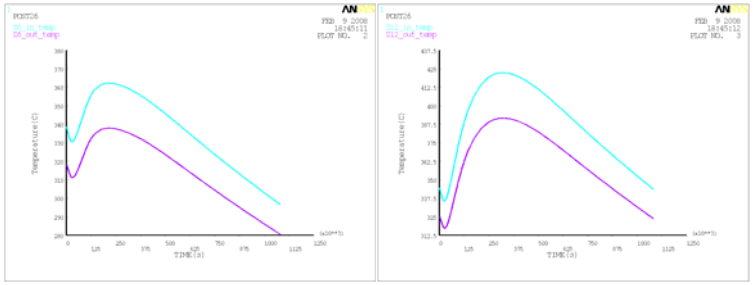

(a) Inner wall (b) Outer wall

Figure 5.6 Temperature histories of the RPV of Case 1 at the selected elevations

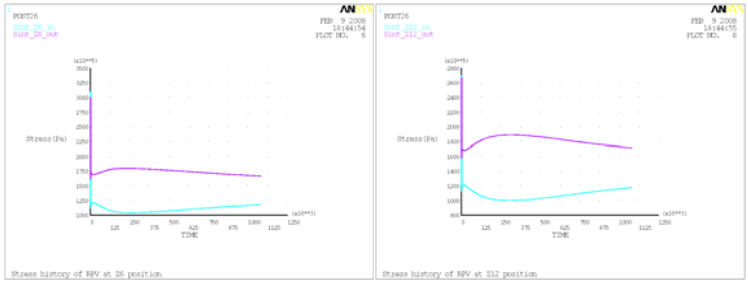

(a) Inner wall (b) Outer wall

Figure 5.7 Stress intensity histories of the RPV of Case 1 at the selected elevations

For total 8 transient cases listed in Table 5.1, the location and corresponding time for maximum stress intensity occurrence and load controlled stress limits are compared with ASME criteria as shown in Tables 5.6 and 5.7. As shown in Table 5.6, primary membrane stress intensities, P_m, induced by the constant pressure loadings during the transients are dominating. The maximum values of average wall temperature, T_{max_m}, exceed the limiting temperature of 371℃ except for Case 3 and 7. Especially Case 2 and Case 6 reveal very high average wall temperatures and their margins are somewhat smaller than others. Although the dominating stress intensities are not functions of temperature in Table 5.6, the margins are varying with temperature because the allowable stress intensities decrease with the increase of temperature.

At elevated temperatures above 371℃, in addition to P_L+P_b criteria, $P_L+0.8P_b$ criteria needs to be satisfied as required in the ASME NH. The factor of 0.8 to P_b is originated

from the creep compensation of bending stress across the wall thickness. $P_L+0.8P_b$ should be smaller than the temperature and time dependent stress intensity S_t. Here, S_t value for 1000 hours for maximum averaged wall temperature is used conservatively, since total time is limited to 1000 hours for metal temperatures exceeding 427℃ per the CC N-499. Table 5.7 shows that the design is adequate for all the cases at this conceptual stage, even though Cases 2 and 6 show relatively small design margins due to high temperatures.

Table 5.6 Design margins for primary stress limits (S_m and $1.5S_m$)

Case Number	Loc.	P_m (MPa)	P_L+P_b (MPa)	S_m (MPa)	S_{mt}^{+} (MPa)	$1.5S_m$ (MPa)	T_{max_m} ( )	Margin	
1	Z16	145	151	184	184	276	414.6	0.3*	0.8***
2	Z12	145	151	160	160	240	494.1	0.1*	0.6***
3	Z16	145	151	184	184	276	363.4	0.3**	0.8***
4	Z12	145	151	180	180	270	434.4	0.2*	0.8***
5	Z16	145	151	184	184	276	418.9	0.3*	0.8***
6	Z12	145	151	160	160	240	499.2	0.1*	0.6***
7	Z16	145	151	184	184	276	368.1	0.3**	0.8***
8	Z12	145	151	180	180	270	439.0	0.2*	0.8***

+: S_{mt} which is the lower of S_m and S_t for 1000 hours is used conservatively, where S_m is time-independent allowable stress intensity and S_t is time-dependent allowable stress intensity, respectively.
*: S_{mt}/P_m -1 **: S_m/P_m − 1 ***: $1.5S_m/(P_L+P_b)$ - 1

Table 5.7 Design margins for primary stress limits (S_t^*)

Case Number	Loc.	$P_L+0.8P_b$ (MPa)	P_L+P_b+Q (MPa)	S_t^* (MPa)	$3\overline{S_m}$ (MPa)	T_{max_i} (℃)	T_{max_o} ( )	Margin
1	Z16	150	195	300	531	429.7	399.5	1.0
2	Z12	150	230	193	480	518.9	469.4	0.3
3	Z16	150	196	358	552	379.0	348.5	1.4
4	Z12	150	231	310	480	459.0	409.9	1.1
5	Z16	150	196	318	531	435.1	404.0	1.1
6	Z12	150	232	180	360	524.9	473.9	0.2
7	Z16	150	197	358	531	383.9	352.4	1.4
8	Z12	150	234	300	503	464.4	413.9	1.0

*: Time dependent stress intensity S_t for 1000 hours is used conservatively.

In Table 5.7, P_L+P_b+Q and corresponding allowable value $3\overline{S}_m$ are provided to compare with each other. $3\overline{S}_m$ is called as modified $3S_m$ since it is determined by

considering the stress relaxation during high temperature above the jurisdiction of the Subsection NB. This is required to apply elastic analysis approach of the Subsection NH and P_L+P_b+Q for all cases satisfied these limits well.

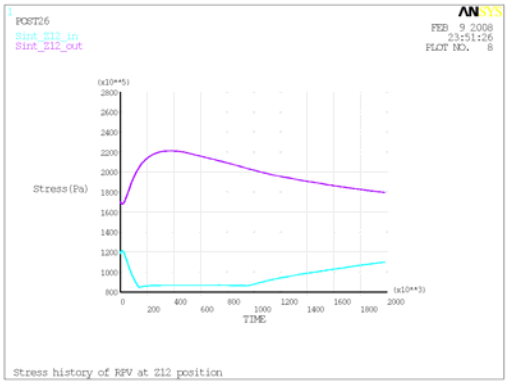

Figure 5.8 Stress intensity histories at elevation Z12 of the RPV

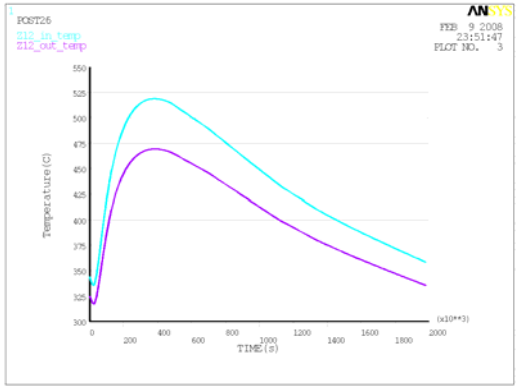

Figure 5.9 Temperature histories at elevation Z12 of the RPV

It is noteworthy that the value of S_t decreases rapidly as temperature increase and the limiting transient cases are Cases 2 and 6 for LPCC accident condition with air cooled RCCS. Maximum stress intensity occurs at around Z12 to Z16 region for Case 2 and the maximum temperature of Z12 location is higher than the other locations, while Z16 location suffers higher temperature transient for Case 1. Fig. 5.7 and Fig. 5.8 show the stress intensity histories on the inner and outer surfaces of the RPV at Z12 location for Case 2 and the corresponding temperature histories along the inner and outer surfaces are shown in Fig. 5.9. Since the maximum stress occurs during the high temperature response at Z12 when the time dependent allowable stress limit S_t decreases to a half, its design margin is relatively small as explained above. Case 6 has the same reason.

As described in Table 5.4, the maximum accumulated inelastic strain limits should be satisfied in regions expecting elevated temperatures. Simplified method T-1330 of Subsection NH is applied to evaluate the accumulated inelastic strains for each case. The maximum strain location for each case is selected and corresponding results are shown in Table 5.8.

Table 5.8 Accumulated inelastic strains and strain ranges

Case Number	Loc.	X	Y	Z	σ_c(MPa)	$\Delta\varepsilon_c$	$\Delta\varepsilon_{max}$	ε_t
1	Z16	0.4800	0.0655	0.4800	150	0.0000	0.00018	0.00018
2	Z12	0.4774	0.1698	0.4774	115	0.0004	0.00047	0.00087
3	Z16	0.4492	0.0585	0.4492	128	0.0000	0.00014	0.00014
4	Z12	0.4584	0.1643	0.4584	125	0.0000	0.00042	0.00042
5	Z16	0.4636	0.0541	0.4636	127	0.0000	0.00016	0.00016
6	Z12	0.4764	0.1736	0.4764	114	0.0005	0.00046	0.00096
7	Z16	0.4535	0.0406	0.4535	127	0.0000	0.00010	0.00010
8	Z12	0.4950	0.1458	0.4950	134	0.0000	0.00036	0.00036

In Table 5.8, X and Y denote a primary stress intensity index and a secondary stress intensity range index, respectively. Z represents the effective creep stress parameter determined by X and Y values according to T-1330 of the Subsection NH. An effective creep stress is obtained by $\sigma_c = ZS_{yL}$ where S_{yL} is yield stress for the lower of the averaged wall temperatures and the total inelastic strain (creep-ratcheting strain) is determined by multiplying σ_c by 1.25 and one can assume that the creep strain associated with the $1.25\sigma_c$ stress held constant throughout the temperature-time of the entire service life. In this evaluation, the number of occurrences of each transient is assumed one, and the isochronous curves of the CC N-499 were used to obtain total creep strain ($\Delta\varepsilon_c$). As shown in Table 5.8, negligible amount of inelastic strains were calculated for the cases except Case 2 and Case 6. The inelastic strains for Cases 2 and 6 are 0.04% and 0.05% respectively, which are far below the allowable limit, 1%, shown in Table 5.4 for single occurrence of transient. Even with the allowable

maximum number of occurrences, 3 by CC N-499, of HPCC and LPCC accidents, the accumulated inelastic strain seems negligible.

The maximum values of the calculated strain ranges ($\Delta\varepsilon_{max}$) were obtained by post-processing the results and the total strain ranges (ε_t) were evaluated according to T-1432 of the Subsection NH. The allowable number of cycles (N_d) is determined by applying the total strain ranges (ε_t) into the design fatigue curve, Figure. 5.10.

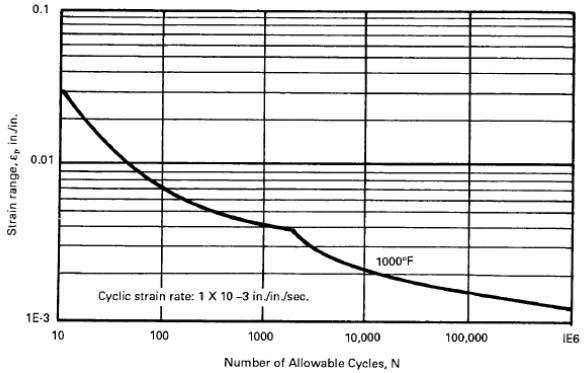

Figure 5.10 Design fatigue range for SA533, Grade B, Class 1

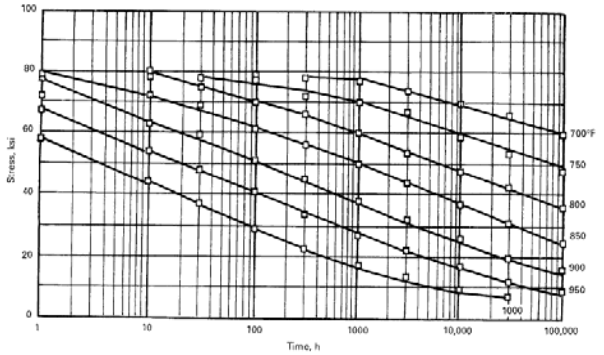

Figure 5.11 Minimum stress-to-rupture as function of time and temperature

T-1433 procedure of Subsection NH provides the procedure to evaluate creep damage. In these analyses, stress level S_j obtained by total strain range (ε_t) and isochronous curve

is used to determine minimum stress-to-rupture time (T_r) as shown in Figure 5.11. The stress level S_j is assumed to be maintained constant during hot hold time.

Table 5.9 shows the fatigue damage and creep damage for single occurrence of each transient. Fatigue damage (D_f) is the ratio of number of transient occurrence over allowable number of cycles, and creep damage (D_c) is the ratio of time duration over stress rupture time. Creep damage for Case 6 is turned out to be noticeable and other values are negligibly small. The effect of the creep-fatigue interaction is determined using the curve shown in Figure 5.12 in which the region under the bi-linear curve indicates safe area. It is shown that the results for all cases are in the safe area.

Table 5.9 Creep-fatigue damage evaluations

Case Number	Loc.	T_{max_i} (°C)	T_{max_o} (°C)	>371°C (hr)	S_j (MPa)	N_f	T_r(hr)	D_f	D_c
1	Z16	429.7	399.5	230	17	>1000000	>100000	0.00	0.00
2	Z12	518.9	469.4	440	138	>1000000	8250	0.00	0.05
3	Z16	379.0	348.5	89	25	>1000000	>100000	0.00	0.00
4	Z12	459.0	409.9	369	70	>1000000	>100000	0.00	0.00
5	Z16	435.1	404.0	226	27	>1000000	>100000	0.00	0.00
6	Z12	524.9	473.9	440	150	>1000000	2000	0.00	0.22
7	Z16	383.9	352.4	110	17	>1000000	>100000	0.00	0.00
8	Z12	464.4	413.9	372	60	>1000000	>100000	0.00	0.00

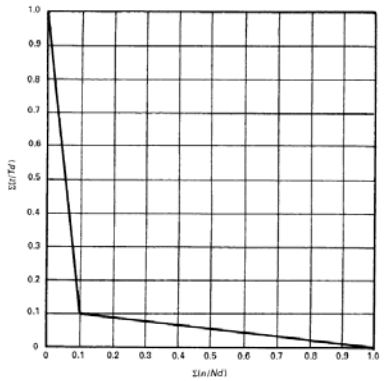

Figure 5.12 Creep-fatigue damage envelop

Through these analyses, the design adequacy of the NGNP RPV made of SA533 Grade B, Class 1 is confirmed with respect to the four normal operating conditions and the eight transient cases. Transient Case 2 and Case 6 result in relatively small design margins since the temperature increases above 500℃ and the material properties of SA533 Grade B Class 1 degrades rapidly at these temperature ranges. Considering, however, that the constant internal pressure load, 7MPa, is assumed in the structural analysis although Case 2 and Case 6 are the LPCC accident cases of no RPV internal pressure load and with air-cooled RCCS, the results for those cases are heavily conservative.

6. SUMMARY

A preliminary thermo-fluid and structural analysis for a cooled NGNP SA508/533 RPV under normal operating conditions and anticipated transients has been performed. A brief summary for the results is described as below.

Cooled-vessel concept

A cooled-vessel concept was derived based on the NGNP PCD study, which is characterized by the inlet flow path to the core inside the graphite structures and by the forced vessel cooling by cold helium flow to the space between the core barrel and the RPV. The flow path consists of the inlet plenum, the riser, and the upper plenum. Among them, the upper plenum configuration is one of key parts in the cooled-vessel design in a view of how to stack the graphite blocks to make the coolant coming from the riser holes in the permanent side reflector guided to the core.

The upper plenum configuration suggested in this study is composed of the supporting post and the distribution block. The supporting post has a simple cylindrical shape and supports the upper reflector. The distribution block has a seat for installing the supporting post and provides flow paths that connect the upper plenum and the coolant channels in the fuel block assembly. Two options of distribution block were provided.

The cooled-vessel design is very preliminary and has many issues to be resolved before its realization. One of the issues is an additional bypass flow arisen by the internal flow path design. Although the bypass flow due to relatively high pressure gradients between the riser and the core can be limited by installing steel tubes in the riser holes, a question still remains how to reduce leakage in the upper plenum before the coolant reaches the core inlet. The use of larger sized graphite blocks may reduce the leakage, but its materialization should be carefully considered.

Thermo-fluid analysis using the GAMMA+ and CFX codes

The system thermo-fluid analysis was performed using the GAMMA+ system analysis code. For the four normal operating conditions with two different helium inlet temperatures (490^{o}C and 590^{o}C) and two different RCCS options (air-cooled and water-cooled), the steady-state conditions satisfying the target RPV peak temperature of 350^{o}C were obtained by adjusting the vessel cooling flow. For the cases with the helium inlet

temperature of 490°C, the RPV peak temperatures are maintained below the target temperature even without the vessel cooling flow. The transient analyses were performed for the two limiting accidents, High-Pressure Conduction Cooldown (HPCC) and Low-Pressure Conduction Cooldown (LPCC), from the four different normal operating conditions. In all the analysis cases, the RPV temperatures exceed the SA533/SA508 temperature limit of 371°C. However, they are still within the limit specified in the ASME code case N-499, that is, below 538°C for less than 1000 hrs.

Detailed steady state analysis for normal operating conditions was conducted by using the CFX code, a commercial CFD code, not only to investigate detailed flow and heat transfer phenomena that occur in the cooled-vessel design but also to verify the GAMMA+ results. Three cases for the air-cooled RCCS and one case for the water-cooled RCCS were analyzed. The cases of air-cooled RCCS are for the core inlet temperature of 490°C without vessel cooling flow, 590°C with vessel cooling flow injected from the bottom side, and 590°C with vessel cooling flow from the top side. For the air-cooled RCCS, the GAMMA+ results were well reproduced by the CFX code both for the maximum vessel temperature and for the heat loss to the RCCS. A little difference in the case of top-injected vessel cooling flow is due to the one-dimensional modeling of the gap between the core barrel and the RPV in the GAMMA+ analysis. For the water-cooled RCCS, one case, the inlet temperature of 490°C without the vessel cooling, was selected for the CFX analysis. In comparison with the GAMMA+ results, there is not much reduction of the vessel temperature by the water-cooled RCCS. This is due to a highly circulating multi-dimensional flow in the reactor cavity affected by the temperature difference between the reactor cavity wall and the RCCS duct.

It is shown from the analysis results that the vessel temperature is maintained below the design limit of 371°C during normal operating conditions for the core inlet temperature of 490°C and the vessel cooling is not required. This is a very promising result because the vessel cooling system, if it is needed, should be a reactor safety system which increases system complexity and licensing difficulty.

Structural analysis

Preliminary structural analyses and evaluations of structural integrity for the NGNP RPV adopting cooled vessel concepts with inlet temperatures of 490℃ and 590℃ and with the air- and water-cooled RCCS have been performed. In the analyses and evaluations, four normal operating conditions and eight limiting transient, such as HPCC and LPCC accidents stating at each normal operating condition, has been

considered. Cooled-vessel concept allows the use of conventional SA533 Grade B, Class 1 alloy steel as RPV material. Design criteria of the ASME Boiler and Pressure Vessel Code, Section III, Subsection NB were applied in the structural integrity evaluation procedure for the metal temperature below 371℃ and the Subsection NH was applied for metal temperature above 371℃ by the requirements of the Code Case N-499 which provides general design guidelines and the material properties of SA533 Grade B, Class 1 alloy steel in the elevated temperature. Design criteria for Levels A&B Service Conditions were used instead of the criteria for Levels C&D Service Conditions for conservative purpose. In all cases considered, the evaluations confirm the structural integrity of the cooled-vessel with appropriate margins. The primary stress intensity generated by the operating pressure, 7MPa, is dominant and the structural integrities were confirmed with acceptable design margins. The effect of the thermal loads from the normal operations and the transients are very minor on the design margins.

The design adequacy of the NGNP RPV is confirmed by considering the RPV internal pressure and the RPV wall temperature for the cases of normal operations and transients of HPCC and LPCC accidents. However, it should be noted that the discussion so far is based on a simplified vessel configuration without nozzles, flanges, or supports. Also, seismic events are to be considered for detailed assessments later.

REFERENCES

[ANSYS, 2006] ANSYS Inc., ANSYS CFX Introduction, ANSYS CFX Release 11.0, Dec. 2006.

[ASME, 2004] ASME, Boiler and Pressure Vessel Code, Section III, Division 1 – Subsection NB-3324, New York, 2004

[GA, 1996] General Atomics, "Gas Turbine-Modular Helium Reactor (GT-MHR) Conceptual Design Description Report," Jul. 1996.

[GA, 2002] General Atomics, "GT-MHR Conceptual Design Description Report," GA/NRC-337-02, August 2002.

[Holman, 2986] J. P. Holman, Heat Transfer, Chapter 7, Sixth Edition, McGraw-Hill Book Company, 1986.

[IAEA, 2000] "Heat Transport and Afterheat Removal for Gas Cooled Reactors under Accident Conditions," IAEA-TECDOC-1163, International Atomic Energy Agency (2000).

[INEEL, 2005] ATHENA PMR input from INEEL, 2005.

[Keyhani, 1983] M. Keyhani, F.A. Kulacki, R.N. Christensen, "Free Convection in a Vertical Annulus with Constant Heat Flux on the Inner Wall," J. Heat Transfer, Vol. 105, pp. 454-459, Aug. 1983.

[Kim, 2007] Kim, M. H., "Thermal Fluid and Safety Analyses of a Preliminary Cooled-Vessel Design for NHDD Plant", Calc. Note, NHDD-KA-07-RD-CD-001, KAERI, March 2007.

[Lim, 2006] H.S. Lim, H.C. No, "GAMMA Multi-dimensional Multi-component Mixture Analysis to Predict Air Ingress Phenomena in an HTGR," Nuclear Science and Engineering, Vol. 152, pp. 87-97, Jan. 2006.

APPENDIX B – KAERI Recommendations for Sensitivity Studies

Parameters for TF sensitivity (GAMMA+ analysis)

This table lists the recommended parameters for TF sensitivity analysis for the LPCC and HPCC transients. Higher priority parameters selected by KAERI are marked in the last column.

Sensitivity parameters	Description	Current approach	Δ T_{RPV}	HPCC	LPCC	Selection by
Graphite block emissivity	Affects the effective thermal conductivity in core and reflectors	Variable by temperature	±	O	O	
Emissivity in CB/RPV annulus	Determines the heat transport by radiation	0.8	±	O	O	KAERI
Emissivity in reactor cavity	Determines the heat removal by radiation	0.8	±	O	O	KAERI
Bypass gap size	Affects the flow distribution in core and reflectors	2 mm for horizontal gap Average 1.5 mm for vertical gap between fuel blocks The worst case is selected.	±	O	Minor	KAERI
Core power redistribution by Gamma and neutron slowing down heating	Smoothing the temperature distribution and then more heat transport to the RCCS	No Gamma heating in reflectors	+	O	O	
Axial power shape change by CR insertion and core life	Shifting the hot spot on the RPV	No power shape changed	±	O	O	KAERI
Reduced system pressure	Depending on system configuration if the PCU is connected or by inventory control	Fixed at 70 bar	+	O	N/A	KAERI
Effect of different fixed-Orifice sizing	Affects the flow distribution in core and reflectors It should be coupled with 3-D solid modeling if considered	Not considered	±	O	Minor	
Degraded heat transfer in mixed convection regime	The recent experiment reports the degradation of heat transfer in the mixed convection region	General package from Burmeister's book (laminar, transition, turbulent)		minor	Minor	

Sensitivity parameters	Description	Current approach	Δ T_{RPV}	HPCC	LPCC	Selection by
Effective thermal conductivity in core	Affects on the heat distribution by conduction and radiation	Equivalent resistance method considering bypass gap and coolant holes $\lambda_{eff\_x}^{core} = \frac{L_{gap} + L_{FA}}{\frac{L_{FA}}{\lambda_{eff}^{FA}} + \left(1-\varphi_{gap}^{FA}\right)\frac{L_{gap}}{\lambda_{eff}^{FA}} + \varphi_{gap}^{FA}\left[\frac{\lambda_{gas}^{gap}}{L_{gap}} + \frac{4\sigma T^3}{2/\varepsilon_r - 1}\right]^{-1}}$ $\lambda_{eff\_z}^{core} = \left(1-\varphi_{gap}^{FA}\right)\lambda_{eff}^{FA} + \varphi_{gap}^{FA}\lambda_{gas}^{FA}$ where $\lambda_{eff}^{FA} = \left(1-\varphi_{void}\right)\lambda_{graphite} + \varphi_{void}\left(\lambda_{gas}^{void} + \lambda_{rad}^{void}\right)$	±	O	O	
Irradiation-dependent Graphite properties at replaceable reflectors	Well-known characteristics of irradiated graphite, but no sufficient data available. Also fast neutron fluence depends on the lifetime of replaceable graphite	Single curve as a function of irradiation temperature (no effect of different irradiation levels considered)	±	O	O	KAERI
Graphite properties of permanent reflectors	If non-isotropic graphite is used, graphite conductivity has direction-dependency.	Isotropic assumption is used. The same with replaceable graphite for permanent side reflector Carbon brick for the O.P. graphite	±	O	O	KAERI
Water-cooled RCCS						
RCCS panel design	Specific geometry design is expected.	The same geometry with air-cooled RCCS panel	±	O	O	
RCCS temperature boundary	Depending on water-loop design and operation condition	Fixed at 65°C at normal operation Linearly increased in 5 hrs then fixed at140°C	±	O	O	
Heat loss from concrete outer wall to environment	Depending on containment design	Heat transfer coefficient of 5 W/m^2-K, an emissivity of 0.6 with an air temperature of 30°C	±	minor	minor	

APPENDIX C – KAERI Report on Analyses of High-Cr NGNP RPV

KAERI

Nuclear Hydrogen Project

Calculation Note

Document No: NHDD-KA-08-ME-CA-001

Title : A Preliminary Analysis for a High-Cr NGNP Reactor Pressure Vessel

Prepared by :	Dong-Ok Kim	Date : Mar. 21. 2008
Reviewed by :	Hong-Sik Lim	Date : Mar. 25. 2008
Reviewed by :	Min-Hwan Kim	Date : Mar. 25, 2008
Approved by :	Won-Jae Lee	Date : Mar. 26, 2008

SUMMARY

This report is on a high-Cr vessel study which is a part of NGNP CDS subtask, WBS NHS.000.S01-RPV and IHX Pressure Vessel Alternatives. The main purpose of the task is to perform a preliminary structural analysis for a high-Cr NGNP RPV under a normal operating condition and anticipated transients. It is assumed that the reactor inlet and outlet temperature are 490℃ and 950℃ respectively. The concept of the high-Cr vessel with air-cooled RCCS and key dimensions for the analysis were based on the 600MW GT-MHR design. Thermal boundary conditions for the structural analysis were obtained from the thermo-fluid analysis using GAMMA+ code. The structural analysis was performed using ANSYS code and the integrity of RPV was confirmed in accordance with the design criteria of the ASME B & PV Code.

Record of Revisions

No.	Date	Description	Prepared by
00	Mar. 26, 2008	Initial Issue	Dong-Ok Kim

NHDD-KA-08-ME-CA-001

NHS.000.S01 #2130

A Preliminary Thermo-fluid and Structural Analysis for a High-Cr NGNP Reactor Pressure Vessel

March 26, 2008

RPV and IHX Pressure Vessel Alternatives

NGNP Project - Conceptual Design Studies

Korea Atomic Energy Research Institute

TABLE OF CONTENTS

LIST OF FIGURES

LIST OF TABLES

1. INTRODUCTION

The higher operating temperatures for the reactor vessel in the NGNP necessitate the use of high-Cr steel as the material of the reactor pressure vessel, which provides good creep resistance at high temperatures. The objective of this task is to perform a preliminary structural analysis for a 9Cr-1Mo-V reactor vessel under a normal operating condition and anticipated transients.

To achieve this goal, the GT-MHR with modified flow configuration is selected as the reference reactor of which the coolant inlet and outlet temperatures are 490℃ and 950℃, respectively. While the inlet coolant flows through riser channel boxes between the core barrel and the reactor pressure vessel in the original GT-MHR, the inlet flow is routed through holes in the permanent side reflector in the modified flow configuration to avoid direct contact of the high temperature helium with the pressure vessel.

GAMMA+ code is used for the thermal-fluid analysis to generate the T-H loads for the structural analysis. The GAMMA+ code input is prepared based on the NGNP pre-conceptual engineering services reflecting the modified design concept. Structural analysis is conducted by using ANSYS code, and the results are evaluated to confirm the vessel integrity based on the ASME B&PV Code Section III, Subsections NB & NH.

2. Description of Core and RPV for High-Cr Vessel

The GT-MHR [1] of which the coolant inlet/outlet temperatures are 490^{o}C and 850^{o}C is selected as a reference reactor for the analysis of high-Cr reactor vessel. For the GT-MHR, the inlet coolant flow is routed through riser channel boxes between the core barrel (CB) and the reactor pressure vessel (RPV).

The NGNP selected 950^{o}C as a design point of the coolant outlet temperature. Without changing the core design of the GT-MHR, the increase of coolant outlet temperature results in an increase of coolant inlet temperature by 100^{o}C to 590^{o}C. GA indicated that this higher coolant inlet temperature will result in the RPV temperatures that could exceed the limits for high-Cr steels if the current GT-MHR inlet flow configuration is used [2]. GA also suggested a modified configuration routing the inlet flow through holes in permanent side reflector to prevent a direct contact of high temperature coolant with the RPV.

Recently GA fixed the coolant inlet temperature of the NGNP at 490^{o}C. Although this inlet temperature would allow the use of high-Cr vessel for all operating conditions with the GT-MHR flow configuration, a modified flow configuration routing the inlet flow through the reflector is preferred to secure a sufficient design margin for the RPV. In the present study, thus, a modified flow configuration is used for the analysis, as shown in Figure 2.1, keeping the dimensions of the GT-MHR related to the CB and the RPV. The modified flow configuration is the same as the cooled-vessel design [3] in which the coolant coming from the outside of co-axial ducts is supplied to the core through the inlet plenum, the riser, and the upper plenum.

Figures 2.2 and 2.3 show horizontal and vertical cross-sectional views for the NGNP high-Cr vessel, respectively. The number of the riser holes in the permanent reflector and its dimension are the same as those for the cooled-vessel design but the radial location of the holes moved near to the core due to the fixed dimensions of the CB that are taken from the GA report [4]. Table 2.1 represents basic dimensions for the analysis

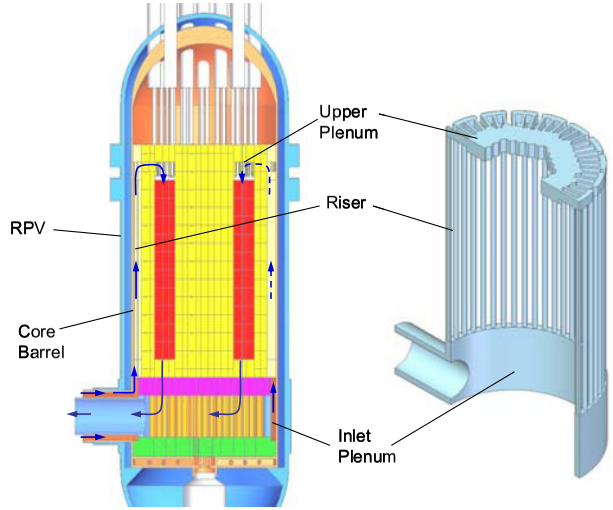

Figure 2.1 Flow paths of the helium coolant for the high-Cr vessel concept

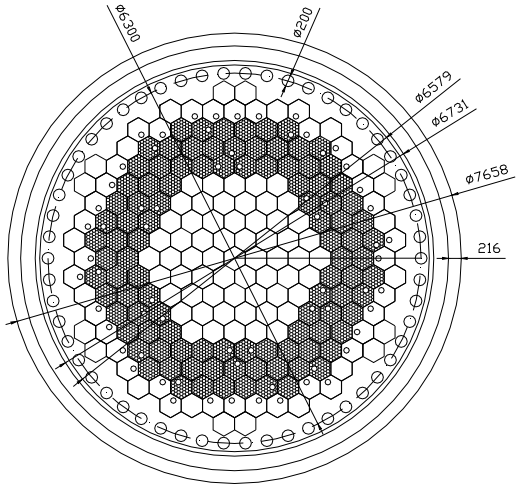

Figure 2.2 Schematic horizontal cross-sectional view of the high-Cr vessel

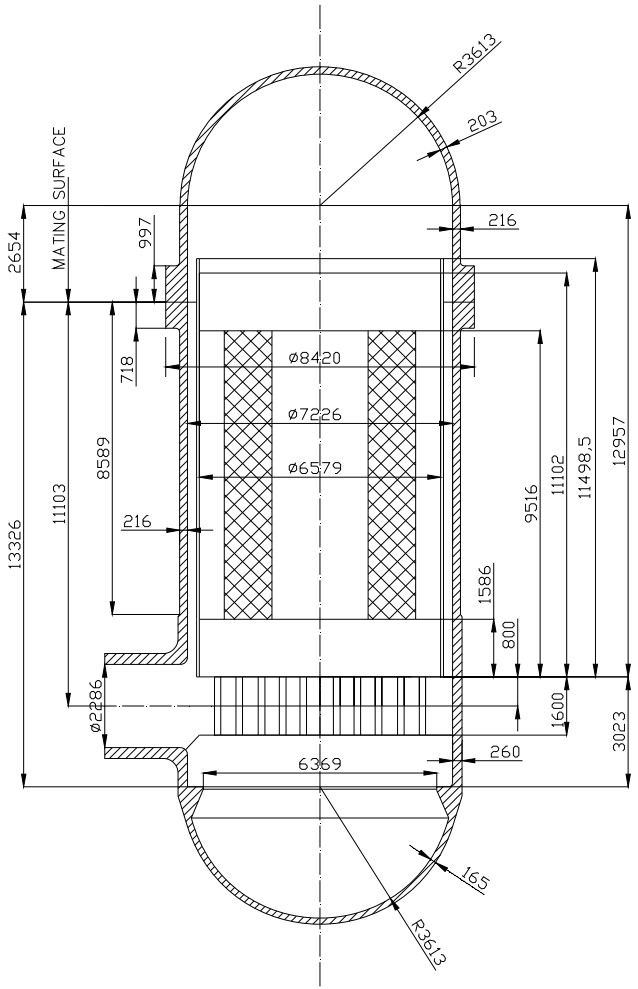

Figure 2.3 Schematic vertical cross-sectional view of the high-Cr vessel

Table 2.1 Basic dimensions for the high-Cr vessel analysis

RPV	Material	Mod. 9Cr-1Mo steel
	Height	23.206m
	Inner Diameter	7.226m
	Outer Diameter	7.658m (cylinder) 8.420m (flange)
	Thickness	0.216m (thin) 0.260m (thick) 0.203m (top shell) 0.165m (bottom shell)
Core Barrel	Material	Alloy 800H
	Inner Diameter	6.579m
	Outer Diameter	6.731m
	Thickness	0.076m
Riser	Number of Holes	54
	Hole Diameter	0.2m
	Diameter of Hole Position	6.3m
Core	Height of Active Region	7.93m
	Height of Upper Reflector	1.586m
	Height of Lower Reflector	1.586m
Lower Plenum Height		1.6m

3. GAMMA+ Thermo Fluid Analysis

3.1 GAMMA+ Code Analysis Model

The GAMMA code [5] was developed for the analysis of VHTR thermo-fluid transients including air ingress phenomena. The code capability was extended and the GAMMA+ code was developed to have enhanced capability for the following models; fluid transport and material properties, multi-dimensional heat conduction, multi-dimensional fluid flow, chemical reactions, multi-component molecular diffusion, fluid heat transfer and pressure drop, heat generation and dissipation, and radiation heat transfer.

The reference analysis inputs for the GT-MHR are taken from the GT-MHR conceptual design report [1] and the INEEL ATHENA PMR input [6]. Based on the reference inputs, the GAMMA+ code input [7] was prepared for the NGNP preconceptual engineering services in 2007. In order to reflect the modified design for the high-Cr vessel concept, some modifications are made in the previous GAMMA+ code input.

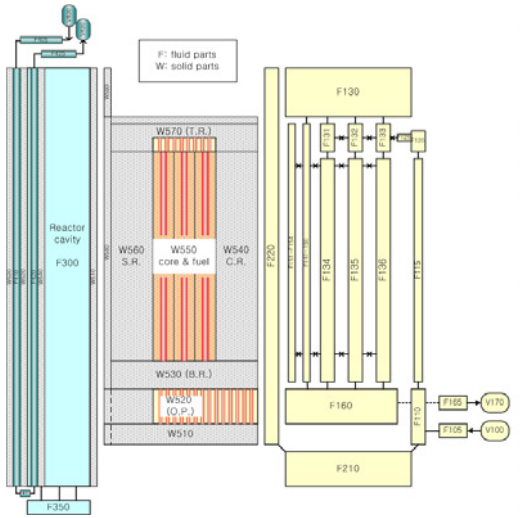

Component	Description	Meshes
F105,F165	Coaxial pipe	1,2
F110	Inlet bottom plenum	2
F115	Inlet riser holes	12
F120, F125	Inlet top plenum	1,2
F130	Top head	1
F131~3	Core top void	3
F134	Inner coolant channel	12
F135	Middle coolant channel	12
F136	Outer coolant channel	12
F141~150	FA bypass channel	15
F151,154	CR bypass channel	15
F152,153	RSC bypass channel	13
F160	Outlet plenum	4
F210	SCS volume	1
F220	CB/RPV annulus	3x21
F300	Reactor cavity (RCCS)	3x23
F350	Reactor cavity (remain)	1
F405	RCCS inlet header	1
F410	RCCS downcomer	14
F415	RCCS lower plenum	1
F420	RCCS tube riser	14
F425	RCCS outlet header	1
W510	Bottom support	14x3
W520	Outlet plenum	14x2
W530	Bottom reflector	11x2
W540	Central reflector	5x10
W550	Fuel & core reflector	3x10
W560	Side reflector	3x10
W570	Top reflector	11x3
W580	Core barrel	3x15
W590	Upper shroud	4x3
W610	Reactor pressure vessel	5x23
W620	RCCS downcomer wall	3x23
W630	Reactor cavity wall	4x23
W640	RCCS panel	2x23x4

Figure 3.1 Analysis model of the GAMMA+ code for the high-Cr vessel concept

Figure 3.1 shows the whole system modeling using the GAMMA+ code. It consists of the reactor coolant system, the reactor cavity and the reactor cavity cooling system (RCCS). All solid regions are two- or three-dimensionally modeled having total meshes of 752. The fluid regions are modeled by the combination of two- and one-dimensional flow networks with total meshes of 432. In particular the reactor cavity and the annulus between the core barrel and the RPV are modeled two-dimensionally in order to consider the natural circulation flow characteristics. The thermal radiation heat transfers are considered in the top plenum, the annulus between the core barrel and the RPV, the reactor cavity containing the RCCS panels, and the annulus between the downcomer wall and the reactor cavity wall.

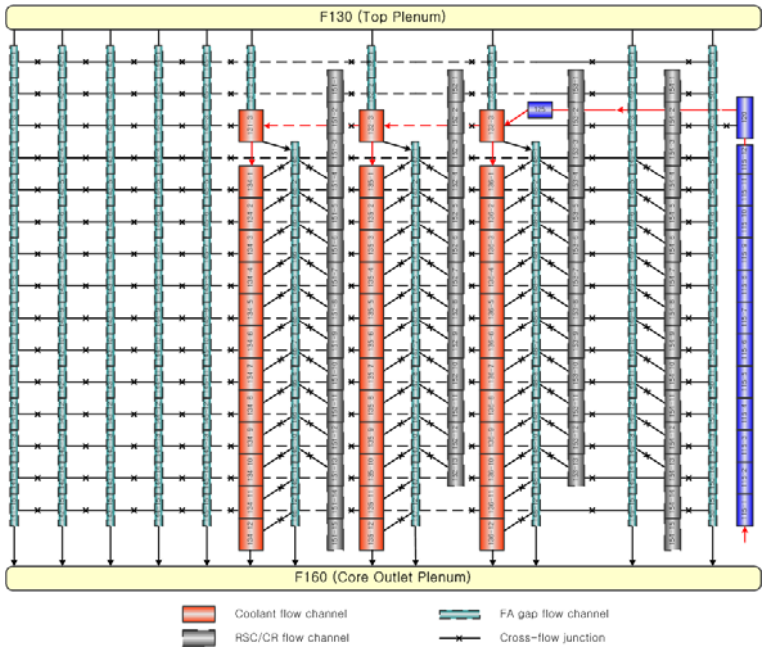

Figure 3.2 The flow network model of the GAMMA+ code for the inlet riser, core coolant, FA gap bypasses, and RSC/CR channels

The core fluid region is modeled in more detail to consider all the bypass flow paths, as shown in Figure 3.2. The bypass flow paths modeled are those through the vertical and horizontal gaps between the fuel blocks, through the reserved shutdown and control rod holes. The cross-flow model is applied between the vertical bypass channels for lateral flow. The gap sizes used in the current analysis are 2 mm for the horizontal gaps and 1.5 mm for the vertical gaps between the fuel blocks, respectively.

The core power distribution is obtained from the GAMMA+/VSOP linkage calculation. Figure 3.3 shows the power distribution for the core condition with the helium inlet and outlet temperatures of 490°C and 950°C. The beginning-of-cycle (BOC) core condition has higher peaking and, thus, conservatively selected for the analysis.

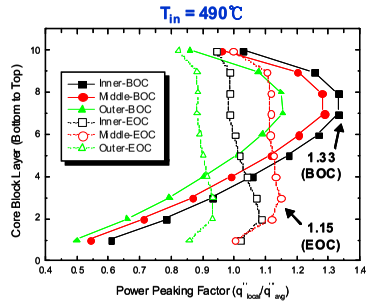

Figure 3.3 The core power distributions from the GAMMA+/VSOP linkage calculation

Free convection heat transfer occurs in the reactor cavity and the annulus between the core barrel and the RPV during the steady-state and the transients. In order to quantify the heat transfer from the core to the RCCS, the following heat transfer correlation for a vertical annulus by Keyhani [8] is used:

$$Nu = 1.406 Ra^{0.077}, \quad \text{for } Ra \le 6.6\times10^{3} \quad \text{(conduction regime)}$$
$$Nu = 0.163 Ra^{0.322}, \quad \text{for } Ra > 6.6\times10^{3} \quad \text{(boundary layer regime)}$$

To consider the effect of the aspect ratios of height and radius, the correlation is re-formulated as follows:

$$Nu = 0.800 Ra^{0.077} H^{-0.052} K^{0.505}, \quad \text{for } Ra \le 6.6\times10^3$$
$$Nu = 0.187 Ra^{0.322} H^{-0.238} K^{0.442}, \quad \text{for } Ra > 6.6\times10^3$$

where H is the aspect ratio, height/width, and K is the radius ratio, Ro/Ri. The Rayleigh number is based on the width, Ro-Ri.

The air-cooled RCCS is modeled one-dimensionally, referencing the GT-MHR design and assuming the inlet pressure and temperature of 1 bar and 43°C, respectively.

3.2 Analysis Cases and Major Parameters from the Analysis

The analysis case considered for the high-Cr vessel option is the helium inlet and outlet temperatures of 490°C and 950°C with the air-cooled RCCS. Table 3.1 shows the major system parameters and the steady state conditions obtained from the analysis.

Table 3.1 Major system parameters and steady state results from the analysis

Major parameters	Values	Remarks
Core thermal power, MWth	600	
RCCS cooling type	**Air-cooled RCCS**	inlet temperature of 43 °C at 1 bar
RCS helium pressure, bar	70	
RCS inlet/outlet temperature, °C	490/950	
RCS helium coolant flow, kg/s	250.55	calculated
Heat removal by RCCS, MW	1.63	calculated
Peak RPV temperature, °C	357	calculated
Peak fuel temperature, °C	1127	calculated

The transient analyses are performed for the High Pressure Conduction Cooldown (HPCC) accident that is the limiting case for vessel heatup at high pressure condition, and the Low Pressure Conduction Cooldown (LPCC) accident that is the limiting case for vessel heatup at low pressure. Transient flow and pressure boundary conditions for the transient calculation are described in Table 3.2. The predicted peak fuel and RPV temperatures show the consistent trend, lower temperatures for HPCC with larger convective heat transfer under high pressure condition.

Table 3.2 Transient cases and major parameters from the analysis

Initiation event	HPCC	LPCC
Peak fuel temp., °C	1369 (at 70 hrs)	1527 (at 83 hrs)
Peak RPV temp., °C	466 (at 93 hrs)	566 (at 100 hrs)
Event scenarios and assumptions	1. Core power switches to GA decay curve at time zero 2. RCS helium flow decreases to zero in 60 seconds (HPCC), and in 10 seconds (LPCC) 3. RCS helium pressure remains at 70 bar (HPCC), and decrease to 1 bar in 10 seconds (LPCC)	

3.3 RPV and fuel temperature transients

Figure 3.4 shows the RPV temperature profile in the axial direction at full power normal operation. The RPV temperature profile is almost flat along the RPV wall and the hottest point locates beside the top reflector region, due to the natural circulation in the annulus between the core barrel (CB) and the RPV. The temperature difference between the inside and outside surfaces of the RPV is non-uniform along the RPV, because of the different vessel thickness as shown in Figure 2.3.

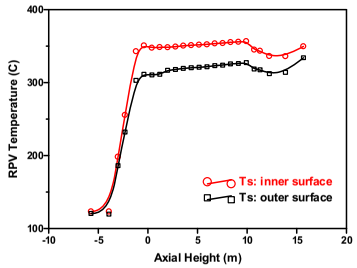

Figure 3.4 Reactor vessel temperature profiles at the inside and outside surfaces for NGNP high-Cr vessel analysis

Figure 3.5 shows the RPV temperature transients during the HPCC/LPCC accidents. The peak RPV temperature locations are different in the HPCC and LPCC accidents. In the case of the HPCC accident where the RCS pressure remains at 70 bars, the peak RPV temperature occurs at the top reflector region like the steady-state case due to the

natural circulation inside the CB/RPV annulus. In case of the LPCC accident where the RCS pressure is at 1 bar, the peak RPV temperature occurs at the center elevation of the active core because the radiation heat transfer is dominant and the effect of free convection inside the CB/RPV annulus is negligible.

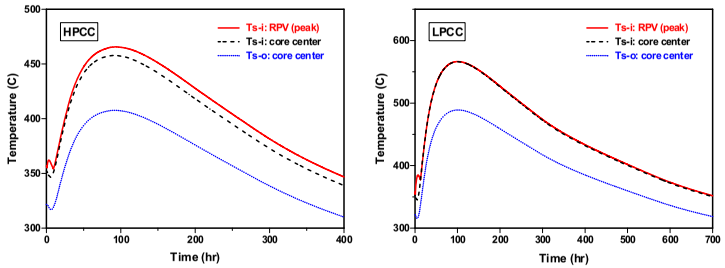

Figure 3.5 Reactor vessel temperature transient for NGNP high-Cr vessel analysis (HPCC/LPCC)

The peak fuel temperatures transients during the HPCC and LPCC accidents are compared in Figure 3.6. The peak fuel temperatures reach 1527°C at 83 hours in the LPCC accident and 1369°C at 70 hours in the HPCC accident, respectively.

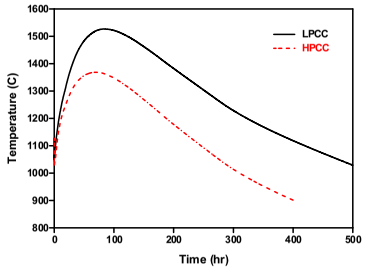

Figure 3.6 Peak fuel temperature transients during the HPCC and LPCC accidents

4. STRUCTURAL ANALYSIS

The objective of structural analysis is to evaluate the structural integrity of the high-Cr NGNP RPV which adopts the modified 9Cr-1Mo-V steel [9] as its material under a normal operating condition and accidents. The vessel material modified 9Cr-1Mo-V steel has a variety of applications in pressure retaining components at elevated temperature. The normal operating condition selected for the analysis is the core inlet and outlet temperature of 490°C and 950°C with the air-cooled RCCS. Two thermal transient conditions, HPCC (High Pressure Conductions Cooldown) and LPCC (Low Pressure Conductions Cooldown), initiated from the normal operating condition is considered in the evaluation of the structural integrity as the accident conditions. The structural integrity is evaluated in accordance with ASME B&PV Code Section III, Subsections NB and NH [10, 11]. As described in the section 3, since the vessel temperature during the normal operation is maintained below 371℃ in all parts of the RPV, the subsection NB is applicable for the structural integrity evaluation in which the stress intensities from the structural analysis are the evaluation items. During the accident conditions the maximum vessel temperatures exceeds 371℃ and the high temperature design criteria of the subsection NH is applicable in which the high temperature creep effects are to be additional items of the evaluation.

Structural analyses of the High-Cr reactor vessel with thermal and mechanical loads are performed using ANSYS code during the normal operation and the transient conditions. The thermal loadings during the normal operation and the HPCC/LPCC transients are given from the thermal fluid analysis results of GAMMA+ system analysis code. The adequacy of the reactor vessel structure under the normal operation load and the given transient loads is evaluated by checking its structural responses with the ASME Code stress limits and the structural deformation limits. Analysis details and evaluation results are summarized and described below. Figure 4.1 shows a schematic of the high-Cr vessel concept with the evaluation elevations indicated by the red line at elevations Z1 to Z23. All the results for the structural damage in this report are calculated by the CHECK-ASME post-processing program of Ref. [12] developed in connection with the ANSYS code.

4.1 ASME Code design criteria

The structural integrity of ASME Code Class 1 component is evaluated in accordance with the requirements of the ASME Section III, Subsection NB and NH. The subsection

NB provides the design criteria for class 1 components at relatively low temperature below 371℃ for ferritic steels and below 427℃ for austenitic stainless steels. The subsection NH provides the high temperature design criteria for Class 1 components having metal temperatures exceeding those covered by the subsection NB.

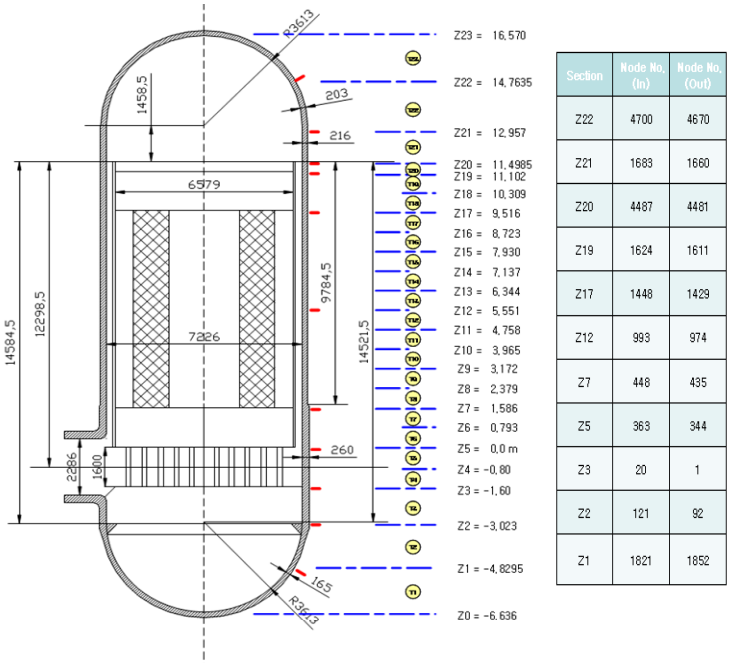

Section	Node No. (In)	Node No. (Out)
Z22	4700	4670
Z21	1683	1660
Z20	4487	4481
Z19	1624	1611
Z17	1448	1429
Z12	993	974
Z7	448	435
Z5	363	344
Z3	20	1
Z2	121	92
Z1	1821	1852

Figure 4.1 Schematic of the high temperature vessel concept with the evaluation cross sections

The elevated temperature criteria of the subsection NH are subdivided into the load controlled rules and the strain and deformation controlled rules. The strain controlled rules are further subdivided into strain limits and a creep-fatigue evaluation. Because of the continuing deformation and redistribution of the stress and strain due to creep, the elevated temperature design criteria are significantly more complex than those for temperatures below the creep temperature range. The design and service limits for Subsection NB and NH are summarized in Table 4.1.

Table 4.1 Design and service limits of Subsection NB and Subsection NH

		Design Condition	Level A and B	Level C	Level D
NB <371°C	Primary	$P_m < S_m$ $P_L+P_b < 1.5S_m$	P_m <110% S_m P_L+P_b < 110% (1.5S_m) (for Level B)	$P_m < 1.2S_m$ $P_L+P_b < 1.8S_m$ (or 1.5S_y)	$P_m < 2.4S_m$ $P_L+P_b < 3.6S_m$
	Secondary	-	$P_L+P_b+Q < 3S_m$ $P_L+P_b+Q+F<S_a$	-	-
N-499-2 >371°C (NH)	Load controlled stress limits	$P_m < S_o$ $P_L+P_b < 1.5S_o$	$P_m < S_{mt}$ $P_L+P_b < 1.5S_m$ $P_L+0.8P_b < S_t$	P_m < 1.2Sm, S_t $P_L+P_b < 1.8S_m$ $P_L+0.8P_b < S_t$	P_m<2.4S_m, 0.7S_u, 0.67S_r $P_L+P_b < 3.6S_m$ $P_L+0.8P_b$<0.67S_r
	Strain and deformation limits	-	-ε(membrane) <1% -ε(membrane+bending)< 2% -ε(peak) < 5% -Creep fatigue damage : $D_c + D_f < D$		-

P_m : Primary membrane stress intensity
P_b : Primary bending stress intensity
S_m : Allowable stress intensity (time independent)
S_t : Allowable stress intensity (temperature and time dependent)
S_{mt} : Allowable stress intensity (lower value of S_m and S_t)
S_r : Expected minimum stress-to-rupture strength
S_o : Allowable stress intensity for design loadings
D_f : Fatigue damage value
P_L : Primary local membrane stress intensity
Q : Secondary stress intensity
D_c : Creep damage value
D : Total creep-fatigue damage

4.1.1 Load controlled limits

The design criteria for the primary or load controlled stress at elevated temperature are similar to those below the creep range with several exceptions. At elevated temperatures the allowable stresses are time dependent and thus a function of load duration. Also, due to the strain redistribution effects, the primary bending stress must be modified by a shape factor function prior to being combined with the primary membrane stress components. The criteria are similar to those for elastic analysis; both are based on the stresses determined in equilibrium with the external loads.

4.1.2 Strain controlled limits

There are two routes in the subsection NH to satisfy deformation controlled limits. What considered as the fundamental approach is through a time dependent inelastic analysis. To implement this approach, complex constitutive relationships are required which model the time dependent and independent flow characteristics of the material.

The other route in the subsection NH to satisfaction of strain controlled limits is by means of elastic analysis. The concept is to have a simpler methodology than the full inelastic analysis which would not require a detailed modeling of time dependent flow characteristics. To check the strain controlled limits, the elastic analysis method is used in this report.

4.2 Preparation of structural analysis

4.2.1 Modeling of the high-Cr reactor vessel

The reactor vessel is composed of a vertical cylinder, hemispherical top and bottom closures, and nozzle. Its key dimensions are 7.7 m in diameter, 23.2 m in height and the thicknesses are various at different elevations as shown in Table 4.2 and Figure 4.1. The finite element analysis was performed using a finite element analysis software ANSYS. Two dimensional axisymetric FE model without nozzle, flange and supports is presented in Figure 4.2. The vessel is analyzed for the internal pressure and thermal loads from the thermo fluid analyses.

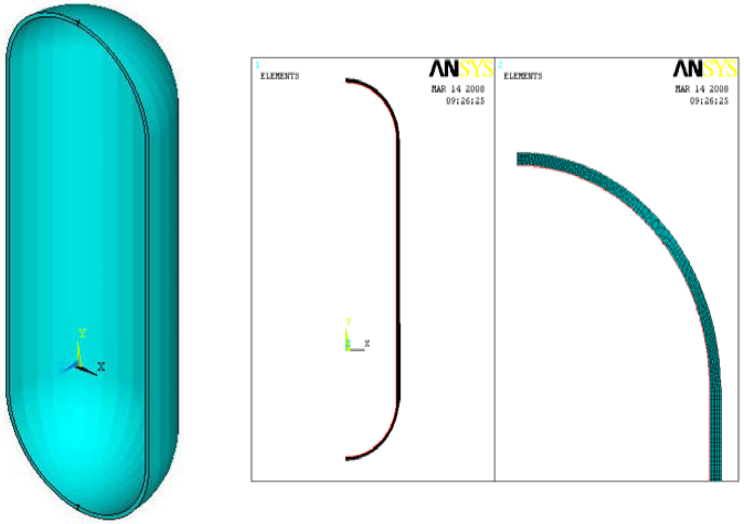

Figure 4.2 Finite element model of the high temperature vessel concept

4.2.2 Loading conditions

The thermal loadings of the normal operating condition and the transient conditions are obtained by the thermal fluid analysis using GAMMA+ system analysis code. The major design parameters are presented in Table 4.2. During the normal operation the inlet and outlet gas temperatures are 490℃ and 950℃, respectively and the reactor internal pressure is assumed constant 7MPa in all analysis cases, conservatively. The limiting transient conditions considered in this analyses are HPCC (High pressure Conduction Cooldown) and LPCC (Low pressure Conduction Cooldown) accidents.

Table 4.2 Major design parameters of the high-Cr vessel

Vessel inside pressure	7 MPa
Helium gas temperature at reactor inlet/outlet	490/950 ℃
Vessel inside diameter	7.23 m
Vessel height	23.2 m
Vessel thickness	
- Hemispherical top closure	203 mm
- Hemispherical bottom closure	165 mm
- Vertical cylinder(upper part)	216 mm
- Vertical cylinder(lower part)	260 mm

Table 4.3 Mechanical and physical properties of modified 9Cr-1Mo steel

Temp. (℃)	Thermal conductivity (J/s.m.℃)	Specific heat (J/Kg.℃)	Density (kg/m^3)	Thermal exp. coefficient (m/m/℃)	Young's modulus (GPa)	Poisson ratio	Yield strength (MPa)
20	22.3	448.85	7730	1.04E-05	213	0.3	414
100	24.4	484.11	7710	1.08E-05	208	0.3	384
200	26.3	523.04	7680	1.12E-05	201	0.3	377
300	27.4	562.69	7650	1.16E-05	195	0.3	377
400	27.9	609.96	7610	1.19E-05	187	0.3	358
500	27.9	671.75	7580	1.22E-05	179	0.3	306
600	27.6	754.96	7540	1.25E-05	168	0.3	218

4.2.3 Material properties

The material of the high-Cr reactor vessel is modified 9Cr-1Mo steel. The temperature dependent material properties are based on ASME Section II, Parts A and D and Section III, Subsection NH. Table 4.3 summarizes the mechanical and physical properties of modified 9Cr-1Mo steel.

4.3 Structural analysis results and structural integrity evaluations

4.3.1 Normal operating condition

The structural integrity of the reactor vessel is evaluated for thermal and mechanical loads during the normal operation. Table 4.4 shows the design margins of the reactor vessel for the normal operating condition. The maximum temperatures of the reactor vessel at all evaluation elevations are below 371℃ in the normal operating condition as shown in Table 4.4, and the design criteria for the design condition and Level A&B Service Conditions of the subsection NB are applicable for the evaluation. The mechanical and thermal stresses are compared with the ASME NB stress limit. The calculated stress levels in all evaluation elevations are below the allowable stress limits with adequate margins.

Table 4.4 Design margins for the normal operating condition

Evaluation section	P_m (MPa)	P_L+P_b (MPa)	P_L+P_b+Q (MPa)	S_m (MPa)	$1.5S_m$ (MPa)	$3S_m$ (MPa)	T_{mean} (℃)	Margin		
								*	**	***
Z22	63.9	70.2	90.5	195	293	585	333.4	2.1	3.2	5.5
Z21	92.3	99.2	122.8	195	293	585	324.6	1.1	1.9	3.8
Z20	122	129.6	156.9	195	293	585	329.2	0.6	1.3	2.7
Z19	122.1	128.3	158.8	195	293	585	330.9	0.6	1.3	2.7
Z17	120.5	127.3	162.3	195	293	585	341.5	0.6	1.3	2.6
Z12	120.4	127.2	164.6	195	293	585	336.7	0.6	1.3	2.6
Z7	107.9	124.3	155.1	195	293	585	331.2	0.8	1.4	2.8
Z5	99.9	106.7	165	195	293	585	330.1	1.0	1.7	2.5
Z3	99.9	108.4	155.7	195	293	585	294.6	1.0	1.7	2.8
Z2	78.1	101.8	92.7	195	293	585	190	1.5	1.9	5.3
Z1	78.6	86	90.8	195	293	585	121.7	1.5	2.4	5.4

*: $(S_m/P_m)-1$ **: $1.5S_m/(P_L+P_b)-1$ ***: $3S_m/(P_L+P_b+Q)-1$

The design margins for the primary membrane stress induced by the design pressure 7MPa range from 0.6 to 2.1, and those for the primary stress plus secondary stresses including the thermal load range from 2.5 to 5.5. The results of the analysis show that a reactor vessel is structurally adequate for the normal operating condition considered. Figure 4.3 shows the stress intensity profile along the location from bottom of the reactor vessel for the normal operating condition. The temperature distribution and the stress intensity distribution for the normal operating condition of a reactor vessel are shown in Figure 4.4 (a) and (b), respectively.

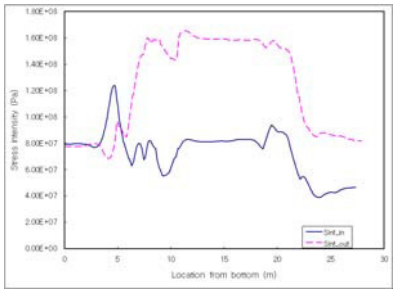

Figure 4.3 Stress intensity profile along the location from bottom for the normal operating condition

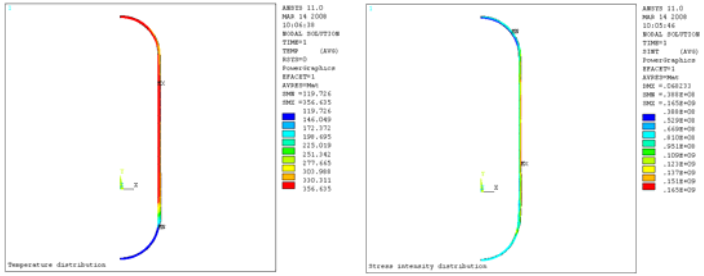

(a) Temperature distribution (b) Stress intensity distribution

Figure 4.4 Temperature and stress intensity distribution for the normal operating condition

4.3.2 Accident conditions

The structural integrity of the high-Cr reactor vessel is evaluated for thermal and mechanical loads during the accident conditions such as HPCC and LPCC. At the elevations where the maximum temperature of the reactor vessel exceeds 371℃ during the transient, the design criteria of the subsection NB are applicable for the evaluation. Figure 4.5 (a) and (b) show the temperature histories of the reactor vessel at the evaluation elevations in the high temperature region during the HPCC accident. As shown in these figures, the maximum temperature position is at Z12 and Z17 sections in HPCC condition. Also, it can be seen that the maximum temperatures at six evaluation

elevations exceed 371℃. Figure 4.6 shows the temperature histories of the reactor vessel at the evaluation elevations in the high temperature region during the LPCC accident. At the elevations where the temperature remains below 371℃ and the subsection NB is applicable, one can assume that the structural integrities for those elevations confirmed already in the previous evaluations for the normal operating condition since the loading conditions, 7MPa internal pressure, and the criteria are the same.

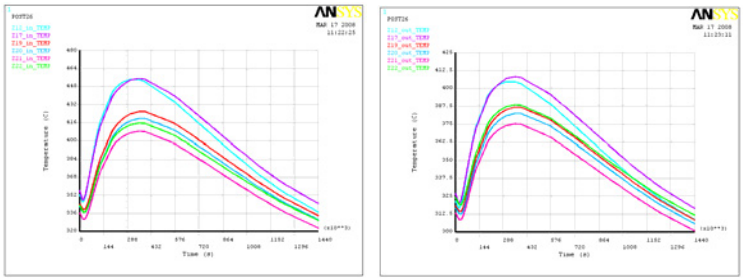

(a) Inside location (b) outside location

Figure 4.5 Temperature histories at the evaluation elevations located in the high temperature regions of the reactor vessel in HPCC condition

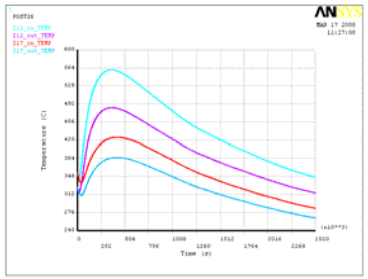

Figure 4.6 Temperature histories at the section located in the high temperature regions of the reactor vessel in LPCC condition

To evaluate the structural integrity at those evaluation elevations where the maximum temperature exceeds 371℃, the load controlled and the strain controlled design limits per the subsection NH shown in Table 4.1 should be applied. Note that the criteria for the Level A&B Service Conditions are applied in this evaluation instead of the criteria for the Level C&D Service Conditions for conservative evaluation even though the considered accidents of HPCC and LPCC are expected to be in the Level C&D Service Conditions.

Table 4.5 and Table 4.6 show the design margins for the load controlled stresses at the evaluation elevations which is in hot regions when the HPCC and LPCC condition, respectively. As shown in Table 4.5, HPCC cases, the design margins for the primary membrane stress, P_m, range from 0.4 to 1.8, and the design margins for the local membrane and bending stress, $P_L+0.8P_b$, range from 1.4 to 3.6. As shown in Table 4.6, LPCC case, the design margins for the primary membrane stress, P_m, range from 0.1 to 0.5, and the design margins the local membrane and bending stress, $P_L+0.8P_b$, range from 0.4 to 1.5. Those margins for the HPCC and LPCC transients are all acceptable for this structural integrity evaluation per the load controlled stress limit of the subsection NH. The smallest design margins are of the elevation Z12, which are 0.4 for HPCC and 0.1 for LPCC but all acceptable. The stress intensity histories at these evaluation elevations are presented in Figure 4.7 and Figure 4.8.

Table 4.5 Design margins for load controlled stress (HPCC)

Evaluation section	P_m (MPa)	P_L+P_b (MPa)	$P_L+0.8P_b$ (MPa)	S_{mt}^+ (MPa)	$1.5S_m$ (MPa)	S_t (MPa)	T_{max_m} (℃)	Margin		
								*	**	***
Z22	63.9	70.2	68.9	178.4	266.7	316.2	402.1	1.8	2.8	3.6
Z21	92.3	98.6	97.4	180.3	270	319.6	391.9	1.0	1.7	2.3
Z20	122	127.2	126.2	178.7	267.1	316.6	401.1	0.5	1.1	1.5
Z19	122.1	128.3	127.1	177.2	265.1	314.4	406.4	0.5	1.1	1.5
Z17	120.5	127.3	126	170.1	255.4	299.5	431.7	0.4	1.0	1.4
Z12	120.4	127.1	125.8	170.7	256.4	302.3	429.5	0.4	1.0	1.4

$^+$: S_{mt} which is the lower value of S_m and S_t where S_m is time-independent allowable stress intensity and S_t is time-dependent allowable stress intensity, respectively.
*: S_{mt}/P_m -1 **: $1.5S_m/(P_L+P_b)$-1 ***: $S_t/(P_L+0.8P_b)$ - 1

Table 4.6 Design margins for load controlled stress (LPCC)

Evaluation section	P_m (MPa)	P_L+P_b (MPa)	$P_L+0.8P_b$ (MPa)	S_{mt}^+ (MPa)	$1.5S_m$ (MPa)	S_t (MPa)	T_{max_m} (℃)	Margin		
								*	**	***
Z17	120.5	127.3	126	177.4	265.3	314.6	409.9	0.5	1.1	1.5
Z12	120.4	127.1	125.8	137.1	206	171.7	522.4	0.1	0.6	0.4

$^+$: S_{mt} which is the lower value of S_m and S_t where S_m is time-independent allowable stress intensity and S_t is time-dependent allowable stress intensity, respectively.
*: S_{mt}/P_m -1 **: $1.5S_m/(P_L+P_b)$-1 **: $S_t/(P_L+0.8P_b)$ - 1

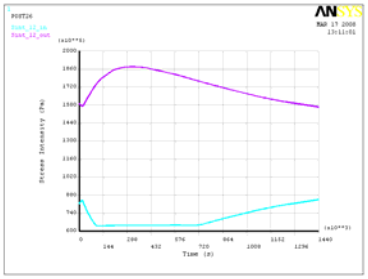

Figure 4.7 Stress intensity histories along at Z12 section in HPCC condition

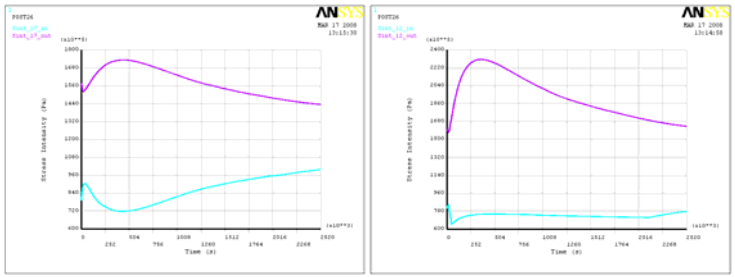

(a) Z17 section (b) Z12 section

Figure 4.8 Stress intensity histories along at Z17 and Z12 section in LPCC condition

The subsection NH allows an elastic analysis method, a simplified inelastic analysis method, and a creep-fatigue damage evaluation method for checking the design adequacy for the strain and deformation limits. In the elastic analysis method, the criteria of the inelastic strain limits are considered being satisfied if any one of the test A-1, A-2 or A-3 in T-1320 of Ref. [11] is satisfied. In these tests, X and Y are important variables which are defined in terms of the maximum local primary membrane and the bending stress intensities and the maximum range of secondary stress intensity, and the average yield stress during loadings. This evaluation study follows the test A-2 of the elastic analysis method to check the design adequacy per the strain and deformation limits. Table 4.7 and Table 4.8 show the inelastic strain check results by the elastic approach in HPCC and LPCC condition, respectively. As shown in these tables, it can be seen that the inelastic strain results satisfy the allowable limit, 1.0.

Table 4.7 Inelastic strain check results by the elastic approach (HPCC)

Evaluation elevation		Max.(P_m+P_b/K_t), (MPa)	Max.(Q_R) (MPa)	X	Y	X + Y ≤ 1.0	
						X + Y	Remark
Z22	Inner	68.9	16.3	0.1881	0.0445	0.2326	< 1.0
	Outer	68.9	16.3	0.1881	0.0445	0.2326	< 1.0
Z21	Inner	97.4	18.3	0.2643	0.0496	0.3139	< 1.0
	Outer	97.4	17.8	0.2643	0.0483	0.3126	< 1.0
Z20	Inner	126.2	18.6	0.3442	0.0506	0.3948	< 1.0
	Outer	126.2	20.5	0.3442	0.0560	0.4002	< 1.0
Z19	Inner	127.1	20.2	0.3479	0.0553	0.4032	< 1.0
	Outer	127.1	22.9	0.3479	0.0626	0.4105	< 1.0
Z17	Inner	126	37.2	0.3503	0.1034	0.4537	< 1.0
	Outer	126	36.9	0.3503	0.1026	0.4529	< 1.0
Z12	Inner	125.8	35.5	0.3488	0.0984	0.4472	< 1.0
	Outer	115	34.9	0.3189	0.0969	0.4158	< 1.0

Table 4.8 Inelastic strain check results by the elastic approach (LPCC)

Evaluation elevation		Max.(P_m+P_b/K_t) (MPa)	Max.(Q_R) (MPa)	X	Y	X + Y ≤ 1.0	
						X + Y	1.0
Z17	Inner	126	29.9	0.3439	0.0817	0.4256	< 1.0
	Outer	115	33.1	0.3140	0.0904	0.4044	< 1.0
Z12	Inner	125.8	93.3	0.3788	0.2810	0.6598	< 1.0
	Outer	115	92.9	0.3464	0.2798	0.6262	< 1.0

The simplified inelastic analysis confirms the design adequacy for the strain and deformation limits when the calculated total creep ratcheting strain is less than 1.0 %. The primary and secondary stress intensities are used to determine an effective creep stress, σ_c, which in turn is used to determine a total ratcheting creep strain. The dimensionless parameter Z for any combination of loading is given in Figure T-1332-1 for Test No. B-1 and in Figure T-1332-2 for Test No. B-2 of Ref. [3]. The creep ratcheting strain is determined by multiplying σ_c by 1.25 and evaluating the creep strain associated with the $1.25\sigma_c$ stress held constant throughout the temperature time history of the entire service life. The isochronous stress strain curves gives the creep ratcheting strains based on the above variables.

Table 4.9 and Table 4.10 show the inelastic strain check results by the simplified

inelastic approach in HPCC and LPCC condition, respectively. The creep ratcheting strains shown in Table 4.9 are all zeros, which mean that the creep ratcheting is not expected during HPCC condition. As shown in Table 4.10, the maximum inelastic ratcheting strain of LPCC condition is 0.099% at the Z12, which has large margin in comparison with the allowable limits of 1.0 %.

Table 4.9 Inelastic strain check by the simplified inelastic approach (HPCC)

Elevation		Creep Stress Parameter Z(%)	Effective Creep Stress(MPa)	Creep Ratcheting Strain(%)	Allowable Limits(%)	Hold Temp.(°C)
Z22	Inner	0.1917	71.7	0.0000	1.0	402.1
	Outer	0.1917	71.8	0.0000	1.0	
Z21	Inner	0.2677	100.5	0.0000	1.0	391.9
	Outer	0.2677	100.5	0.0000	1.0	
Z20	Inner	0.3466	130	0.0000	1.0	401.1
	Outer	0.3472	130.2	0.0000	1.0	
Z19	Inner	0.3531	132.2	0.0000	1.0	406.4
	Outer	0.3539	132.4	0.0000	1.0	
Z17	Inner	0.3551	132.6	0.0000	1.0	431.7
	Outer	0.3550	136.2	0.0000	1.0	
Z12	Inner	0.3560	133.4	0.0000	1.0	429.5
	Outer	0.3262	122.2	0.0000	1.0	

Table 4.10 Inelastic strain check by the simplified inelastic approach (LPCC)

Section		Creep Stress Parameter Z(%)	Effective Creep Stress(MPa)	Creep Ratcheting Strain(%)	Allowable Limits(%)	Hold Temp.(°C)
Z17	Inner	0.3579	134.9	0.0000	1.0	405.9
	Outer	0.3282	123.7	0.0000	1.0	
Z12	Inner	0.3855	144.3	0.0989	1.0	522.4
	Outer	0.3545	132.7	0.0651	1.0	

The subsection NH confirms the design adequacy for the accumulated creep-fatigue damage limit when the following equation is satisfied with the load combinations of the Level A, B and C Service Conditions;

$$\sum_{j=1}^{p}\left(\frac{n}{N_d}\right) + \sum_{k=1}^{q}\left(\frac{\Delta t}{T_d}\right) \le D \qquad (3)$$

Where D is total creep-fatigue damage, $(N_d)_j$ is the number of design allowable fatigue cycles for a cycle type j, $(T_d)_j$ is the allowable time duration determined from the stress to rupture curve, $(n)_j$ is the number of repeated cycles of type j, $(\Delta t)_k$, the duration of time interval k.

Table 4.11 and Table 4.12 represent the fatigue and creep damages calculated for one cycle of each transient. In all cases, the fatigue damages do not have any noticeable value. The creep damages by the HPCC accident are quite small in all evaluation elevations and the maximum creep damage by the LPCC accident is 0.0073 at the inner surface of Z12. Noting that the allowable creep damage limit with no fatigue damage is 1.0 which is provided by the creep-fatigue interaction diagram of the subsection NH, the creep-fatigue damage values are far below the allowable limit as listed in the table below.

Table 4.11 Creep-fatigue damage (HPCC)

Elevation		Total Strain Range, ε_t(%)	Fatigue Damage	Creep Damage	Hold Temp.(°C)
Z22	Inner	0.0078	0.0000	0.0001	402.1
	Outer	0.0085	0.0000	0.0001	
Z21	Inner	0.0078	0.0000	0.0001	391.9
	Outer	0.0090	0.0000	0.0001	
Z20	Inner	0.0074	0.0000	0.0002	401.1
	Outer	0.0135	0.0000	0.0002	
Z19	Inner	0.0079	0.0000	0.0002	406.4
	Outer	0.0120	0.0000	0.0002	
Z17	Inner	0.0166	0.0000	0.0002	431.7
	Outer	0.0185	0.0000	0.0002	
Z12	Inner	0.0176	0.0000	0.0002	429.5
	Outer	0.0189	0.0000	0.0002	

Table 4.12 Creep-fatigue damage (LPCC)

Section		Total Strain Range, ε_t(%)	Fatigue Damage	Creep Damage	Hold Temp.(°C)
Z17	Inner	0.0130	0.0000	0.0003	405.9
	Outer	0.0177	0.0000	0.0003	
Z12	Inner	0.0989	0.0000	0.0073	522.4
	Outer	0.0815	0.0000	0.0022	

5. SUMMARY

A preliminary thermo-fluid and structural analysis for the NGNP high-Cr reactor pressure vessel under the normal operating condition and anticipated transients has been performed, and the structural integrity is confirmed. A brief summary for the results is described as below.

Thermo-fluid analysis with GAMMA+ code

The system thermo-fluid analysis was performed using the GAMMA+ system analysis code. The steady analysis for the modified high-Cr vessel configuration with the air-cooled RCCS was performed for the normal operating condition with the helium inlet and outlet temperatures of 490℃ and 950℃ at 70 bars. The transient analyses were conducted for the two limiting accidents, High Pressure Conduction Cooldown (HPCC) and Low Pressure Conduction Cooldown (LPCC), thus producing the detailed temperature distribution of the reactor pressure vessel for the structural analysis.

Preliminary structural analysis

The structural analyses of the NGNP high-Cr RPV under the normal operating condition and the transient conditions (HPCC/LPCC) are performed, and the structural integrity of the vessel is confirmed per the ASME B&PV Code, Section III, Subsections NB and NH. The design criteria for the Level A&B Service Conditions are applied in the evaluation of the structural integrity of the vessel instead of those for the Level C&D Service Conditions conservatively. The vessel material is modified 9Cr-1Mo-V steel and it is assumed that during the normal operation the core inlet and outlet gas temperatures are 490℃ and 950℃, respectively, and the reactor internal pressure is constant, 7MPa, in all conditions considered, conservatively.

The reactor vessel temperature is maintained below 371℃ during the normal operation and the structural integrity of the vessel is confirmed with proper margin per the design criteria of the subsection NB. All the check items for the stress intensities given by the structural analysis and post-process are below the certain allowable limits required in the subsection NB. Even though the reactor vessel temperature exceeds 371℃ during the transients of the HPCC and LPCC for time, the structural integrity of the vessel is confirmed with proper margin per the design criteria in the subsection NH. All the check items for the stress intensities, the creep strains and the creep-fatigue damage given by the structural analysis and post-process are below the corresponding allowable limits required in the subsection NH.

In summary, the structural integrity and design adequacy of the NGNP high-Cr RPV was confirmed through this preliminary evaluation study. However, it should be noted that the evaluation and discussion so far is preliminary and is based on the simplified vessel configuration in which the important loadings such as nozzle loads, or support loads, seismic loads, and flange effects are not considered.

REFERENCES

[1] General Atomics, “GT-MHR Conceptual Design Description Report,” GA/NRC-337-02, August 2002.

[2] General Atomics, “H2-MHR Pre-Conceptual Design Report: SI-Based Plant,” GA-A25401, April, 2006.

[3] M.H. Kim, Calc. Note, “A Preliminary Thermo-fluid and Structural Analysis for a Cooled SA-508/533 NGNP Reactor Pressure Vessel,” NHDD-KA-07-RD-CA-022, Feb 2008.

[4] General Atomics, TAC2D Model Calculation Report, No. 910673, 1994.

[5] H.S. Lim, H.C. No, "GAMMA Multi-dimensional Multi-component Mixture Analysis to Predict Air Ingress Phenomena in an HTGR," Nuclear Science and Engineering, Vol. 152, pp. 87-97, Jan. 2006.

[6] ATHENA PMR input from INEEL, 2005.

[7] H.S. Lim, “GAMMA Code Input Calcs. for the PMR 600MWt”, NHDD-KA05-RD003-01, October 30, 2006

[8] M. Keyhani, F.A. Kulacki, R.N. Christensen, "Free Convection in a Vertical Annulus With Constant Heat Flux on the Inner Wall," J. Heat Transfer, Vol. 105, pp. 454-459, Aug. 1983.

[9] ASME Boiler & Pressure Vessel Code Section II, Part A, Part D, 2004.

[10] ASME Boiler & Pressure Vessel Code Section III, Subsection NB, 2004.

[11] ASME Boiler & Pressure Vessel Code Section III, Subsection NH, 2004.

[12] G. H. KOO, Computer program of SIE ASME-NH code, KAERI/TR-3526/2008, 2008.

APPENDIX D – KAERI Report on RPV Manufacturability

Manufacturability Evaluation

for

NGNP Pressure Vessels

2008.03.12

Table of Contents

1. Background and Purpose

This report was prepared according to GA subcontract SOW. As described in WBS NHS.000.S01 (RPV and IHX Pressure Vessel Alternatives) Task 3, the following items were evaluated in this document.

- A discussion of the manufacturability of SA508/533 vessels and high-Cr steel vessels
- Impact of material selection on vessel transportation
- Impact of material selection on ability to fabricate components on-site

2. Manufacturability of SA508/533 and High-Cr Steel Vessels

(1) Steel Manufacture Process

- Plate

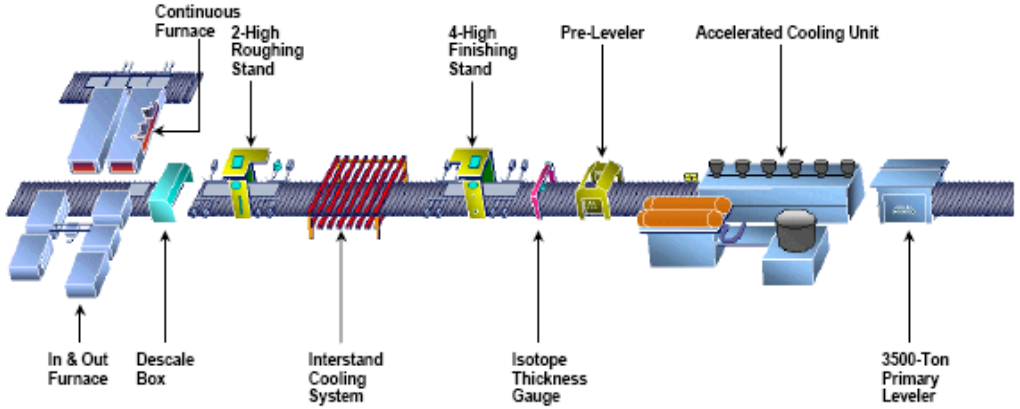

Slabs are heated in a furnace to a temperature in a typical range of 1150~1270˚C. The furnace incorporates machinery to transport a stream of slabs through it. These processes cause an oxide layer (scale) built up on the outer surface of the slab. High pressure water sprays are used to remove it (descale).
The descaled slab is gradually cooled while being passed through a series of straightening rolls. Once the required dimensions and thickness has been reached in the mill, the plate undergoes cooling. For many steel grades and applications, the cooling path is as influential in the plates' metallurgical development as the strain path in the mill. Systems for the controlled cooling are known as accelerated cooling systems, and are designed to reduce the plate temperature at high rates.
Leveling is a stress-relieving process carried out through low and controlled elongation in a multi-roller machine.

- Forging

Scrap iron is melted in the electric furnace and alloy materials (Cr, Ni etc.) are controlled in the refining ladle furnace to meet the chemical requirements in the steel foundry shop. This Al-killed and vacuum degassed steel is poured into the mold to make ingot. Forging Maker(Korean local supplier) has manufactured ingots ranged from 2 tons to 500 tons. These ingots are shaped into shells, heads, nozzles, blocks and bars by using forging presses of 10,000 tons, 4,200 tons and 1,600 tons.
Heat Treatment, such as normalizing, quenching and tempering is performed for stress relieving and mechanical property improvement. Test coupon is removed from the forged material, and then simulated PWHT is performed for mechanical and metallurgical test.
When all requirements are accepted, the forged material is finally machined for required dimensions. These forged materials are delivered to Manufacturing shop for fabrication with CMTR (Certified Material Test Report). The below photos show typical forging process


Steel Melting & Chemical Analysis


Pouring Vacuum Degassing


Ingot


Heating for Forging


Forging


Normalizing & Tempering


Machining before Quenching & Tempering


Quenching & Tempering


Mechanical & Metallurgical Test


Final Machining

(2) Material Purchase Specification (MPS) Requirements for Each Material

Description		SA508 Gr.3 Cl.1	SA533, Type B, Cl.1	2.25Cr-1Mo (SA387, Gr.22)	9Cr-1Mo (SA387, Gr.91)
Chemical Composition **Req't**	Carbon	0.25	0.25	0.05 ~ 0.15	0.08 ~ 0.12
	Mg	1.20 ~ 1.50	1.15 ~ 1.50	0.30 ~ 0.60	0.30 ~ 0.60
	Copper (Max.)	0.07	0.15	-	-
	Phosphorus (Max.)	0.012	0.015	0.035	0.020
	Sulfur (Max.)	0.010	0.005	0.035	0.010
	Vanadium	0.03	-	-	0.18 ~ 0.25
	Aluminum (Max.)	0.04	-	-	0.04
	Nickel	0.40~1.00	0.40~0.70	-	0.40
	Chromium	0.25	-	2.00 ~ 2.50	8.00 ~ 9.50
	Si	0.15 ~ 0.40	0.15 ~ 0.40	0.50	0.20 ~ 0.50
Mechanical Req't	Tensile strength (ksi)	70 ~ 95	80 ~ 100	60 ~ 85	85 ~ 110
	Yield strength, min. 0.2% offset (ksi)	36	50	30	60
	Elongation 2 in min (%)	20	18	18	18
	Reduction of area, min (%)	38	-	45	-

* Refer to attached CMTR (Certified Material Test Report) for detail information.

(3) Evaluation of the Weldability and Manufacturability for Each Material

Description	SA508 Gr.3 Cl.1 /SA 533 B 1	2.25Cr-1Mo (SA387 Gr.22)	9Cr-1Mo (SA387 Gr.91)
Classification	Carbon Steel	Heat Resisting Steel (Boiler equip't)	Heat Resisting Steel (LNG Tank Ship)
Material Manufacturability	Good	Poor (Due to segregation)	Poor (Due to segregation)
Welding Rod	EA-3 Type (Mn-Mo-Ni Alloy) ASME Sec.II Part C SFA 5.23 (Annex A7.1.1)	EB-3 Type ASME Sec.II Part C SFA 5.23 (Annex A7.1.2)	EB-9 Type ASME Sec.II Part C SFA 5.23 (Annex A7.1.2.1)
Weldability	Satisfactory	Poor (Weld crack)	Poor (Weld crack)

The material manufacturability and weldability of carbon steel are satisfactory, and it has been qualified in the overall areas of industries. Korean local supplier has the accumulated experience and knowledge about carbon steel.

Meanwhile, in case of the Cr-Mo steel, it is not easy to fabricate and weld the materials. The preheating and PWHT (Post Welding Heat Treatment) are required to prevent crack in the welding process and special care should be taken when selecting the welding material. Therefore, longer detail design duration and more manufacturing cost are required for the Cr-Mo vessels. In addition, Mock-up for Cr steel is required to verify the manufacturability and weldability in the next step for nuclear application.

(4) Considerations for Steel Manufacture

- Korean local supplier made large vessels (about 10m diameter & 44m height) using 2.25Cr-1Mo for Jammnagar Refinery project, chemical plant (1996~1998). And Korean local supplier has manufactured and supplied many forged materials vessels for nuclear projects. On the basis of these manufacturing experiences, Korean local supplier has a capability to make large vessels using Cr-Mo steel and carbon steel. Korean local supplier is considering the plate bending and forming to make large vessel and forging for nozzles and flanges for NGNP. (Refer to section 3.(2) & 3.(3) of this document)
- Korean local supplier has manufactured many nuclear vessels from rolled plate. Plate forming and bending method is applied to the vessel head and shell manufacture, respectively. For example, Secondary Head of Sequoyah unit 2 (USA) replacement Steam Generator was manufactured using plate forming, and HPECC Tank vessel of Qinshan phase III (CANDU PJT, China) was made using plate bending. Especially, Korean local supplier has experience to manufacture 2.25Cr-1Mo vessel (about 10m diameter) from rolled plate for Jammnagar Refinery project.

Plate Bending

Rolled Half Shell

Vessel for Jammnagar PJT

- Korean local supplier's preferences are 2.25Cr-1Mo for high temperature vessel application and SA508 or SA533 for other application. But it does not mean that Korean local supplier does not want to use of 9Cr-1Mo.
- Through manufacturing experience of similar materials, Korean local supplier has accumulated knowledge about Cr-Mo steel such as steel manufacturing, steel ingot making, forging, heat treatment according to temperature condition, material properties in high temperature, and forging process based on the pressure, etc. Korean local supplier's knowledge about Cr-Mo steel is competitive with other companies'.
- **Restriction on size;** In case of forging shell, the size (based on the weight) can be restricted due to the limitation of melting furnace capacity and other equipments.
- In case of Cr steel (2.25Cr-1Mo and 9Cr-1Mo) manufacture, the elaborate control is required because the segregation can easily occur. Especially, to prevent crack in the forging process, work should be controlled in the narrow temperature range compared to carbon steel.

3. Transportation and Installation of NGNP RPV Subassemblies

(1) Subassemblies by Shop Manufacture

- **Option 1**: Head and 1 piece body are manufactured in the shop, and assembled on the site.
- **Option 2**: Head and 2 piece body (Upper Body and Lower Body) are manufactured in the shop, and assembled on the site.

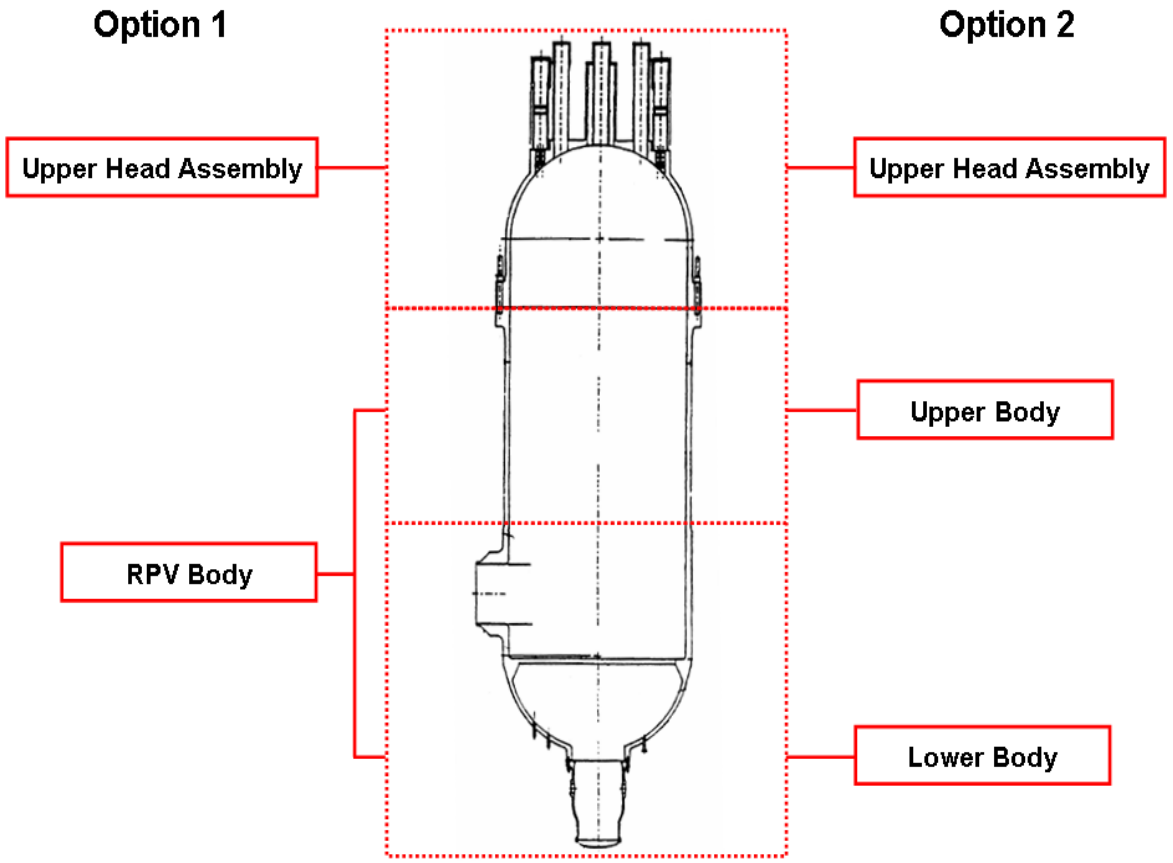

(2) Vessel Manufacturing

- Option 1 (1 Piece Body)

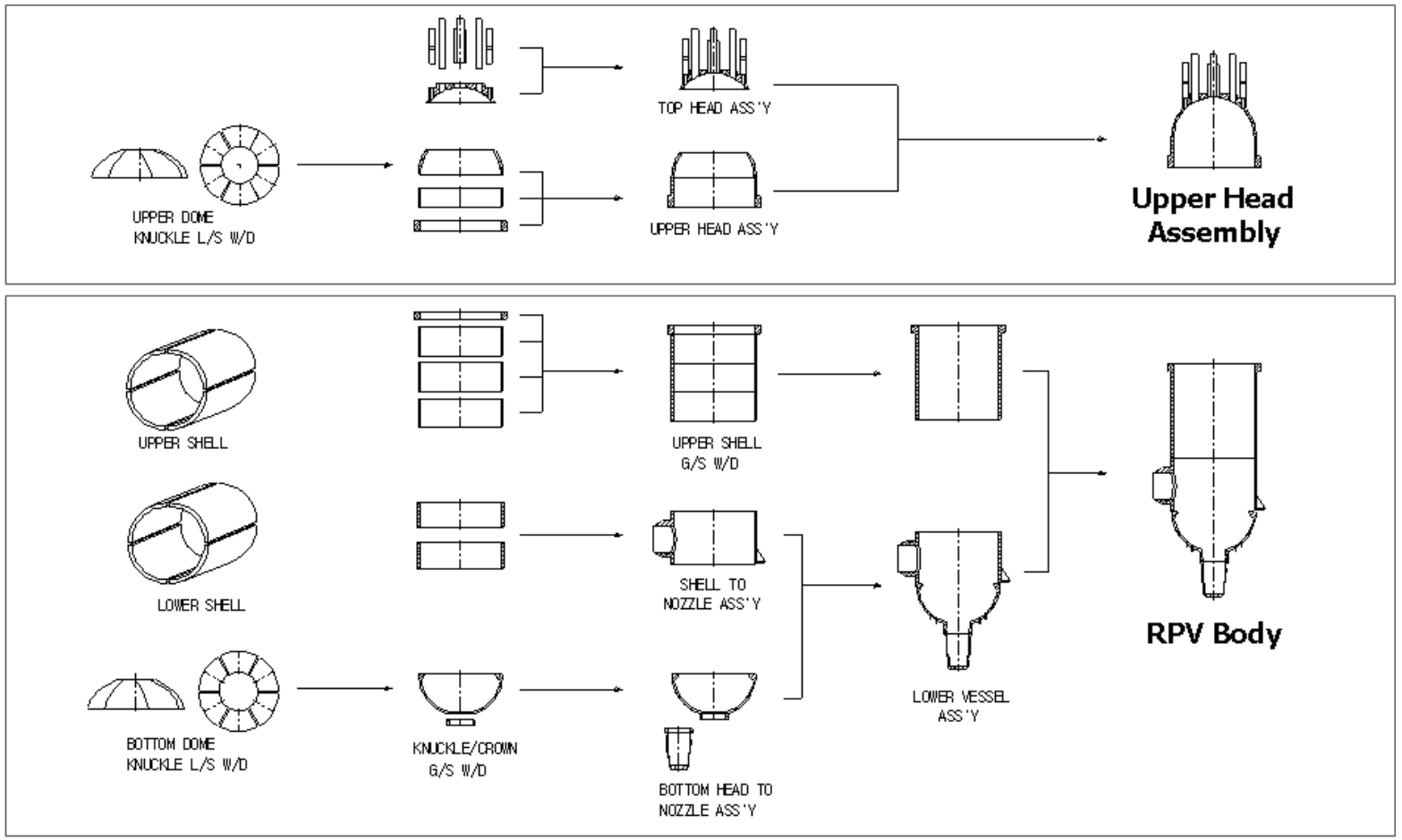

- Option 2 (2 Piece Body)

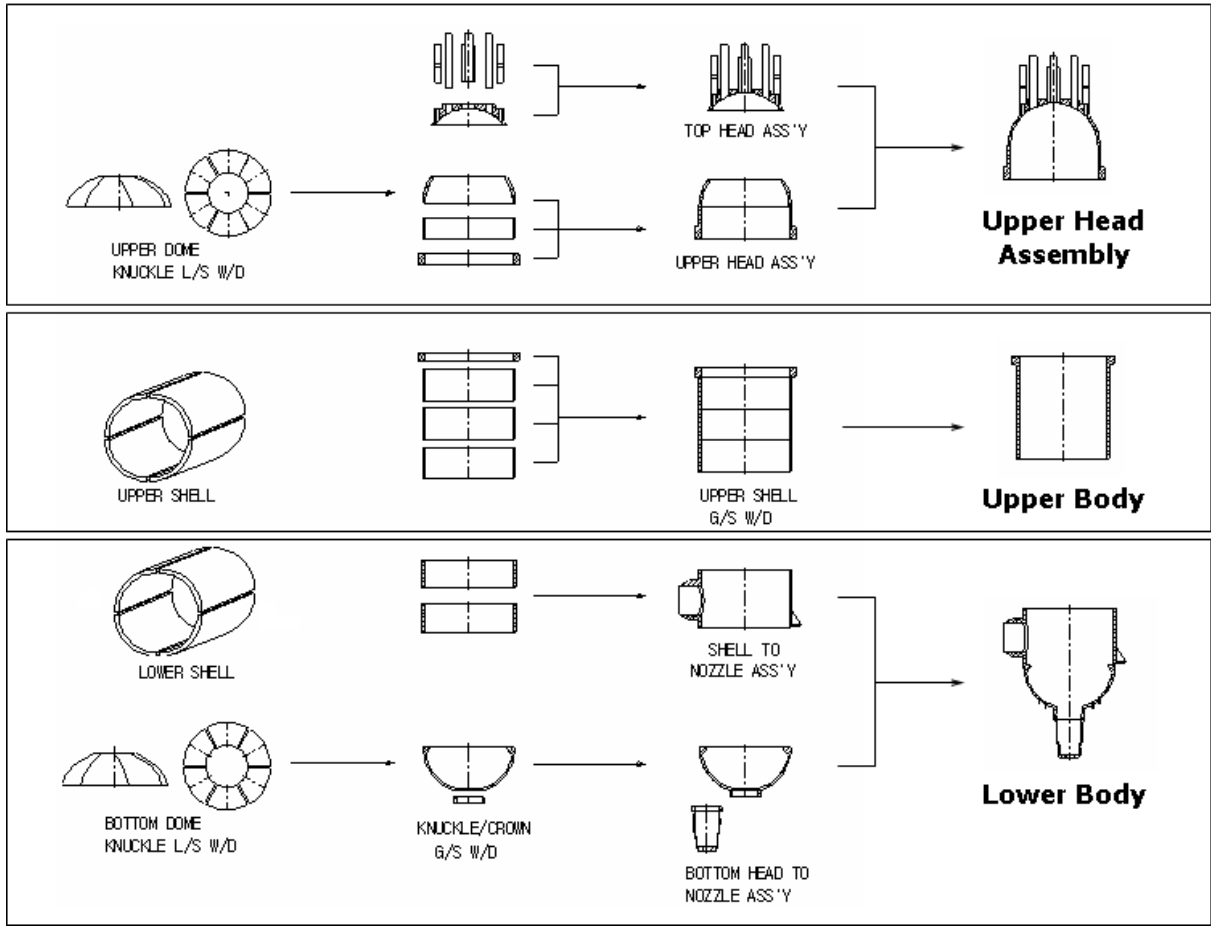

(3) BOM (Bill Of Material) for Vessel Manufacture

- Shell/Head Manufacture by Plate Bending

S/N	Plate Thickness (mm)	Plate Length (mm)		Arrangement	Configuration
		Single	Total		
1	220	2,800	2,800	60°	
2	225	1,660	1,660	90°	
3	600	997	997	90°	
4	600	718	718	90°	
5	225	2,624	7,872	90°	
6	270	2,370	4,740	90°	
7	170	4,620	4,620	60°	
8	50	1,796	1,796	180°	
9	50	508	508	180°	
10	50	712	712	180°	

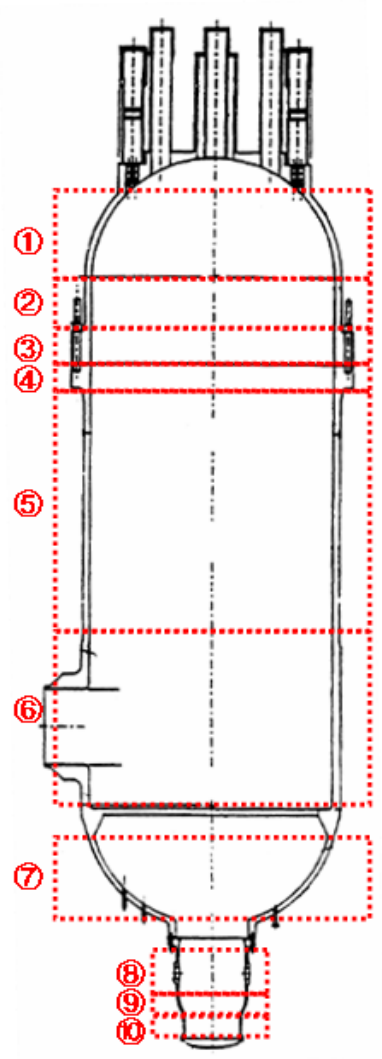

- **Forging**

S/N	OD (mm)	ID (mm)	Depth (mm)	Q'ty	Remark
1	640.0	-	-	31	Nozzle
2	5,718.0	5,163.0	318.7	1	-
3	7,632.7	7,226.3	203.2	2	-
4	7,658.1	7,226.3	215.9	4	-
5	3,046.4	-	260.4	1	Nozzle
6	7,747.0	7226.3	260.4	2	-
7	7,504.4	6807.8	347.4	1	-
8	127.0	-	200.0	45	Nozzle
9	3,060.0	-	181.4	1	Nozzle
10	2,032.0	1,932.0	50.0	2	-
11	533.0	-	50.0	2	Nozzle
12	2,032.0	1,932.0	50.0	1	-

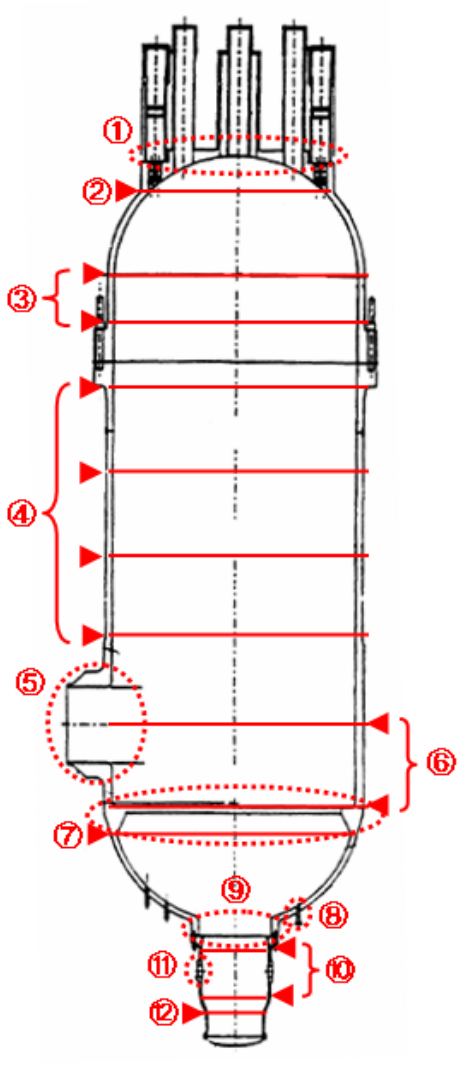

- Hydrostatic Test

a) Option 1 (1 Piece Body): Hydrostatic Test for 2 Assemblies (Head & RPV Body)

Hydrostatic tests are performed for the Head and Body, respectively, and the additional hydrostatic covers are required for the test.
Especially, in case of the hydrostatic test for the Body, the special equipment should be prepared considering the ground subsidence due to the excessive weight (above 1,300 ton)

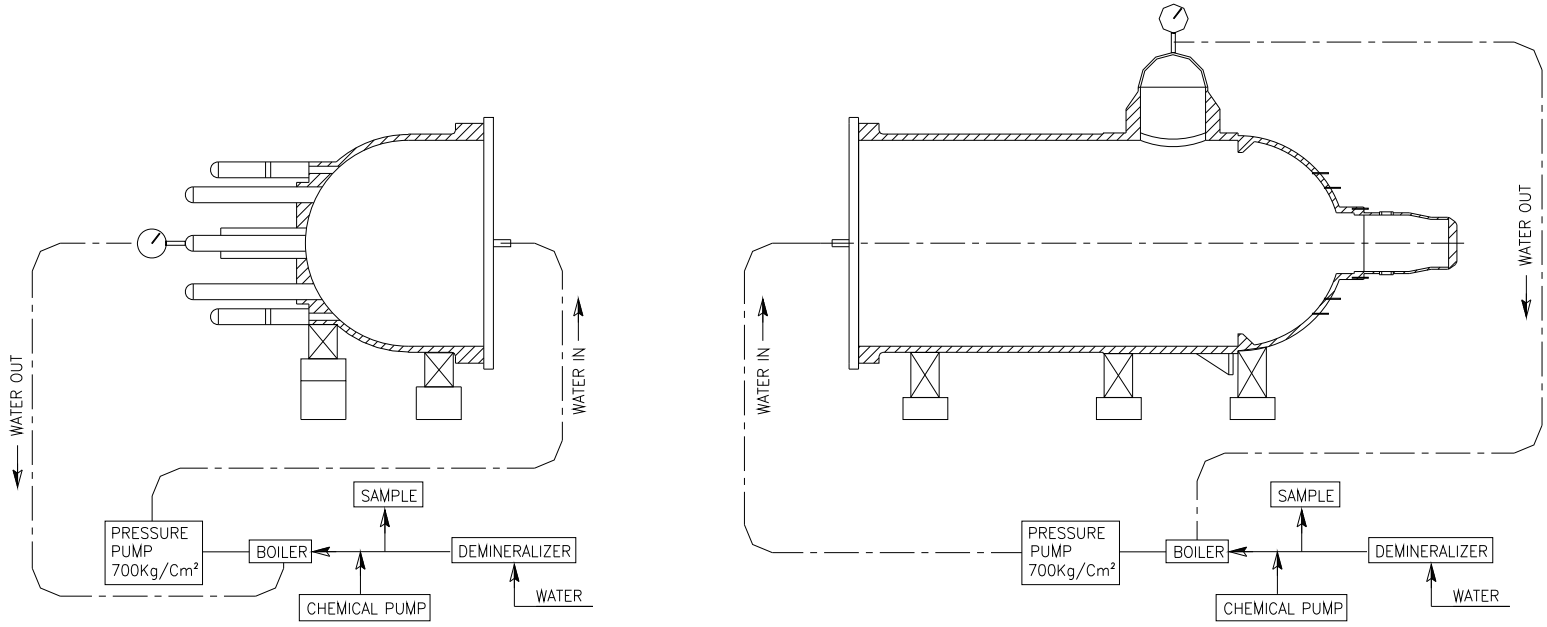

b) Option 2 (2 Piece Body): Hydrostatic Test for 3 Assemblies (Head & 2 Bodies)

Hydrostatic tests are performed for the Head and 2 Bodies, respectively, and the additional hydrostatic covers are required for the test.
2 subassemblies(Bodies) are to be welded on the site, and the system hydrostatic test should be performed after the final welding and PWHT.

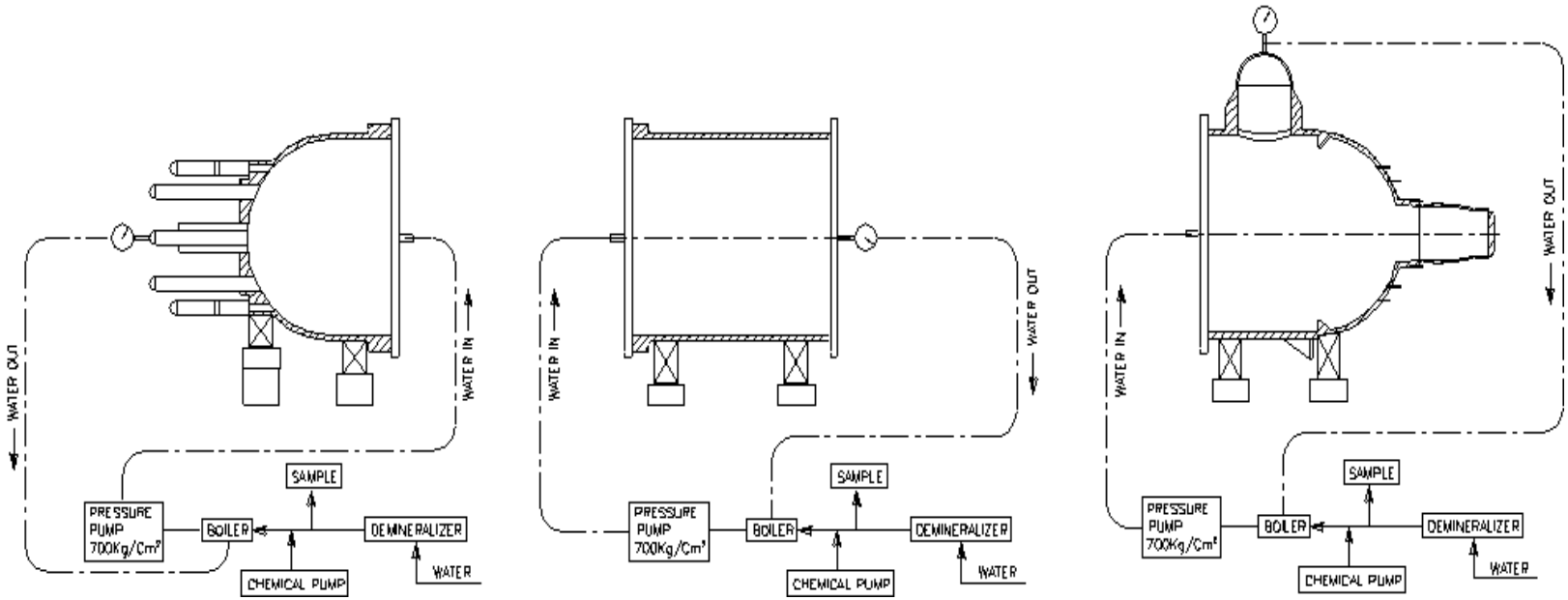

(4) Jigs to Prevent Deformation during the Transportation

To prevent the deformation due to deadweight during the transportation and storage in the field, the following items should be performed.

- Covers installation for opening of shell, nozzles (nitrogen fill-up)
- Internal supports installation for RPV Body. (3 places, 8 directions)

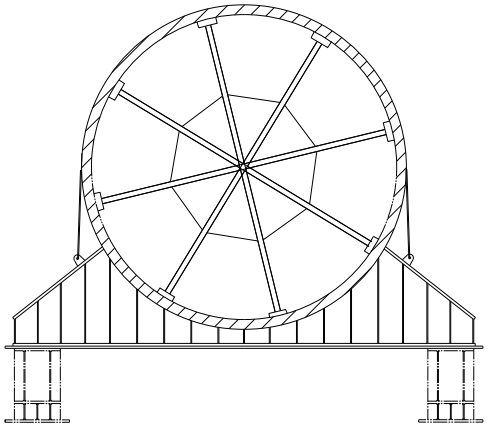

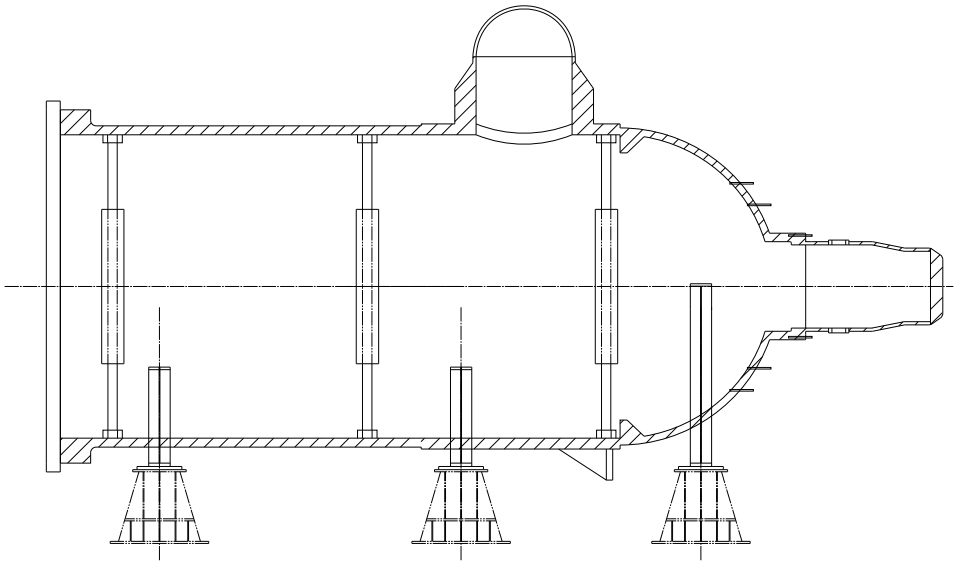

(5) Sketches, Weight and Dimensions of Each Subassembly

Option 1 (1 piece RPV body)

Component		OD (mm)	ID (mm)	Height (mm)	Weight (ton)
RV	Head	8,420.1	7,226.3	10,207.5	435*
	RPV Body	8,420.1	7,226.3	21,008.3	924*
	Total	8,420.1	7,226.3	31,215.8	1,364

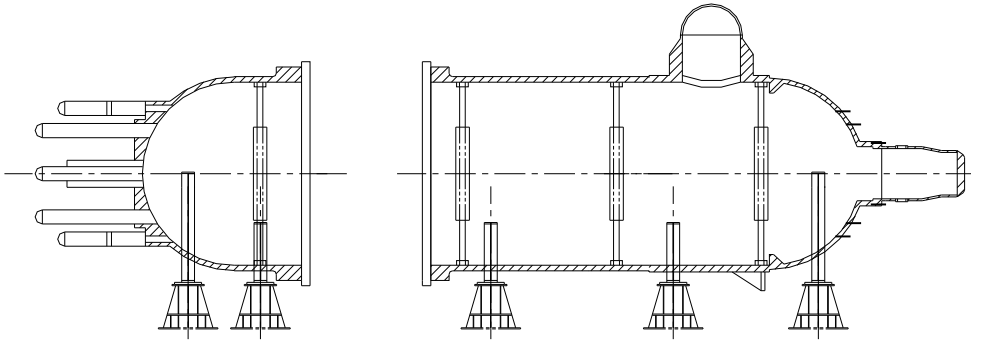

* The weight of stud and gasket is excluded. (But it is included in total weight)

Option 2 (2 RPV piece body)

Component		OD (mm)	ID (mm)	Height (mm)	Weight (ton)
RV	Head	8,420.1	7,226.3	10,207.5	435*
	Upper Body	8,420.1	7,226.3	8588.5	325
	Lower Body	8,420.1	7,226.3	12419.8	599*
	Total	8,420.1	7,226.3	31,215.8	1,364

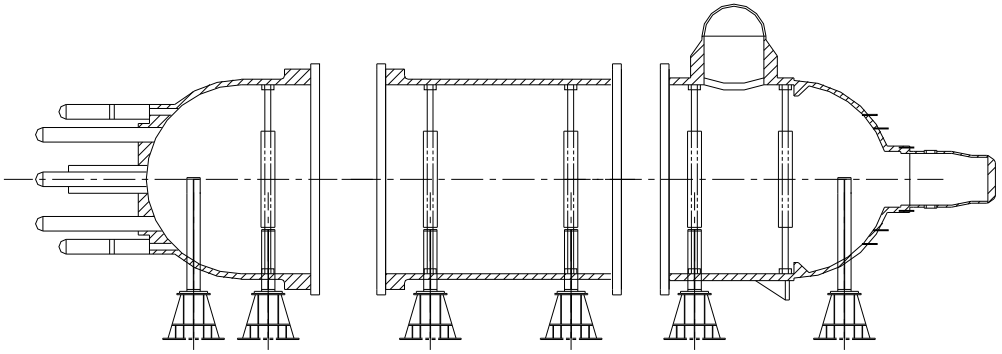

* The weight of stud and gasket is excluded. (But it is included in total weight)

(6) Considerations for the Transportation and On-site Fabrication

- If the transportation and fabrication conditions are same, there is no difference in the vessel transportation among the candidate materials. Both carbon steel and Cr-Mo steel have painting and package requirements, and the internal support to prevent deformation during transportation is required for all materials.
- When the Cr-Mo vessel is assembled on the site, special control is required in the selection of weld material, preheating, and PHWT. Because the Cr-Mo steel has poor weldability compared to carbon steel.

- Considerations for the Ground (Marine) Transportation – Route Survey

a) Bridges, tunnels, roundabout ways in all transportation routes should be investigated.
b) Packing, painting and nitrogen fill-up should be performed to prevent corrosion of the internal/external component.
c) The barge arrival date considering the flux and reflux of the tides should be determined, and the preparation of the pull-up process is required.
d) Cranes, lifting/handling equipment, pedestals and multi-loaders should be prepared for both the ground and marine transportation.
e) The estimated problems should be considered for the approval of the transportation.

- Considerations for the Option 1 (1 Piece Body) Manufacture

a) In case of long-term storage on the site, continuous control is required to prevent corrosion.
b) Saddle, Up/Down Ending method, Tie-Down requirement and the method of using Lift Lugs should be checked.
c) Extra-large crane (1000 ton) for the overweight RPV body is required.
d) When assembling the head and body, a special tensioner equipment is required for the stud/nut assembly.

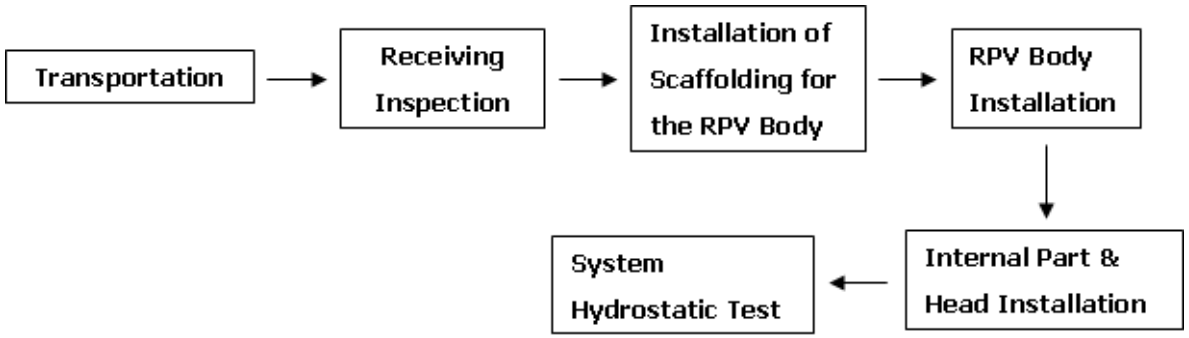

- Considerations for the Option 2 (2 Piece Body) Manufacture

a) In case of long-term storage on the site, continuous control is required to prevent corrosion.

b) Girth seam welding for the bodies is required on the site. Welding is to be performed in the horizontal direction after the installation of the Lower Body. Therefore, the following items should be developed.

- Automatic welding equipment considering the weldability
- Weld preparation
- Requirement for the weld misalignment
- Mock-up for welding
- Welding process

c) Saddle, Up/Down Ending method, Tie-Down requirement and the method of using Lift Lugs should be checked.

d) Extra-large Crane (1000 ton) for the overweight RPV body is required.

e) When assembling the head and body, a special tensioner equipment is required for the stud/nut assembly.

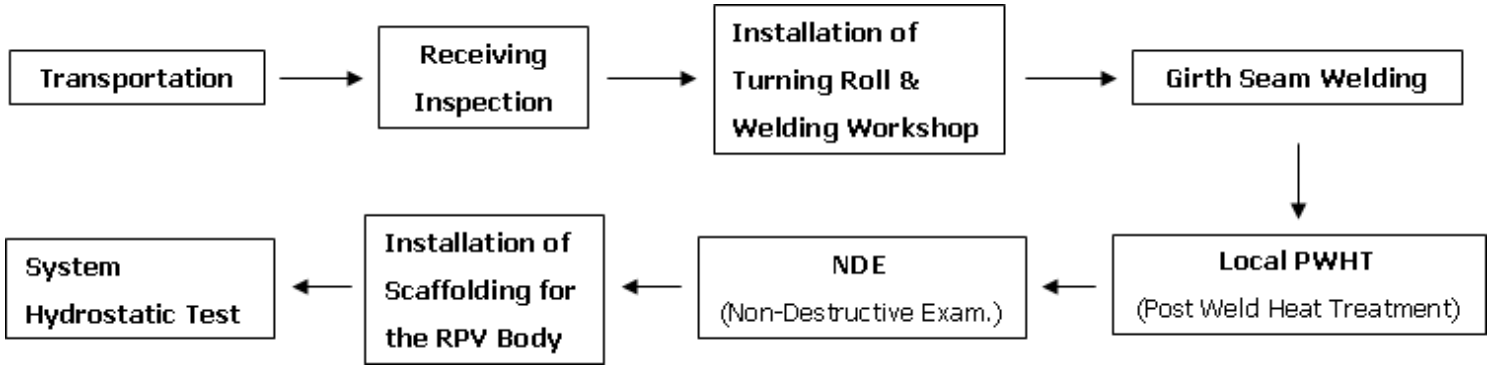

Appendix A. CMTR (Certified Material Test Report)

1. SA508

재 질 증 명 서
MATERIAL CERTIFICATE

공 사 명 Project Name	Shin-Kori Units 3&4 REACTOR VESSEL	고객 발주 번호 Customer PO No.	NPP-SKN34-0003 Rev.2	증명서번호 Certificate No.	F411-N-010
제 품 명 Product Name	UPPER SHELL	고객 사양서 번호 Customer Spec No.	HC-MPS21-006 Rev.1	고 객 Customer	DOOSAN
재 질 Mat'l Spec.	KEPIC MDF A508 등급3 클래스1	도 면 번 호 Drawing No.	C-HC-11100-P03 Rev.2		

순위 No.	제품번호 M/O Serial No.	치수 또는 규격 Size	수량 Q'ty	단 중(kg) Unit Wt	제강번호 Heat No.	화학성분 Chemical Composition %												Weight
						*1	C	Si	Mn	P	S	Ni	Cr	Mo	V	Al	Cu		
1	VF3515 010	Refer to DWG	1ea	92,000	2C34548	H	0.19	0.18	1.30	0.009	0.001	0.79	0.19	0.49	0.003	0.023	0.03		152 Ton
					2C34549	H	0.20	0.19	1.32	0.011	0.001	0.78	0.19	0.48	0.003	0.024	0.03		151 Ton
					WEIGHTED AV.	H	0.19	0.18	1.31	0.010	0.001	0.79	0.19	0.49	0.003	0.023	0.03		303 Ton
						P	0.19	0.21	1.24	0.010	0.001	0.79	0.19	0.49	0.004	0.018	0.03		
-	SPECIFICATION	-		-	-	H	Max.	0.15	1.20	Max.	Max.	0.40	Max.	0.45	Max.	Max.	Max.		
							0.25	0.40	1.50	0.025	0.010	1.00	0.25	0.60	0.03	0.04	0.20		

순위 No.	인장시험 Tensile Test							충격시험 Impact Test													비파괴시험 NDE			열처리 Heat Treatment			
	시편위치 Specimen Location	시편종류 Specimen Type	시험온도 Temp (°F)	항복강도 0.2%Y.S (KSI)	인장강도 T.S (KSI)	연신율 EL %	단면수축율 R/A %	시편위치 Specimen Location	시편종류 Specimen Type	시험온도 Temp (°F)	흡수에너지 Abs Energy(ft-lbs)			Lateral Expansion(Mils)			Shear Area (%)			*2	절차서 Procedure	결과 Result	*3	유지온도 Hold Temp(°C)	유지시간 Hold Time(hr)	냉각율 Cooling Rate
											1	2	3	1	2	3	1	2	3							
-	SPEC.	ASME	Room Temp	Min. 50	80 ~105	Min. 18	Min. 38	SPEC.	ASME	T$_{NDT}$+60°F (Max.70)	Min. 50	Min. 50	Min. 50	Min. 35	Min. 35	Min. 35	-	-	-	UT	FHD-5150	Accept	Q	880	12	W.C
1	AT1	SA370	70	67	88	31	75	AV/1,2,3	SA370,	30	176	166	196	75	89	91	74	74	84							
	BT1	Fig.5		70	90	30	77	(Axial.)	Fig.11											MT	Rev.0	Accept	T	655	12	A.C
	CT1	GL:2"		67	88	29	75	BV/1,2,3	(a)		178	215	183	82	87	87	80	100	86							
	DT1			67	88	29	74	(Axial.)																		

*1 ··· Kind of Analysis
H = Heat Analysis
P = Product Analysis
*2 ··· Kind of Examination
RT , UT , MT , PT , VT
*3 ··· Kind of Heat Treatment
A = Annealing N = Normalizing
Q = Quenching T = Tempering
R = Stress Relieving A.C = Air Cooling
W.C = Water Cooling

* Drop weight test (spec: T$_{NDT}$ & RT$_{NDT}$: ACTUAL Max.10°F)
-. Specimen : P3 Type : Tangential Direction
-. Results : AD3 / BD3 (-20°F) : No break / No break
: AD1 / BD1 (-30°F) : break / break
(T$_{NDT}$ & RT$_{NDT}$ = -30°F)
*Grain Size No : 6.5 (Method : ASTM E112-96)
Remark
1. Direction of Tensile Specimens : Tangential
2. The method locating test specimen is per purchase spec. HC-MPS21-006 Rev.1 3.3.2 1 Without pad.
3. Simulated PWHT for test coupons
- Holding Temp : 615℃ - Heating Rate : 40℃/ Hr
- Holding Time : 30Hrs - Cooling Rate : 30℃/Hr

본 제품은 지정된 자재요구사양에 따라 제조되었고 모든 시험 및 검사 결과가 이에 만족하고 있음을 증명함.

We hereby certify that the contents of this report are correct and accurate and that all test and examination results and operations performed by DOOSAN are in compliance with the applicable material requirements.

Certified by J. K. SANG 11/25/04
주단품질관리부장 CFQC Dept Gen Mgr Date

품질-C-031

A4(210×297mm)

2. SA533

INDUSTEEL
Groupe Arcelor
■ Site de Châteauneuf

CLIENT - Purchaser.	DOOSAN HEAVY INDUSTRIES AND
COMMANDE CLIENT - Purchaser order n°.	ORDER NO. 110058851 rev. 1
PROJET - Project.	
CERTIFICAT N° - Certificat nr.	11023.12
REVISION - Rev.	1
TYPE CERTIFICAT - Form.	
SPECIFICATION Specification	ASME code section II part A + Section III Subsection NB(cl1), +section III Division 1 Appendix P-1000 + 10 CFR part 50 appendix B.1989 Edition without addenda. SPEC. WA-MPS 21-011 REV 1 SPEC PS-11102- REV 1
COMMANDE IND - IND order.	30941F
NUANCE - Quality.	SA 533 TYPE B CL. 2
ETAT DE LIVRAISON - As delivered.	Austenitized, Quenched Tempered -
11023.12 : 1 x [3 400 x 3 500 x 92.1] mm	ITEM 1 DOOSAN TVA Watts Bar Unit-1 RSG Contract # 16346

11023.12 PAGE - Sheet 2/9

ANALYSES CHIMIQUES - Chemical analysis

☒ Conforme - Conforming

N° DE COULEE - Heat n° 11023

ELABORATION - Steel processing ..... Acier électrique, à grain fin, calmé, dégazé sous vide - Electric furnace, fine grain size, killed, vacuum degassed

	UNITES Unit	COULEE - Heat		PRODUIT - Product				
		IMPOSE - Required	OBTENU - Actual	IMPOSE - Required	OBTENU - Actual			
					BD-M	HG-M	-	-
C	%	<=0.25	0.18	<=0.25	0.19	0.19		
Mn	%	1.15 / 1.50	1.49	1.07 / 1.62	1.47	1.47		
Si	%	0.15 / 0.40	0.23	0.13 / 0.45	0.23	0.23		
Ni	%	0.40 / 0.70	0.67	0.37 / 0.73	0.66	0.66		
Cr	%	<=0.30	0.19	<=0.34	0.19	0.19		
Mo	%	0.45 / 0.60	0.51	0.41 / 0.64	0.51	0.51		
Cu	%	<=0.15	0.08	<=0.15	0.07	0.07		
Al	%	INFO	0.027	INFO	0.025	0.025		
S	%	<=0.005	0.001	<=0.005	0.002	0.002		
P	%	<=0.015	0.007	<=0.018	0.007	0.007		
Sn	%	INFO	0.005	INFO	0.006	0.005		
V	%	<=0.030	0.005	<=0.040	0.004	0.004		
Nb	%	<=0.020	0.003	<=0.030	0.003	0.002		

NOUS CERTIFIONS QUE LES PRODUITS ENUMERES CI-DESSUS SONT CONFORMES AUX PRESCRIPTIONS DE LA COMMANDE
We certifiy hereby that the above mentioned products are consistent with the order prescriptions

Résultats vérifiés le / Results checked on 15/05/2003

Dépt. Inspection R. MILLET

3. SA336 F.22

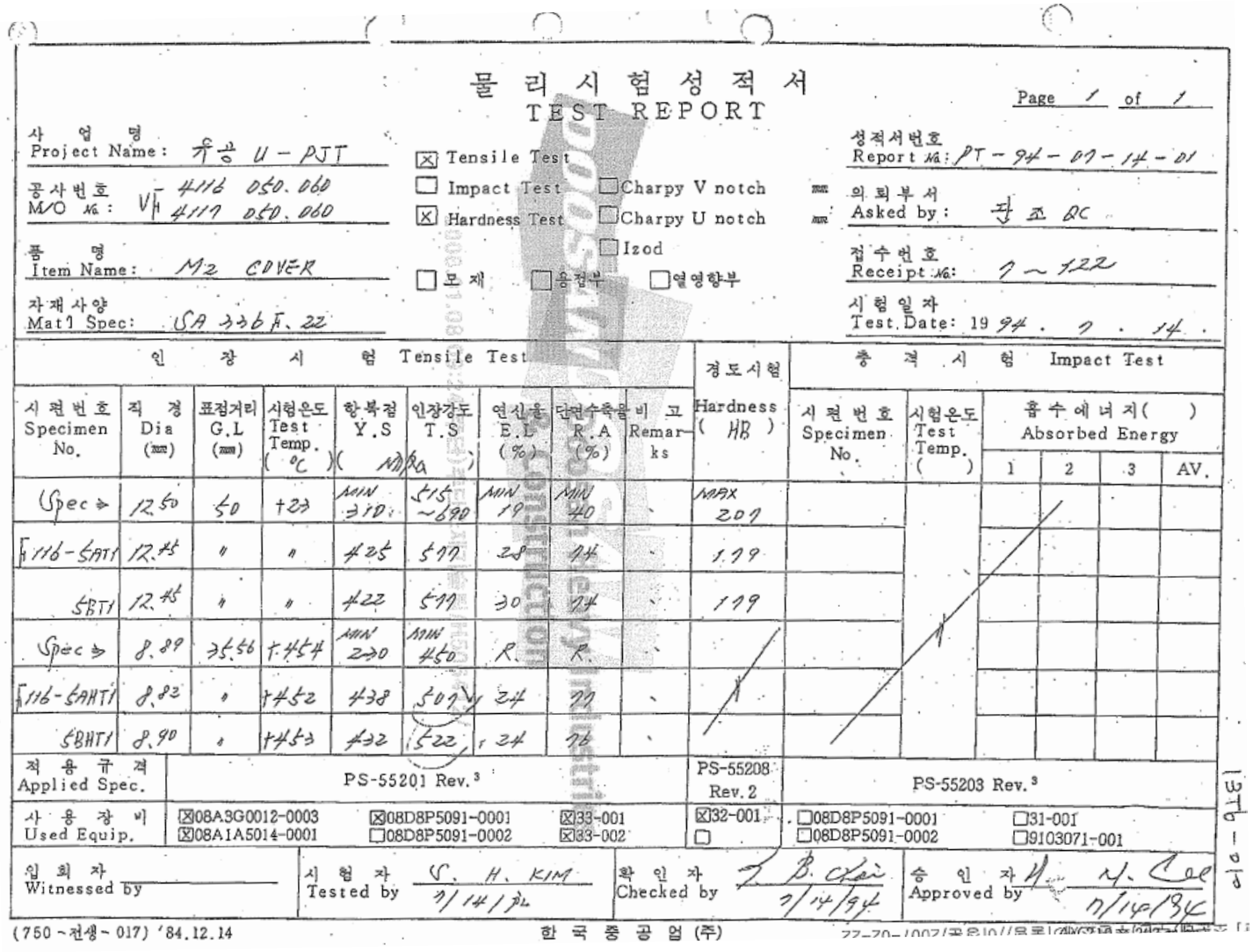

물 리 시 험 성 적 서
TEST REPORT

Page 1 of 1

사 업 명 Project Name: 유공 U-PJT
공사번호 M/O No.: VH 4116 050.060 / 4117 050.060
품 명 Item Name: M2 COVER
자재사양 Mat'l Spec: SA 336 F. 22

☒ Tensile Test ☐ Impact Test ☐ Charpy V notch ☐ Charpy U notch ☒ Hardness Test ☐ Izod
☐ 모재 ☐ 용접부 ☐ 열영향부

성적서번호 Report No.: PT-94-07-14-01
의뢰부서 Asked by: 검사 QC
접수번호 Receipt No.: 1~122
시험일자 Test Date: 1994. 7. 14.

인장시험 Tensile Test									경도시험	충격시험 Impact Test						
시편번호 Specimen No.	직경 Dia (mm)	표점거리 G.L (mm)	시험온도 Test Temp. (°C)	항복점 Y.S (MPa)	인장강도 T.S	연신율 E.L (%)	단면수축율 R.A (%)	비고 Remarks	Hardness (HB)	시편번호 Specimen No.	시험온도 Test Temp. (°C)	흡수에너지 Absorbed Energy 1	2	3	AV.
Spec ≥	12.50	50	+23	MIN 310	515~690	MIN 19	MIN 40		MAX 207						
F116-5AT1	12.45	〃	〃	425	577	28	74		179						
5BT1	12.45	〃	〃	422	577	30	74		179						
Spec ≥	8.89	35.56	+454	MIN 290	MIN 450	R.	R.								
F116-5AHT1	8.82	〃	+452	438	501	24	77								
5BHT1	8.90	〃	+453	432	522	24	76								

적용규격 Applied Spec.	PS-55201 Rev.3	PS-55208 Rev.2	PS-55203 Rev.3
사용장비 Used Equip.	☒08A3G0012-0003 ☒08A1A5014-0001 ☒08D8P5091-0001 ☐08D8P5091-0002 ☒33-001 ☒33-002	☒32-001 ☐	☐08D8P5091-0001 ☐08D8P5091-0002 ☐31-001 ☐9103071-001

입회자 Witnessed by
시험자 Tested by S. H. KIM 7/14/94
확인자 Checked by B. Choi 7/14/94
승인자 Approved by M. M. Lee 7/14/94

(750-전생-017) '84.12.14 한국중공업(주)

GENERAL ATOMICS
P.O. BOX 85608 SAN DIEGO, CA 92186-5608 (858) 455-3000